# Spectroscopic Investigations of Magnetic Anisotropy in Molecular Nanomagnets

ECMM workshop on Magnetic Anisotropy
Karlsruhe, 11th-12th October 2013

Prof. Dr. Joris van Slageren
Institut für Physikalische Chemie

Dr. Shang-Da Jiang
1. Physikalisches Institut

Universität Stuttgart
Germany

# Contents

# Contents



**Literature**

A. Abragam/B. Bleany – Electron Paramagnetic Resonance of Transition Ions, 1970

N.M. Atherton – Principles of Electron Spin Resonance, 1993.

R. Boča – Theoretical Foundations of Molecular Magnetism, 1999

R. Carlin – Magnetochemistry, 1986

C. Görller-Wallrand, K. Binnemans in Handbook on the Physics and Chemistry of Rare Earths, Vol. 23, http://dx.doi.org/10.1016/S0168-1273(96)23006-5

O. Kahn – Molecular Magnetism, 1993

F.E. Mabbs/D.J. Machin – Magnetism and Transition Metal Complexes, Chapman and Hall, London, 1973

K.R. Lea, M.J.M. Leask, W.P. Wolf, J. Phys. Chem. Solids, 23, 1381 (1962)

H. Lueken – Magnetochemie, 1999

H. Lueken – Course of lectures on magnetism of lanthanide ions under varying ligand and magnetic fields, http://obelix.physik.uni-bielefeld.de/~schnack/molmag/material/Lueken-kurslan_report.pdf 2008

D.J. Newman/Ng (Ed.) – Crystal Field Handbook

A.J. Orchard – Magnetochemistry, 2003

1. Introduction
2. Single Crystal Magnetometry
3. High-Frequency EPR Spectroscopy
4. Inelastic Neutron Scattering
5. Electronic Absorption and Luminescence

# Ch. 1. Introduction

## Section 1.1 Magnetic anisotropy



**Magnetic anisotropy. The highly simplified, hand-waving explanation**

- Magnetic anisotropy means that the magnetic properties (of the molecule) have an orientational dependence.
- This means that the response to an external magnetic field depends on the direction in the molecule along which the field is applied, e.g., g-value anisotropy, hard/easy axes of magnetization.
- Susceptibility becomes anisotropic. **M** = $\underline{\chi}$ **H**

$$\underline{\chi} = \begin{pmatrix} \chi_{xx} & 0 & 0 \\ 0 & \chi_{yy} & 0 \\ 0 & 0 & \chi_{zz} \end{pmatrix}$$

- This also means that the magnetic moment of the molecule prefers (lower potential energy) to lie along a certain direction, e.g., double well picture in transition metals.

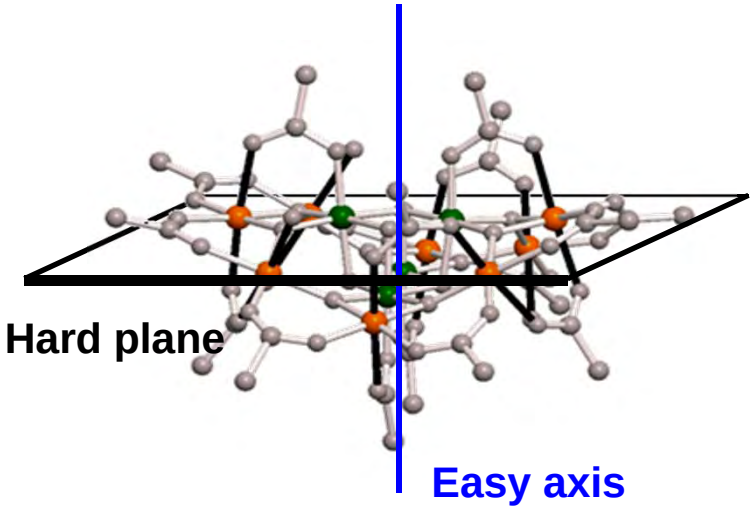


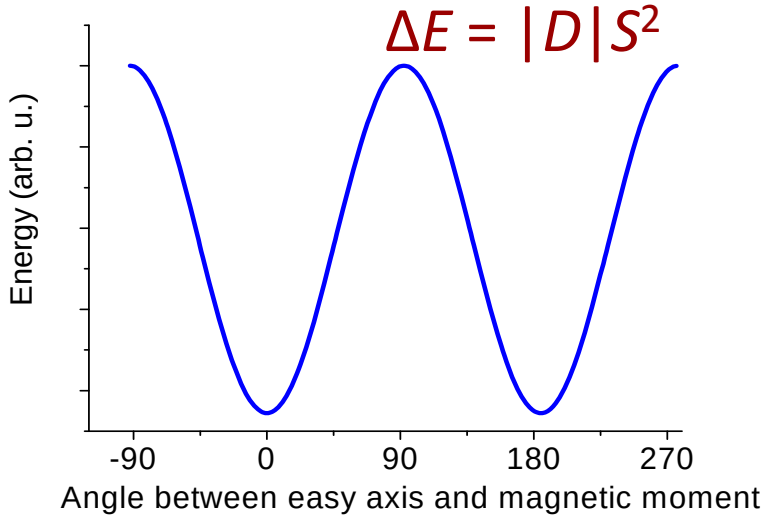

# Ch. 1. Introduction

## Section 1.1 Magnetic anisotropy



**Magnetic anisotropy. The highly simplified, hand-waving explanation**

- Electrons experience the following interactions:
  - attraction to the nucleus (Coulomb)
  - repulsion by other electrons
  - spin-orbit coupling
  - crystal field (Coulomb)
  - magnetic field (Zeeman)

| | | | | | | |
|---|---|---|---|---|---|---|
| $3d^N$ | $H_{ee}$ | $>$ | $H_{LF}$ | $>$ | $H_{SO}$ | weak field |
| | $H_{LF}$ | $>$ | $H_{ee}$ | $>$ | $H_{SO}$ | strong field |
| | $H_{LF}$ | $\approx$ | $H_{ee}$ | $>$ | $H_{SO}$ | intermediate field |
| $4f^N$ | $H_{ee}$ | $>$ | $H_{SO}$ | $>$ | $H_{LF}$ | (a) |
| | $H_{ee}$ | $>$ | $H_{SO}$ | $\gg$ | $H_{LF}$ | (b) |

(a) strong field lanthanide system ; (b) weak field lanthanide system

| Effect | | System | Energy equivalent wavenumber/$cm^{-1}$ [a] |
|---|---|---|---|
| Electron-electron interaction | $H_{ee}$ | 3d, 4d, 5d | $3d > 4d > 5d \approx 10^4$ [b] |
| | | 4f, 5f | $4f > 5f \approx 10^4$ [b] |
| Ligand-field potential | $H_{LF}$ | 3d, 4d, 5d | $3d < 4d < 5d \approx 2 \times 10^4$ [b] |
| | | 4f | $\approx 10^2$ |
| | | 5f | $\approx 10^3$ |
| Spin-orbit coupling | $H_{SO}$ | 3d, 4d, 5d | $3d < 4d < 5d \approx 10^3$ [b] |
| | | 4f, 5f | $4f < 5f \approx 10^3$ [b] |
| Exchange interaction | $H_{ex}$ | $nd$ | $\leq 10^2$ |
| | | 4f | $< 1$ |
| | | $nd$–4f | $< 10$ |
| Magnetic field | $H_{mag}$ | | $\approx 0.5$ (1 T) |

- The main difference between 3d transition metals and f-elements is that the crystal field and exchange interactions are much weaker in the latter, while spin-orbit coupling can be much stronger.

Lueken99, Lueken08

# Ch. 1. Introduction

## Section 1.2 Magnetic anisotropy in Transition Metal Clusters



**A highly simplified, hand-waving explanation.**

- Most free ions have an orbital angular momentum (except $d^5$ high-spin).
- In most complexes, the orbital angular momentum appears to have disappeared. (quenching of the orbital moment).
- This is due to the crystal field splitting of the d-orbitals ("$t_{2g}$-$e_g$").

**Tab. 2.2:** Ionen mit $3d^N$-High-Spin-Konfiguration: Termsymbol (Grundzustand), Einelektronen-Spin-Bahn-Kopplungsparameter $\zeta_{3d}$ [$cm^{-1}$] [178], $S$, $2[S(S+1)]^{1/2}$ und $n_{eff}^{exp}$ (295 K).

| Ion | $3d^N$ | $^{2S+1}L_J$ | $\zeta_{3d}$ | $S$ | $2[S(S+1)]^{1/2}$ | $n_{eff}^{exp}$ |
|---|---|---|---|---|---|---|
| $Sc^{3+a)}$ | $3d^0$ | $^1S_0$ | | | | 0 |
| $Ti^{3+}$ | $3d^1$ | $^2D_{3/2}$ | 154 | 1/2 | 1,73 | 1,65 – 1,79 |
| $V^{3+}$ | $3d^2$ | $^3F_2$ | 209 | 1 | 2,83 | 2,75 – 2,85 |
| $V^{2+}$ | $3d^3$ | $^4F_{3/2}$ | 167 | 3/2 | 3,87 | 3,80 – 3,90 |
| $Cr^{3+}$ | $3d^3$ | $^4F_{3/2}$ | 273 | 3/2 | 3,87 | 3,70 – 3,90 |
| $Cr^{2+}$ | $3d^4$ | $^5D_0$ | 230 | 2 | 4,90 | 4,75 – 4,90 |
| $Mn^{3+}$ | $3d^4$ | $^5D_0$ | 352 | 2 | 4,90 | 4,90 – 5,00 |
| $Mn^{2+}$ | $3d^5$ | $^6S_{5/2}$ | 347 | 5/2 | 5,92 | 5,65 – 6,10 |
| $Fe^{3+}$ | $3d^5$ | $^6S_{5/2}$ | (460) | 5/2 | 5,92 | 5,70 – 6,00 |
| $Fe^{2+}$ | $3d^6$ | $^5D_4$ | 410 | 2 | 4,90 | 5,10 – 5,70 |
| $Co^{3+}$ | $3d^6$ | $^5D_4$ | (580) | 2 | 4,90 | 5,30 |
| $Co^{2+}$ | $3d^7$ | $^4F_{9/2}$ | 533 | 3/2 | 3,87 | 4,30 – 5,20 |
| $Ni^{3+}$ | $3d^7$ | $^4F_{9/2}$ | (715) | 3/2 | 3,87 | |
| $Ni^{2+}$ | $3d^8$ | $^3F_4$ | 649 | 1 | 2,83 | 2,80 – 3,50 |
| $Cu^{2+}$ | $3d^9$ | $^2D_{5/2}$ | 829 | 1/2 | 1,73 | 1,70 – 2,20 |
| $Zn^{2+a)}$ | $3d^{10}$ | $^1S_0$ | | | | 0 |

a) diamagnetisch

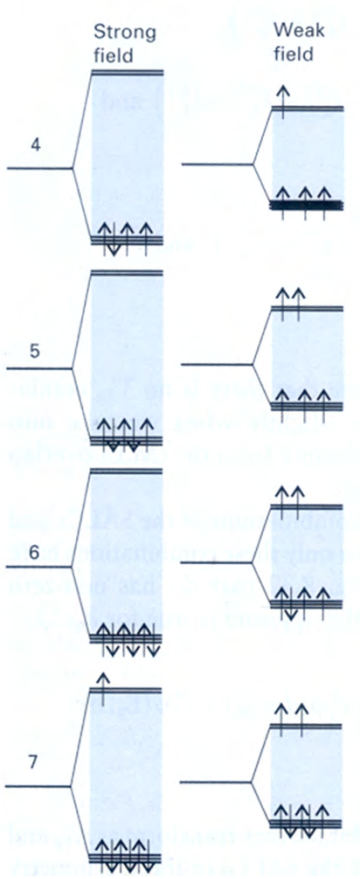


Lueken99, Atkins-PC

# Ch. 1. Introduction

## Section 1.2 Magnetic anisotropy in Transition Metal Clusters



**Quenching of the orbital moment.**

- Orbital angular momentum is generally pictured as a circular motion of electrons around the nucleus.
- The (classical) orbital angular momentum is

$$\vec{l} = \vec{r} \times \vec{p}$$

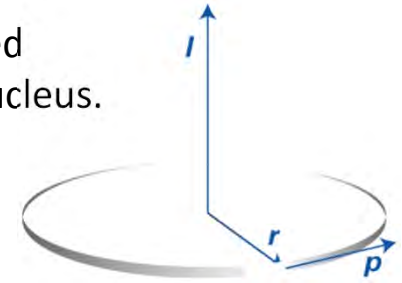


- Translated into quantum mechanics, we can picture orbital angular momentum as being due to a circular motion of the electron through **degenerate** orbitals, that are **related by a rotation.**
- For example:
  - $d_{xz}$ / $d_{xy}$ (x axis)
  - $d_{xy}$ / $d_{x^2-y^2}$ (z axis)
  - $p_x$ / $p_y$ (z axis).

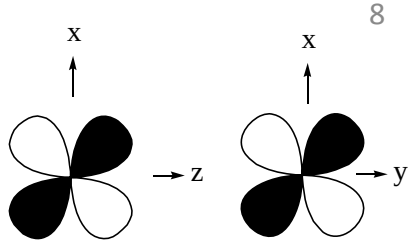


$d_{xz}$ $d_{xy}$

related by 90° rotn. about *x* axis

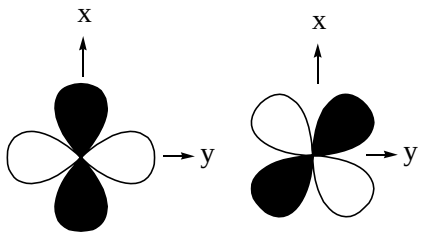


$d_{x^2-y^2}$ $d_{xy}$

related by 45° rotn. about *z* axis

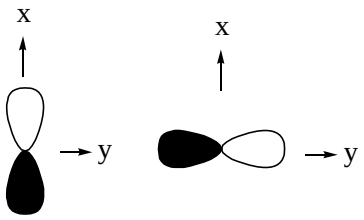


$p_x$ $p_y$

related by 90° rotn. about *z* axis

# Ch. 1. Introduction

## Section 1.2 Magnetic anisotropy in Transition Metal Clusters



**Quenching of the orbital moment.**

- In transition metal complexes, the degeneracy of the d-orbitals is lifted by the interaction with the ligands (crystal/ligand field splitting).
- As a result, the circular motion is no longer possible and the orbital angular momentum disappears.
- For $O_h$ and $T_d$ complexes, only in certain cases an orbital angular momentum is retained

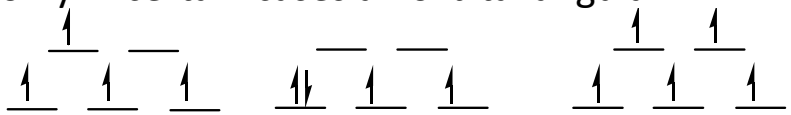

| orbital contribution? | No | Yes | No |
|---|---|---|---|
| ground state type | E | T | A |

- Importantly, in lower symmetry, fewer orbitals are degenerate:

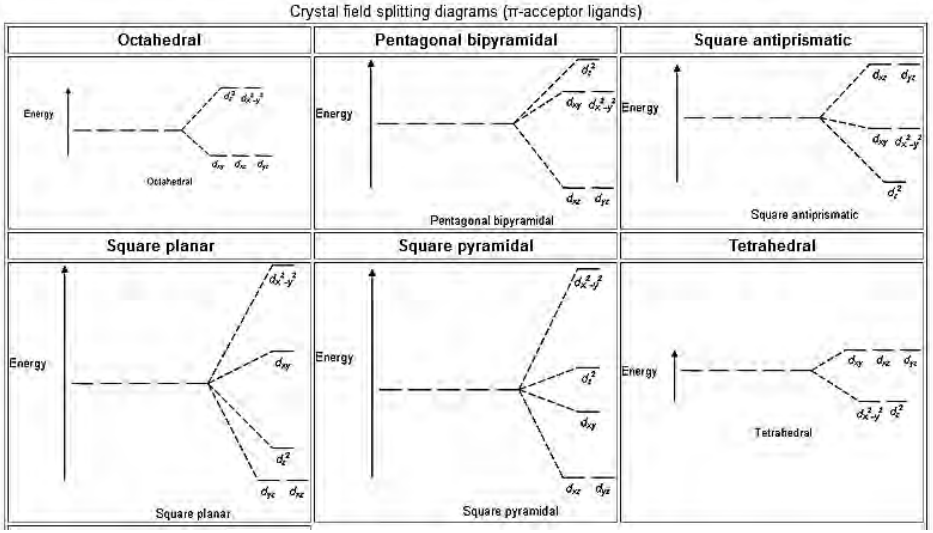


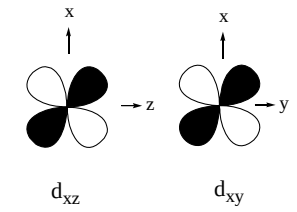


$d_{xz}$ $d_{xy}$

related by 90° rotn. about *x* axis

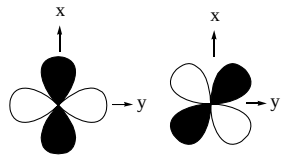


$d_{x^2-y^2}$ $d_{xy}$

related by 45° rotn. about *z* axis

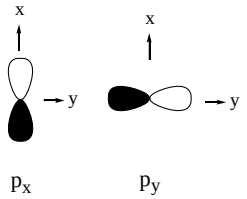


$p_x$ $p_y$

related by 90° rotn. about *z* axis

# Ch. 1. Introduction

## Section 1.2 Magnetic anisotropy in Transition Metal Clusters



**g-Value anisotropy.**

- Spin orbit coupling reintroduces orbital angular momentum (2nd order perturbation).
- Quantitative formula:

$$g_{\alpha\alpha} = g_e + 2\lambda \sum_m \frac{\langle m|\hat{l}_\alpha|0\rangle\langle 0|\hat{l}_\alpha|m\rangle}{E_m - E_0}; \quad g = g_e\mathbf{E} + 2\lambda\mathbf{\Lambda}$$

- $\alpha$ = x, y, or z; $m$ is the excited d-orbital.
- For $d_{xy}$ - $d_{x^2-y^2}$ mixing induced by $l_z$:

$$g_{zz} = g_e + 2\lambda \frac{-2i \times 2i}{E_{xy} - E_{x^2-y^2}} = g_e - \frac{8\lambda}{\left|E_{xy} - E_{x^2-y^2}\right|}$$

- $\lambda > 0$ for $d^1$ $\therefore$ $g_z = g_{||} < g_e$.
- Anisotropy must correspond to point group symmetry.

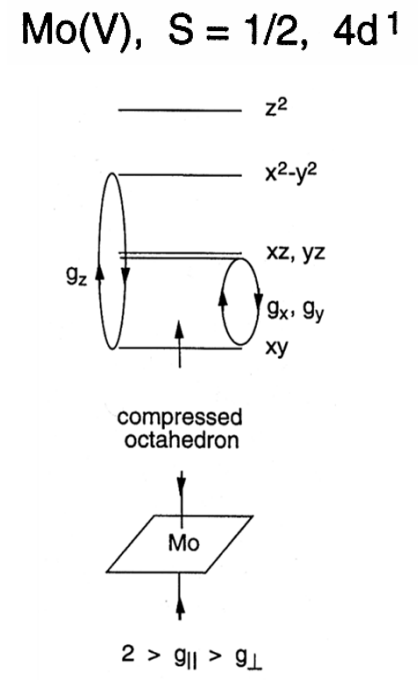


**Table 4.2** [E] Angular momentum operations on the real p and d orbitals

| | $l_x$ | $l_y$ | $l_z$ |
|---|---|---|---|
| $\|x\rangle$ | 0 | $-i\|z\rangle$ | $i\|y\rangle$ |
| $\|y\rangle$ | $i\|z\rangle$ | 0 | $-i\|x\rangle$ |
| $\|z\rangle$ | $-i\|y\rangle$ | $i\|x\rangle$ | 0 |
| $\|x^2-y^2\rangle$ | $-i\|yz\rangle$ | $-i\|xz\rangle$ | $2i\|xy\rangle$ |
| $\|xy\rangle$ | $i\|xz\rangle$ | $-i\|yz\rangle$ | $-2i\|x^2-y^2\rangle$ |
| $\|yz\rangle$ | $i\|x^2-y^2\rangle + \sqrt{3}i\|z^2\rangle$ | $i\|xy\rangle$ | $-i\|xz\rangle$ |
| $\|xz\rangle$ | $-i\|xy\rangle$ | $i\|x^2-y^2\rangle - \sqrt{3}i\|z^2\rangle$ | $i\|yz\rangle$ |
| $\|z^2\rangle$ | $-\sqrt{3}i\|yz\rangle$ | $\sqrt{3}i\|xz\rangle$ | 0 |

Mabbs/Machin; Atherton

# Ch. 1. Introduction

## Section 1.2 Magnetic anisotropy in Transition Metal Clusters



**Types of anisotropy.**

- In transition metals we have three kinds:

1. Zero-field splitting: We can express the **D** tensor in terms of **Λ**.

$$D_{\alpha\alpha} = \lambda^2 \sum_m \frac{\langle m|\hat{l}_\alpha|0\rangle\langle 0|\hat{l}_\alpha|m\rangle}{E_m - E_0}; \quad \mathbf{D} = \lambda^2 \mathbf{\Lambda}$$

$$\mathbf{D} = \begin{pmatrix} D_{xx} & 0 & 0 \\ 0 & D_{yy} & 0 \\ 0 & 0 & D_{zz} \end{pmatrix}$$

$$D = \tfrac{3}{2} D_{zz}, \; E = \tfrac{1}{2} | D_{xx} - D_{yy} |$$

2. g-anisotropy:

$$g_{\alpha\alpha} = g_e + 2\lambda \sum_m \frac{\langle m|\hat{l}_\alpha|0\rangle\langle 0|\hat{l}_\alpha|m\rangle}{E_m - E_0}; \quad g = g_e \mathbf{E} + 2\lambda \mathbf{\Lambda}$$

$$\mathbf{g} = \begin{pmatrix} g_{xx} & 0 & 0 \\ 0 & g_{yy} & 0 \\ 0 & 0 & g_{zz} \end{pmatrix}$$

- Relation between ZFS and g value anisotropy (this relation does not always hold).

$$D = \frac{\lambda}{2}\left[ g_z - \frac{g_x + g_y}{2} \right]$$

$$E = \frac{\lambda}{4}(g_x - g_y)$$

**Table 4.2** [E] Angular momentum operations on the real p and d orbitals

| | $l_x$ | $l_y$ | $l_z$ |
|---|---|---|---|
| $\|x\rangle$ | 0 | $-i\|z\rangle$ | $i\|y\rangle$ |
| $\|y\rangle$ | $i\|z\rangle$ | 0 | $-i\|x\rangle$ |
| $\|z\rangle$ | $-i\|y\rangle$ | $i\|x\rangle$ | 0 |
| $\|x^2-y^2\rangle$ | $-i\|yz\rangle$ | $-i\|xz\rangle$ | $2i\|xy\rangle$ |
| $\|xy\rangle$ | $i\|xz\rangle$ | $-i\|yz\rangle$ | $-2i\|x^2-y^2\rangle$ |
| $\|yz\rangle$ | $i\|x^2-y^2\rangle + \sqrt{3}i\|z^2\rangle$ | $i\|xy\rangle$ | $-i\|xz\rangle$ |
| $\|xz\rangle$ | $-i\|xy\rangle$ | $i\|x^2-y^2\rangle - \sqrt{3}i\|z^2\rangle$ | $i\|yz\rangle$ |
| $\|z^2\rangle$ | $-\sqrt{3}i\|yz\rangle$ | $\sqrt{3}i\|xz\rangle$ | 0 |

3. Anisotropic, antisymmetric exchange interactions

Mabbs/Machin; Atherton; Abragam/Bleaney

# Ch. 1. Introduction

## Section 1.2 Magnetic anisotropy in Transition Metal Clusters



**Zero-Field Splitting in Transition Metal Clusters.**

- The cluster zero-field splitting is a linear combination of:
  - **single-ion** zero-field splittings,
  - **dipolar spin-spin interaction** (usually a minor contribution)

$$\mathbf{D}_S^{si} = \sum_i d_i \mathbf{D}_i + \sum_{i<j} d_{ij} \mathbf{D}_{ij}$$

  - In addition anisotropic and antisymmetric exchange interactions lead to energy splittings in zero field.

**Factors of Importance**

1. **Magnitude and sign of projection coefficients $d_i$.**
2. **Orientation of single ion zero-field splitting.**
3. **Magnitude and sign of single ion zero-field splitting.**

# Ch. 1. Introduction

## Section 1.2 Magnetic anisotropy in Transition Metal Clusters



**Zero-Field Splitting in Transition Metal Clusters.**

**1. Magnitude and sign of projection coefficients $d_i$.**

- Projection coefficients $d_i < 1$.
- For each pairwise coupling $D$ decreases.
- In the end the energy barrier is only linearly dependent on the spin of the ground state:

$$d_i = \frac{S_i(2S_i - 1)}{S(2S - 1)} \qquad \Delta E_{\max} = \left( \sum_{i=1}^{N} \frac{2 - 1/S_i}{2 - 1/S} \right) \left| D^{SI} \right| S_{SI}^2$$

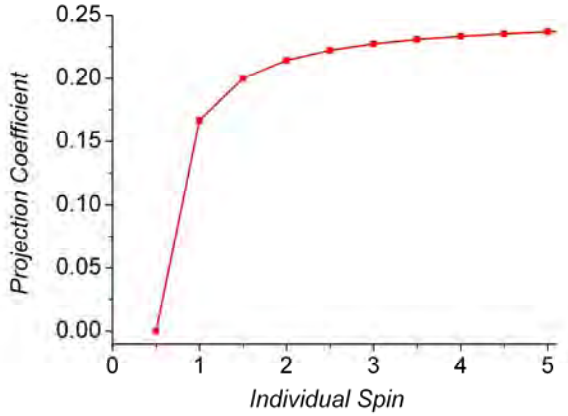


For $S = n \times S_i$ Waldmann, IC,2007; Sessoli, ICA, 2008: "Waldmann's dire prediction" (Hill, DT, 2009)

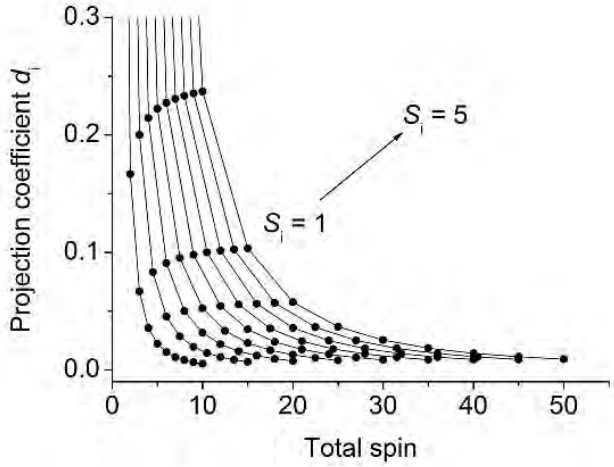


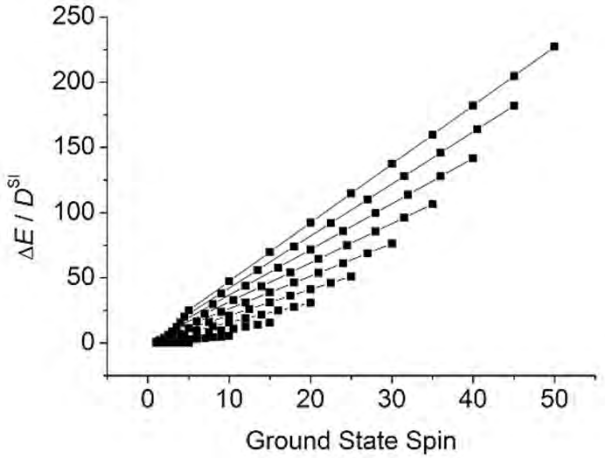

# Ch. 1. Introduction

## Section 1.2 Magnetic anisotropy in Transition Metal Clusters



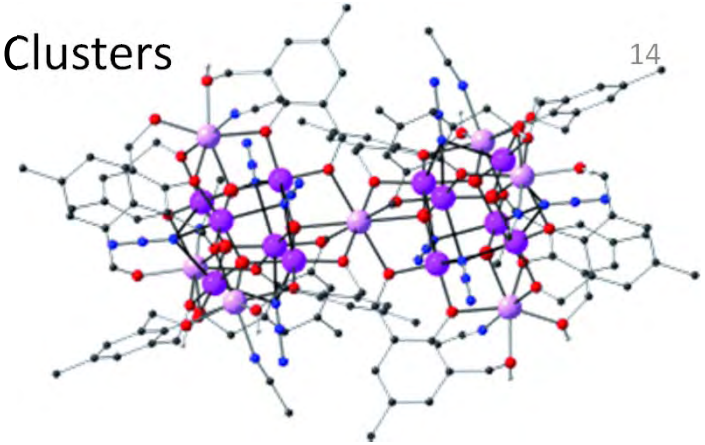

Ako, Powell, ACIE, 2006

**Zero-Field Splitting in Transition Metal Clusters.**

- Example: $Mn_{19}$: $S = 83/2$ but very small $D$. Why?

**2. Orientation of single ion zero-field splitting.**

$$\mathbf{D}_S^{si} = \sum_i d_i \mathbf{D}_i$$

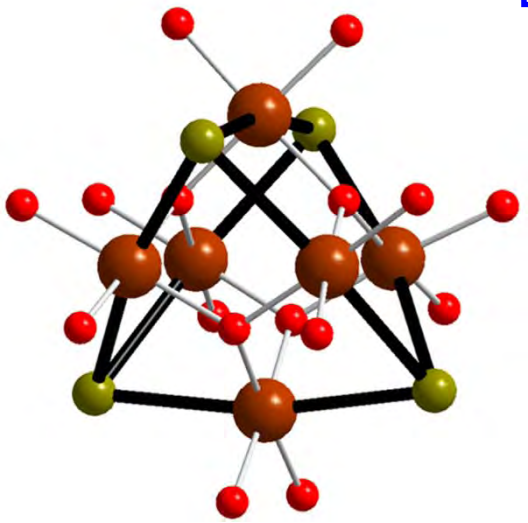

$[Mn_6O_4Br_4(Me_2dbm)_6]$
Aromí, JACS, 99
$S = 12$
$D = 0.009$ cm$^{-1}$

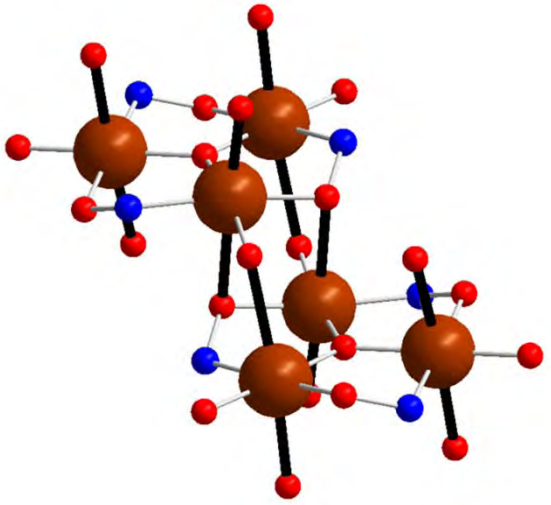

$[Mn_6O_2(sao)_6(O_2CPh)_2(EtOH)_4]$
Milios, JACS, 07
$S = 12$
$D = -0.43$ cm$^{-1}$

# Ch. 1. Introduction

## Section 1.2 Magnetic anisotropy in Transition Metal Clusters



**Energy scales in Transition Metals.**

- Example $Mn^{3+}$, $d^4$ HS

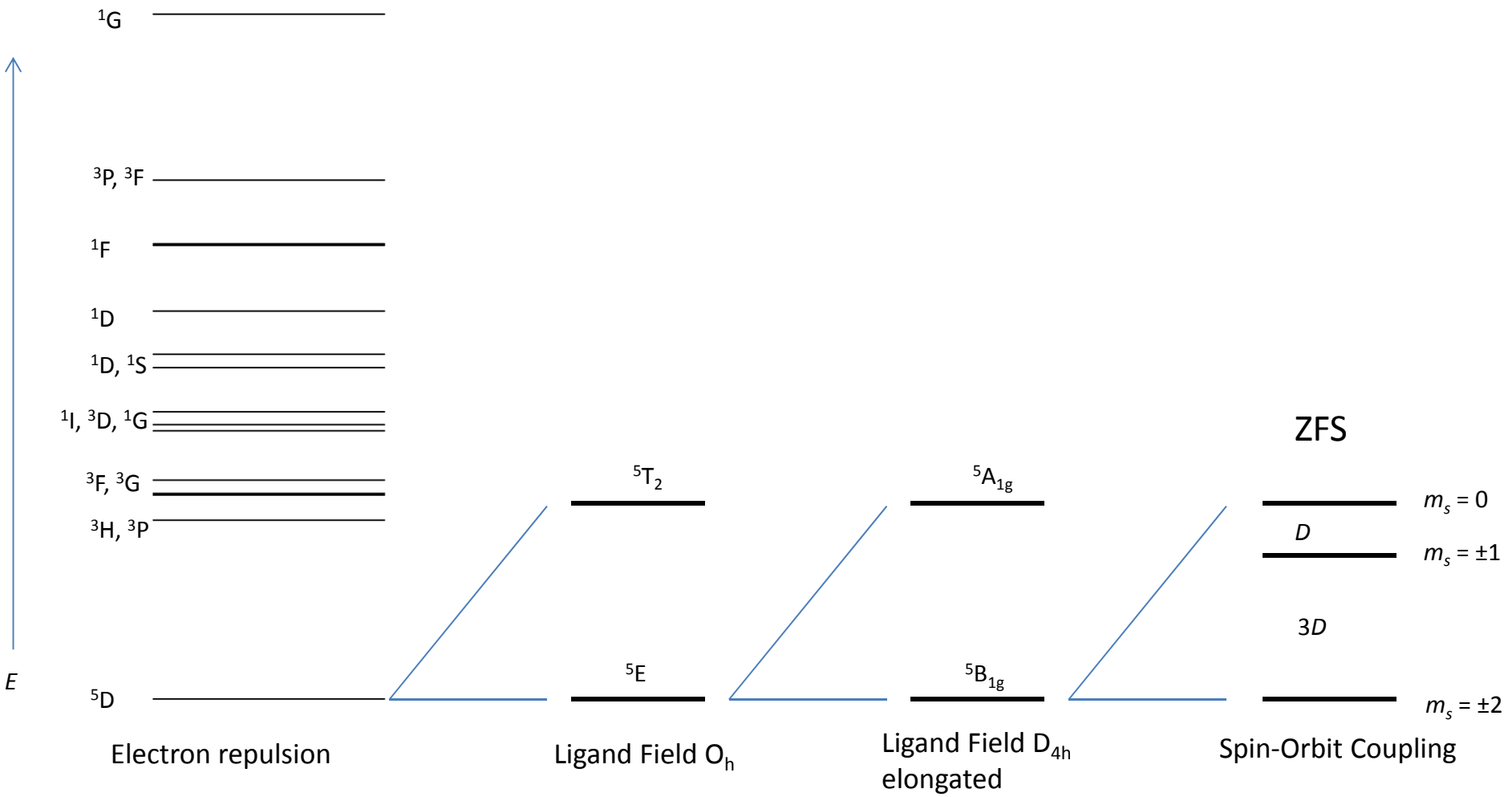

# Ch. 1. Introduction

## Section 1.3 Magnetic anisotropy in f-Elements



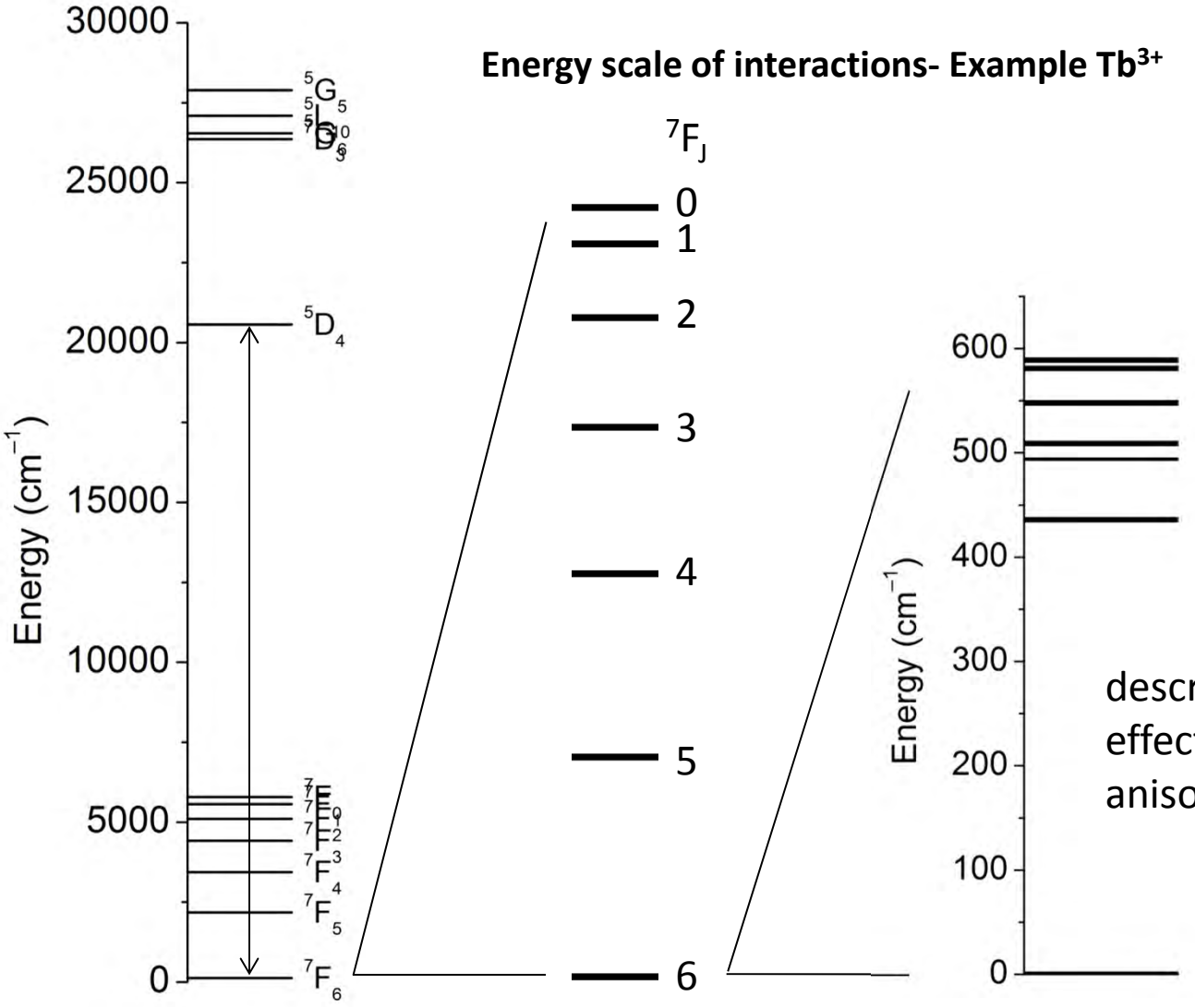

# Ch. 1. Introduction

## Section 1.3 Magnetic anisotropy in f-Elements



**Dieke Diagram**

- Because f-electrons are little influenced by metal-ligand bonding, a general scheme of energy levels in lanthanides can be constructed (Dieke diagram).
- To a first approximation, the energy difference between multiplets that differ in *J* only is due to spin-orbit coupling.
- The energy difference between groups of multiplets that differ in *L* and or *S* is due to electron repulsion.
- Originally obtained by analysis of the optical (absorption/luminescence) spectra of $Ln^{3+}$:$LaCl_3$ and $Ln^{3+}$:$LaF_3$.
- The thickness of the lines indicates the crystal field splitting.

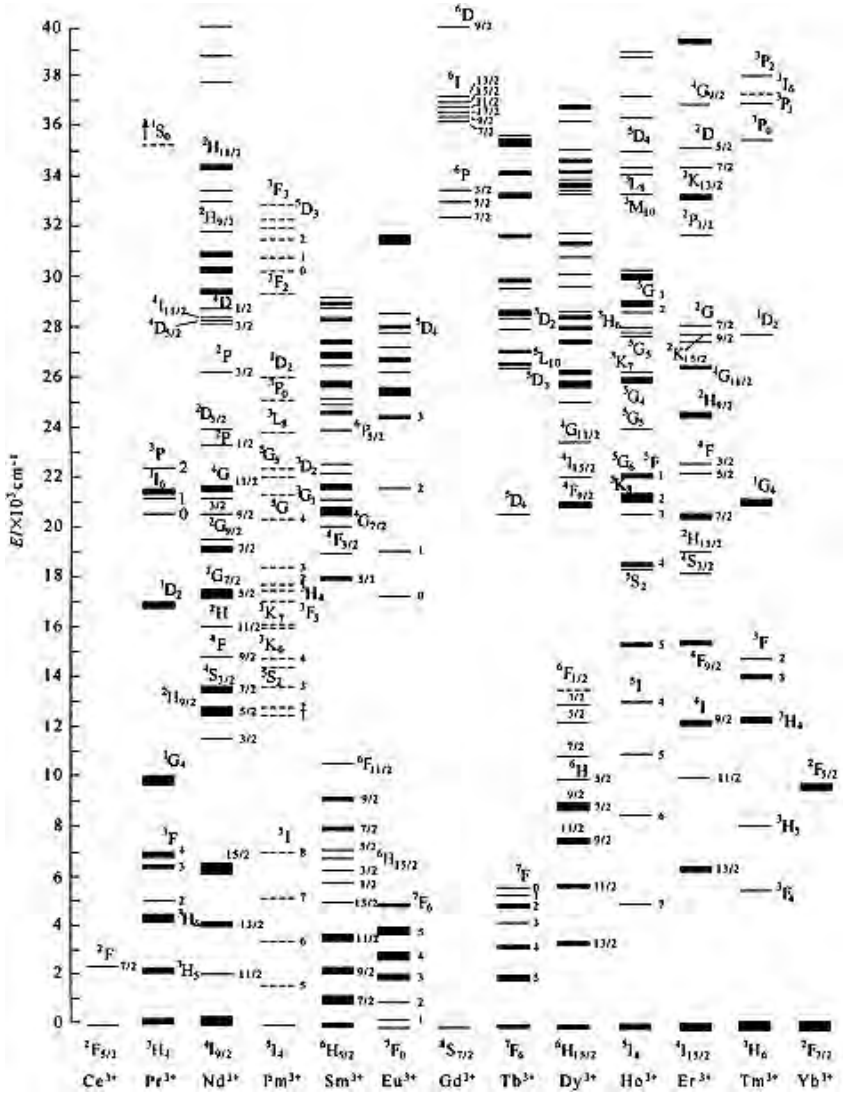

# Ch. 1. Introduction

## Section 1.3 Magnetic anisotropy in f-Elements



**Susceptibility of free ions**

- The susceptibilities of lanthanide compounds at room temperature are often very close to the free ion values.
- Exceptions are $Sm^{3+}$, $Eu^{3+}$ (low lying excited J-multiplets).

Table 2: Lanthanide ions: term symbol (ground state), one-electron spin-orbit coupling parameter $\zeta_{4f}$ [$cm^{-1}$], $g_J$, $g_J J$, $g_J[J(J+1)]^{1/2}$ and $\mu_{eff}^{exp}$(295 K) [7]

| $Ln^{3+}$ | $4f^N$ | $^{2S+1}L_J$ | $\zeta_{4f}$ [a] | $g_J$ | $g_J J$ | $g_J[J(J+1)]^{1/2}$ | $\mu_{eff}^{exp}$ [b] |
|---|---|---|---|---|---|---|---|
| $La^{3+}$ [c] | $4f^0$ | $^1S_0$ | | | | 0 | |
| $Ce^{3+}$ | $4f^1$ | $^2F_{5/2}$ | 625 | 6/7 | 15/7 | 2.535 | 2.3–2.5 |
| $Pr^{3+}$ | $4f^2$ | $^3H_4$ | 758 | 4/5 | 16/5 | 3.578 | 3.4–3.6 |
| $Nd^{3+}$ | $4f^3$ | $^4I_{9/2}$ | 884 | 8/11 | 36/11 | 3.618 | 3.4–3.5 |
| $Pm^{3+}$ | $4f^4$ | $^5I_4$ | 1000 | 3/5 | 12/5 | 2.683 | 2.9 [d] |
| $Sm^{3+}$ | $4f^5$ | $^6H_{5/2}$ | 1157 | 2/7 | 5/7 | 0.845 | 1.6 |
| $Eu^{3+}$ | $4f^6$ | $^7F_0$ | 1326 | 0 | 0 | 0 | 3.5 |
| $Gd^{3+}$ | $4f^7$ | $^8S_{7/2}$ | 1450 | 2 | 7 | 7.937 | 7.8–7.9 |
| $Tb^{3+}$ | $4f^8$ | $^7F_6$ | 1709 | 3/2 | 9 | 9.721 | 9.7–9.8 |
| $Dy^{3+}$ | $4f^9$ | $^6H_{15/2}$ | 1932 | 4/3 | 10 | 10.646 | 10.2–10.6 |
| $Ho^{3+}$ | $4f^{10}$ | $^5I_8$ | 2141 | 5/4 | 10 | 10.607 | 10.3–10.5 |
| $Er^{3+}$ | $4f^{11}$ | $^4I_{15/2}$ | 2369 | 6/5 | 9 | 9.581 | 9.4–9.5 |
| $Tm^{3+}$ | $4f^{12}$ | $^3H_6$ | 2628 | 7/6 | 7 | 7.561 | 7.5 |
| $Yb^{3+}$ | $4f^{13}$ | $^2F_{7/2}$ | 2870 | 8/7 | 4 | 4.536 | 4.5 |
| $Lu^{3+}$ [b] | $4f^{14}$ | $^1S_0$ | | | | 0 | |

[a] The relation between $\zeta_{4f}$ and $\lambda_{LS}$ of the Russell-Saunders ground term is given by $\lambda_{LS} = \pm(\zeta_{4f}/2S)$, where (+) and (−) sign correspond to $N \leq 2l+1$ and $N \geq 2l+1$, respectively.
[b] Definition: $\chi_m = \mu_0 N_A \mu_B^2 \mu_{eff}^2/(3 k_B T)$.
[c] diamagnetic
[d] observed for $Nd^{2+}$ compounds.

# Ch. 1. Introduction

## Section 1.3 Magnetic anisotropy in f-Elements



**Crystal field splitting**

- Going from a free ion to a compound, the symmetry around the f-element ion is lowered, leading to splitting of the states.
- Group theory can be exploited to predict the way in which the terms split (**symmetry aspect**).
- The magnitude of the splitting can be obtained from crystal field theory (purely Coulombic interaction of point dipoles) or ligand field theory (taking into account σ-bonding) (**energy aspect**).

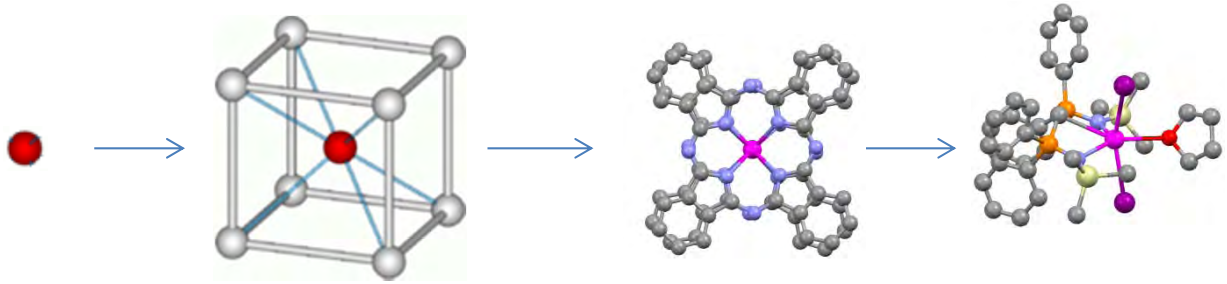

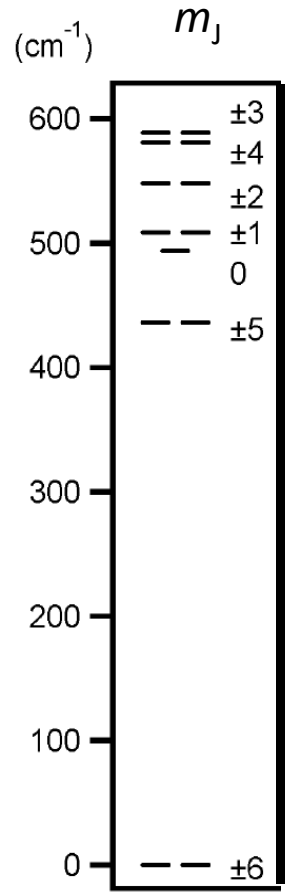

# Ch. 1. Introduction

## Section 1.3 Magnetic anisotropy in f-Elements



**Crystal field splitting: Stevens operator equivalents**

- We can write the electrostatic potential created by the ligands as an expansion in terms of spherical harmonics.
- The resulting operators act on each f-electron separately, hence for each state $|J\ M_J\rangle$, the corresponding wavefunction must be determined. This is rather complicated.
- In order to reproduce the splittings, we can **replace** the coordinates in the spherical harmonics by angular momentum operator components, which have simple properties.
- $x \to \hat{J}_x,\ y \to \hat{J}_y,\ z \to \hat{J}_z,\ r \to \sqrt{J(J+1)}$
- To take into account the noncommutation between the angular momentum operators, we have to form symmetrized products, e.g. $xy \to \frac{1}{2}\left(\hat{J}_x\hat{J}_y + \hat{J}_y\hat{J}_x\right)$
- We end up with a Hamiltonian of the form

f-electrons

$$\hat{H}_{LF} = \sum_{q=-2}^{+2} B_2^q \hat{O}_2^q + \sum_{q=-4}^{+4} B_4^q \hat{O}_4^q + \sum_{q=-6}^{+6} B_6^q O_6^q$$

d-electrons

- The parameters $B_k^q$ are taken as free parameters

Lueken; Boča

# Ch. 1. Introduction

## Section 1.3 Magnetic anisotropy in f-Elements



**Crystal field splitting: Stevens operator equivalents**

- A table of common Stevens operator equivalents and the related spherical harmonics

$$Y_0^2 = \sqrt{\frac{5}{16\pi}}\frac{3z^2 - r^2}{r^2} \qquad \hat{O}_2^0 = 3\hat{J}_z^2 - J(J+1)$$

$$Y_{\pm 2}^2 = \sqrt{\frac{15}{32\pi}}\frac{(x \pm iy)^2}{r^2} \qquad \hat{O}_2^2 = \tfrac{1}{2}\left(\hat{J}_+^2 + \hat{J}_-^2\right)$$

shift operators $\left(\hat{J}_\pm = \hat{J}_x \pm i\hat{J}_y\right)$

$$Y_0^4 = \sqrt{\frac{9}{256\pi}}\frac{35z^4 - 30z^2r^2 + 3r^4}{r^4} \qquad \hat{O}_4^0 = 35\hat{J}_z^4 + \left(25 - 30J(J+1)\right)\hat{J}_z^2 - 6J(J+1) + 3J^2(J+1)^2$$

$$Y_{\pm 4}^4 = \sqrt{\frac{315}{512\pi}}\frac{(x \pm iy)^4}{r^4} \qquad \hat{O}_4^4 = \tfrac{1}{2}\left(\hat{J}_+^4 + \hat{J}_-^4\right)$$

- The properties of the angular momentum operators.

$$\hat{\mathbf{J}}^2 \mid J\ m_J > \ = J(J+1) \mid J\ m_J >$$

$$\hat{J}_z \mid J\ m_J > \ = m_J \mid J\ m_J >$$

$$\hat{J}_+ \mid J\ m_J > \ = \sqrt{J(J+1) - m_J(m_J+1)}\ \mid J\ m_J + 1 >$$

$$\hat{J}_- \mid J\ m_J > \ = \sqrt{J(J+1) - m_J(m_J-1)}\ \mid J\ m_J - 1 >$$

Lueken; Abragam, Bleany.

# Ch. 1. Introduction

## Section 1.3 Magnetic anisotropy in f-Elements



**Crystal field splitting: Symmetry**

- Furthermore, the CF Hamiltonian must have the same symmetry as the complexed ion.
- Hence, with increasing symmetry, more terms must be zero by symmetry
- For example in $D_{4d}$ symmetry, the crystal field Hamiltonian reads: $\hat{H}_{CF} = B_2^0\hat{O}_2^0 + B_4^0\hat{O}_4^0 + B_6^0\hat{O}_6^0$
- A Table of nonzero CF parameters in different symmetries,
  ± means parameters with both +q and –q are nonzero.

| *k* | *\|q\|* | $D_{2h}$ | $D_{3h}$ | $D_{4h}$ | $D_{\infty h}$ | $D_{2d}$ | $D_{4d}$ | $C_{2v}$ | $C_{3v}$ | $C_{4v}$ | $C_{\infty v}$ | $C_{2h}$ | $C_{3h}$ | $C_{4h}$ | $C_2$ | $S_4$ | $C_1$ |
|---|---|---|---|---|---|---|---|---|---|---|---|---|---|---|---|---|---|
| 2 | 0 | + | + | + | + | + | + | + | + | + | + | + | + | + | + | + | + |
| 2 | 1 | | | | | | | | | | | | | | | | ± |
| 2 | 2 | + | | | | | | + | | | | ± | | | ± | | ± |
| 4 | 0 | + | + | + | + | + | + | + | + | + | + | + | + | + | + | + | + |
| 4 | 1 | | | | | | | | | | | | | | | | ± |
| 4 | 2 | + | | | | | | + | | | | ± | | | ± | | ± |
| 4 | 3 | | | | | | | | + | | | | | | | | ± |
| 4 | 4 | + | | + | | + | | + | | + | | ± | | ± | ± | ± | ± |
| 6 | 0 | + | + | + | + | + | + | + | + | + | + | + | + | + | + | + | + |
| 6 | 1 | | | | | | | | | | | | | | | | ± |
| 6 | 2 | + | | | | | | + | | | | ± | | | ± | | ± |
| 6 | 3 | | | | | | | | + | | | | | | | | ± |
| 6 | 4 | + | | + | | + | | + | | + | | ± | | ± | ± | ± | ± |
| 6 | 5 | | | | | | | | | | | | | | | | ± |
| 6 | 6 | + | + | | | | | + | + | | | ± | ± | | ± | | ± |

H. Lueken; Newman/Ng; C. Görller-Wallrand

# Ch. 1. Introduction

## Section 1.3 Magnetic anisotropy in f-Elements



**Crystal field splitting: Kramers Theorem**

- Whatever the symmetry, for an odd number of electrons, all microstates are doubly degenerate, in the absence of a magnetic field.
- This is known as Kramers' theorem, and ions with half integer angular momentum ground states are called Kramers ions.
- This degeneracy has major implications for spin dynamics, in that quantum tunnelling cannot be induced by the crystal field.

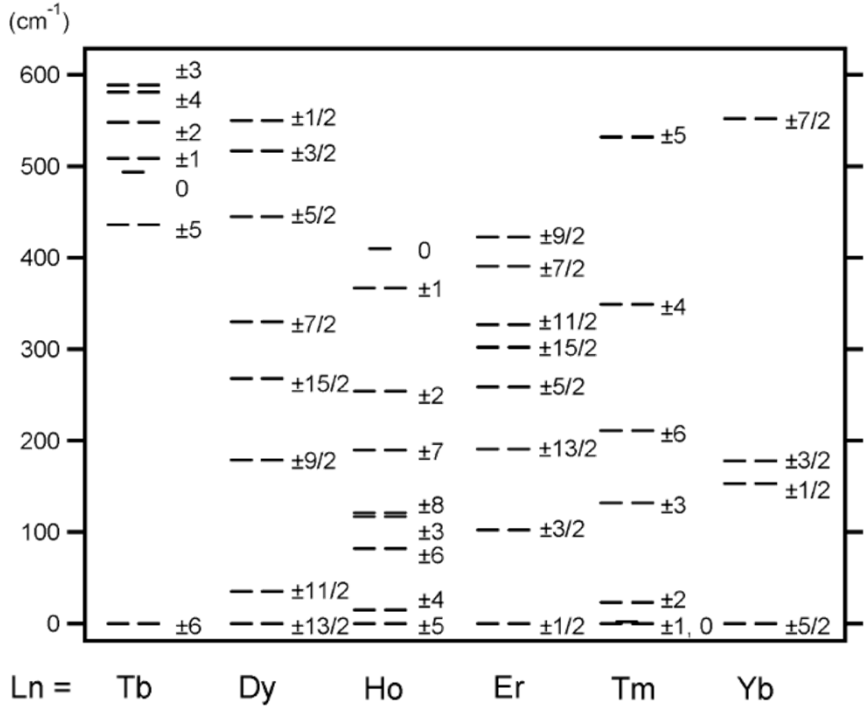


H. Lueken; Abragam/Bleaney

# Ch. 1. Introduction

## Section 1.3 Magnetic anisotropy in f-Elements



**Crystal field splitting: Crystal quantum number**

- A crystal field interaction term $B_k^q \hat{O}_k^q$ will mix $m_J$ states only if $m_J - m_J' = q$.
- We can define a new quantum number, the crystal quantum number μ to designate a group of states satisfying $m_J = \mu$ (mod $q$), i.e. $m_J = \mu + n$ q ($n$ = integer).
- For even numbers of electrons:

$$
\begin{aligned}
q = 2: &\quad \mu = 0^+, 0^-, 1^+, 1^-; \\
q = 3: &\quad \mu = 0^+, 0^-, \pm 1; \\
q = 4: &\quad \mu = 0^+, 0^-, \pm 1;, 2^+, 2^-; \\
q = 5: &\quad \mu = 0^+, 0^-, \pm 1, \pm 2; \\
q = 6: &\quad \mu = 0^+, 0^-, \pm 1, \pm 2, 3^+, 3^-.
\end{aligned}
$$

For odd numbers of electrons:

$$
\begin{aligned}
q = 2: &\quad \mu = \pm\tfrac{1}{2}; \\
q = 3: &\quad \mu = \pm\tfrac{1}{2}, \pm\tfrac{3}{2}; \\
q = 4: &\quad \mu = \pm\tfrac{1}{2}, \pm\tfrac{3}{2}; \\
q = 5: &\quad \mu = \pm\tfrac{1}{2}, \pm\tfrac{3}{2}, \pm\tfrac{5}{2}; \\
q = 6: &\quad \mu = \pm\tfrac{1}{2}, \pm\tfrac{3}{2}, \pm\tfrac{5}{2}.
\end{aligned}
$$

- For odd numbers of electrons, there is a one-to-one correspondence with the irreducible representations that the states belong to.
- For even numbers of electrons, the groups of states can contain states belonging to two different irreducible representations, which can be distinguished using $0^+$, $0^-$ and $1^+$, $1^-$.
- ±μ states are degenerate

Wybourne; Goerller-Wallrand

# Ch. 1. Introduction

## Section 1.3 Magnetic anisotropy in f-Elements



**Crystal field splitting: Crystal field ground states**

- The shape of the electron distribution is different for the different CF states.
- Hence by choosing the ligands, one can influence the CF state energies.
- Hence different ground states can be obtained.
- The ground state and the energy splittings can be influenced by judicious choice of the ligands
- Note that the $m_J$ states are the eigenstates only in $C_{\infty v}$, $D_{\infty h}$ and $D_{4d}$ symmetries.

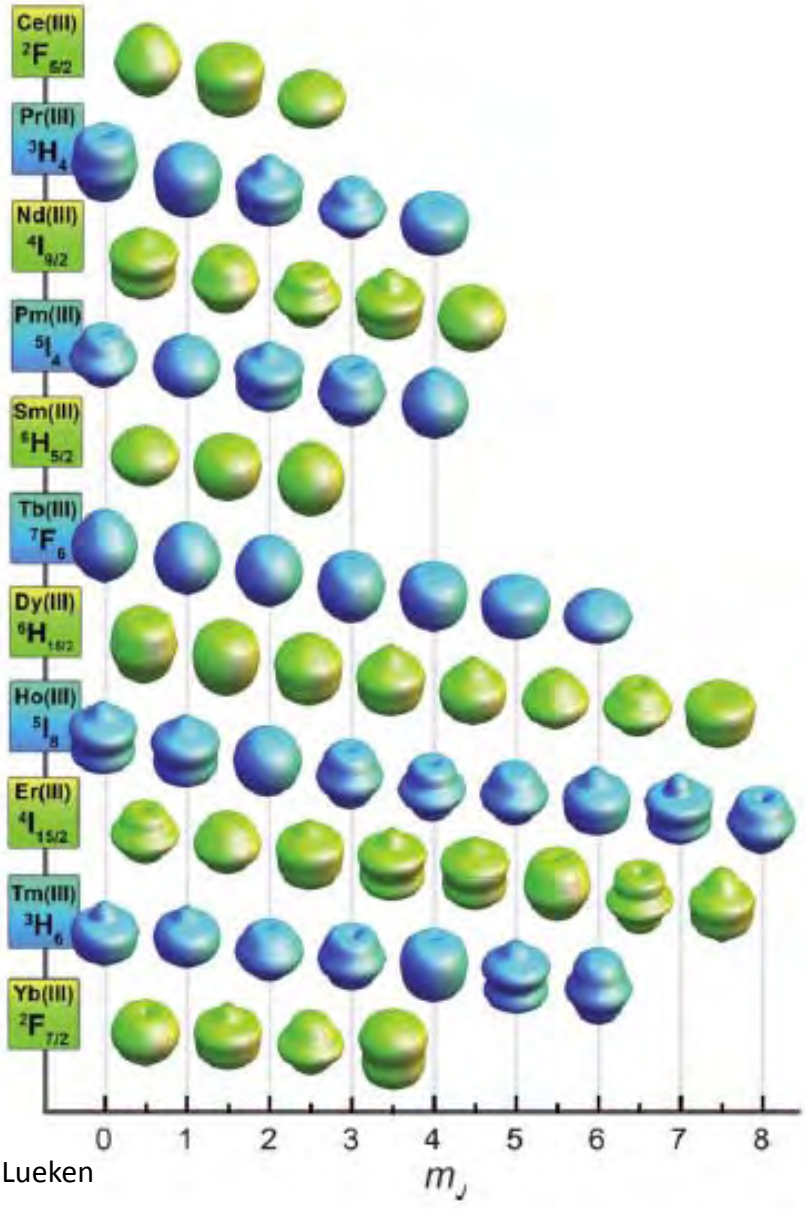


J. Sievers, Z. Phys. B, 45, 289 (1982), J.D. Rinehart, Chem. Sci., 2, 2078 (2011); Lueken

# Ch. 1. Introduction

## Section 1.3 Magnetic anisotropy in f-Elements



**Magnetic and spectroscopic measurements**

- The magnetic susceptibility is the thermal average of the contributions due to the occupied microstates.
- Luminescence spectroscopy allows direct determination of the splitting of the ground Russell-Saunders multiplet.
- Absorption/MCD spectroscopy allows determination of CF splittings of excited states: beyond Russell-Saunders coupling. (intermediate coupling: CF and SOC at same level)
- Far infrared/inelastic neutron scattering allows investigation of intramultiplet excitations.

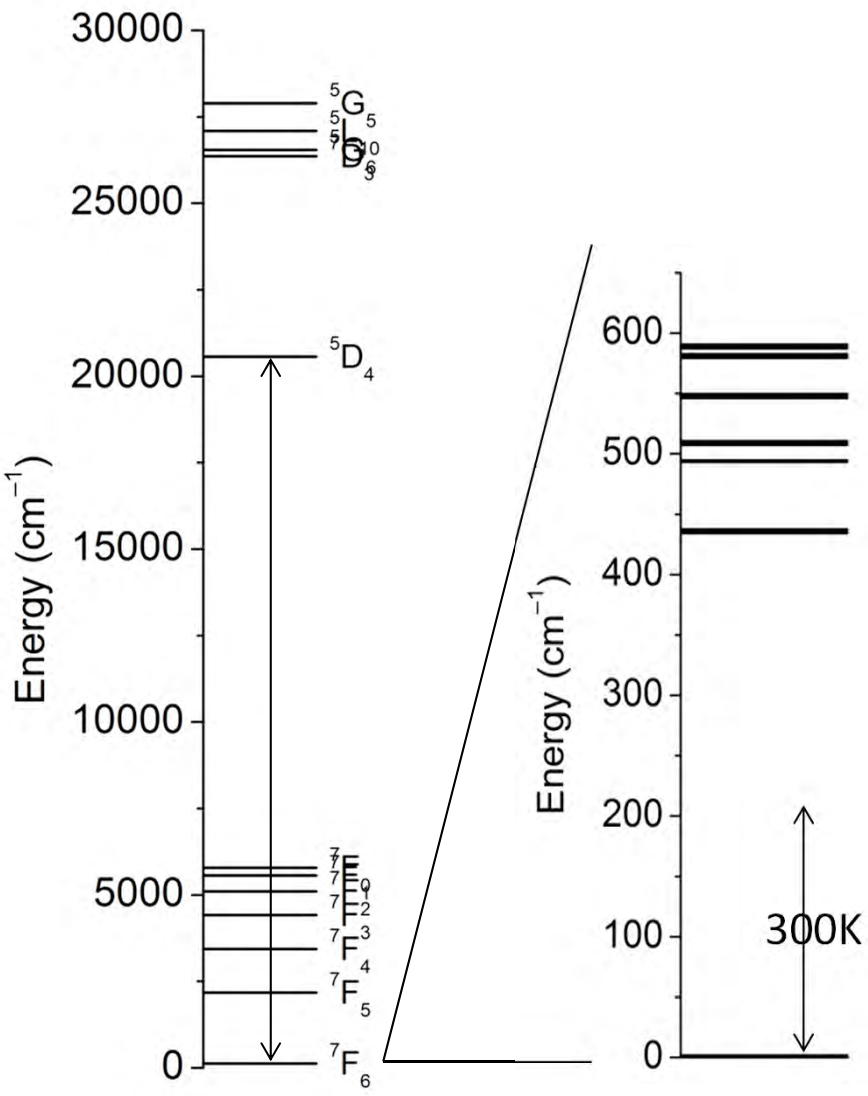

1. Introduction
2. Single Crystal Magnetometry
3. High-Frequency EPR Spectroscopy
4. Inelastic Neutron Scattering
5. Electronic Absorption and Luminescence

# Ch. 2. Single Crystal Magnetometry



**Contents**

# Ch. 2. Single Crystal Magnetometry

## Section 2.1 Motivation



- Determination of the molecular principal axes
- magneto-relations
- Possibility of ground state determination $g_{//}^{eff} = 2g_J \left\langle \pm J_z \left| \hat{J}_z \right| \pm J_z \right\rangle$

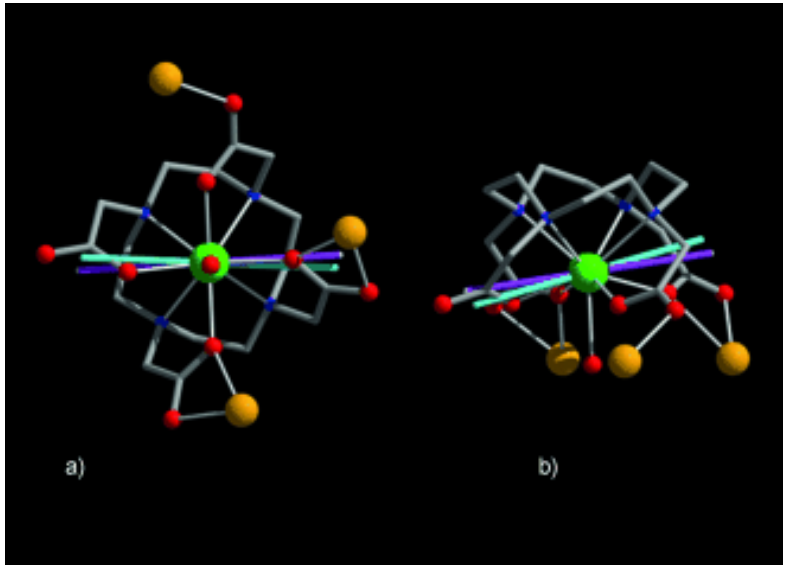


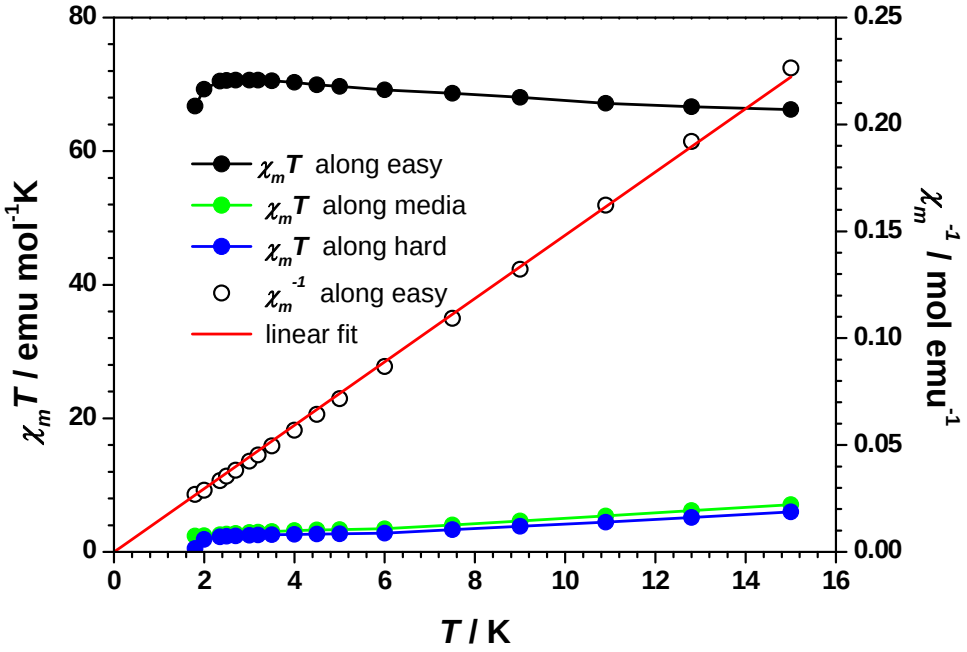


R. Sessoli,*et al, Angew Chem Int Ed* 2012, 164, 1238;

S.-D. Jiang, X.-Y. Wang,*unpublished*;

# Ch. 2. Single Crystal Magnetometry

## Section 2.2 magnetic susceptibility tensor



- Molecular $\chi$ tensor relation: $$\chi_{ij}^{m_q} = \left(A_p^q\right)\chi_{ij}^{m_p}\left(A_p^q\right)^{\dagger}$$

- In the paramagnetic limit, crystal behavior is the sum of all the molecules' one in the unit cell, so is $\chi$ tensor; $$\chi_{ij}^{Cry} = \sum_q \chi_{ij}^{m_q} = \sum_q \left(A_p^q\right)\chi_{ij}^{m_p}\left(A_p^q\right)^{\dagger}$$

- In the paramagnetic limit, the molecular $\chi$ tensor can be fully determined only when **the molecule symmetry is not lower than the crystal symmetry**:

(a) Only one symmetrically independent molecule in the unit cell;

(b1) The molecules are related by inversion center (P-1 space group) or

(b2) The molecule is at highest symmetry position;

Neumann's Principle:

*the symmetry elements of any physical property of a crystal must include all the symmetry elements of the point group of the crystal*

# Ch. 2. Single Crystal Magnetometry

Section 2.3 Determination



**(0) large enough single crystal**

- The background of the rotator provided by Quantum Design MPMS-XL SQUID is around $10^{-4}$ emu;
- The crystal should be larger than 0.5 mg;

**(1) Face index**

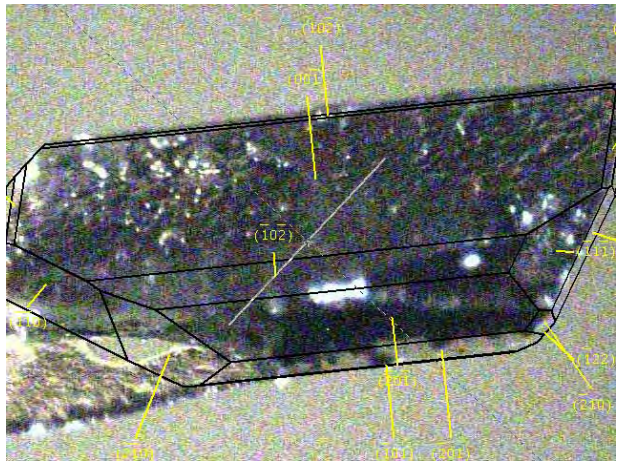

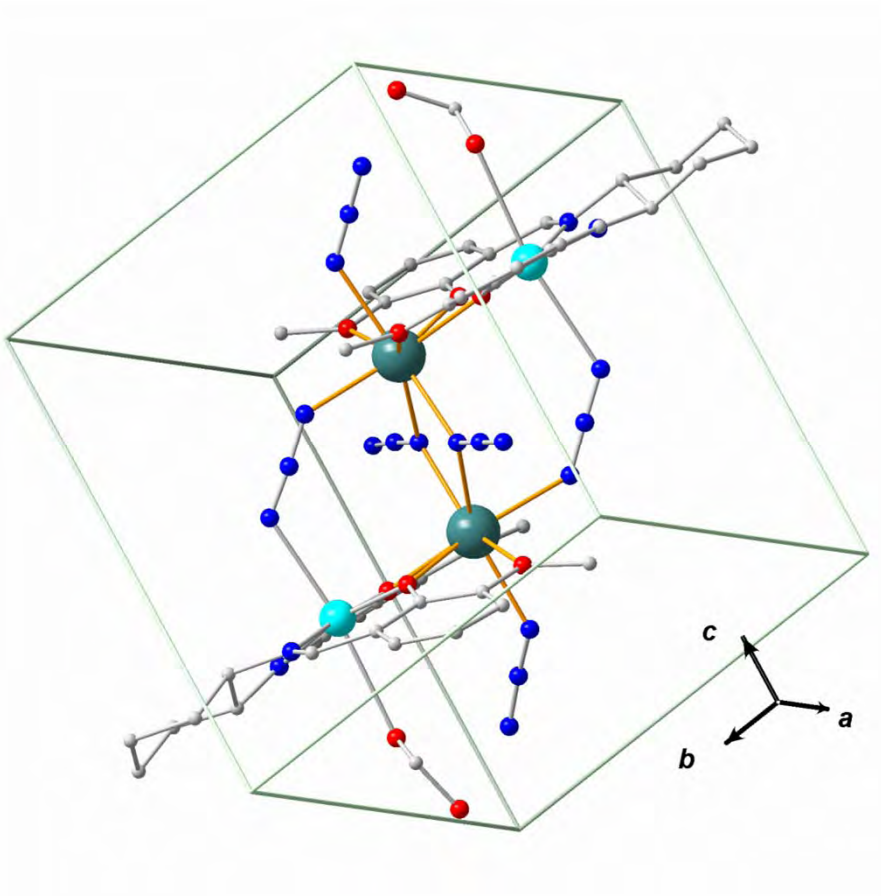

# Ch. 2. Single Crystal Magnetometry

Section 2.3 Determination



**(2) Define the experimental space**

- b as X axis;
- (001) is XY plane;
- Z follows right hand rule;

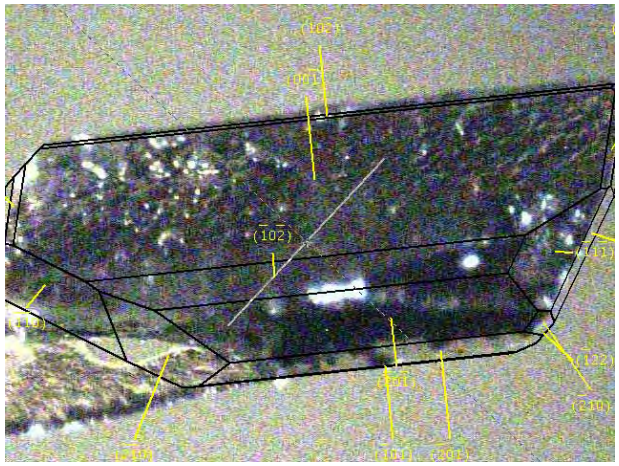

**(3) Transformation matrix**

- Derive the abc unit vector into the same length!
- High school geometry game
- Complicated!

$$\begin{pmatrix} \vec{a} \\ \vec{b} \\ \vec{c} \end{pmatrix} = \begin{pmatrix} 1.78 & 9.41 & 0 \\ 11.93 & 0 & 0 \\ 2.40 & 0.71 & 12.18 \end{pmatrix} \begin{pmatrix} \vec{X} \\ \vec{Y} \\ \vec{Z} \end{pmatrix}$$

# Ch. 2. Single Crystal Magnetometry

Section 2.3 Determination



**(4) Mount the crystal**

- L shaped Cu-Be support: small background;
- Fixed with Apiezon N-grease;

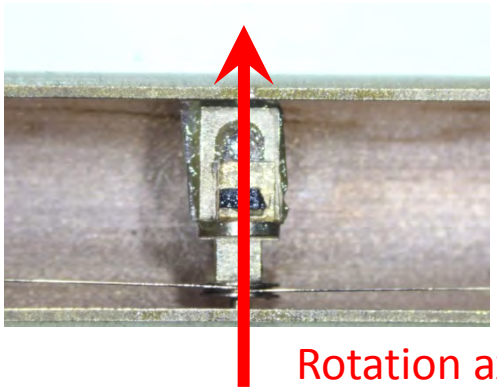


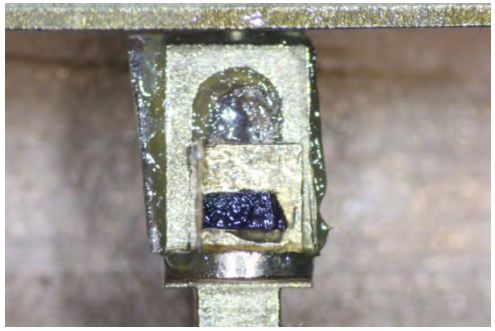

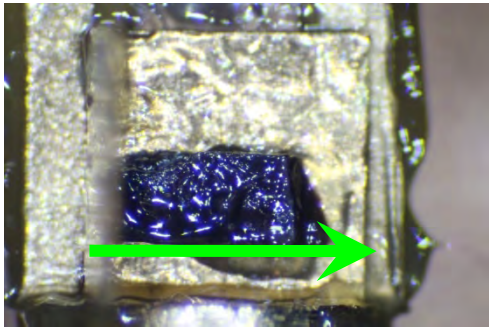


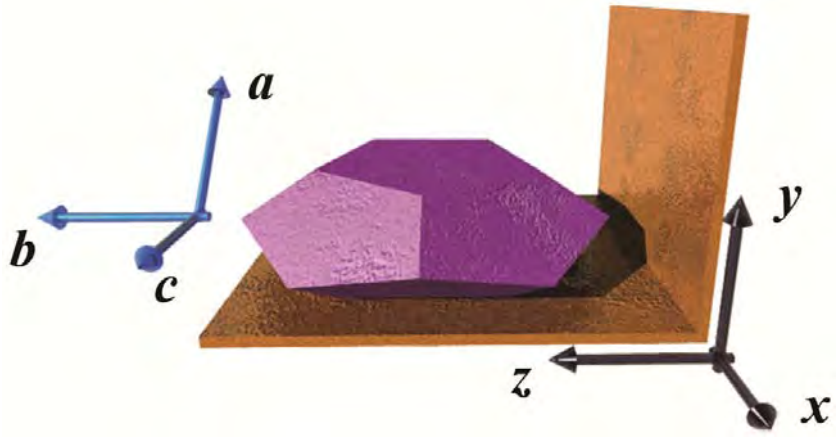


This abc-XYZ relation is not the one defined before

# Ch. 2. Single Crystal Magnetometry

Section 2.3 Determination



## (5) Three orthogonal rotations

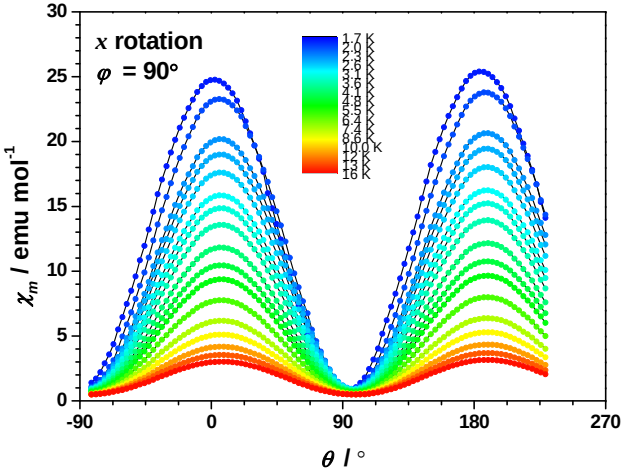


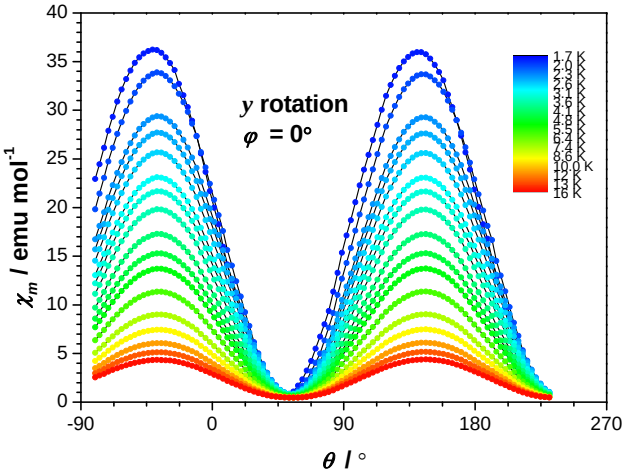


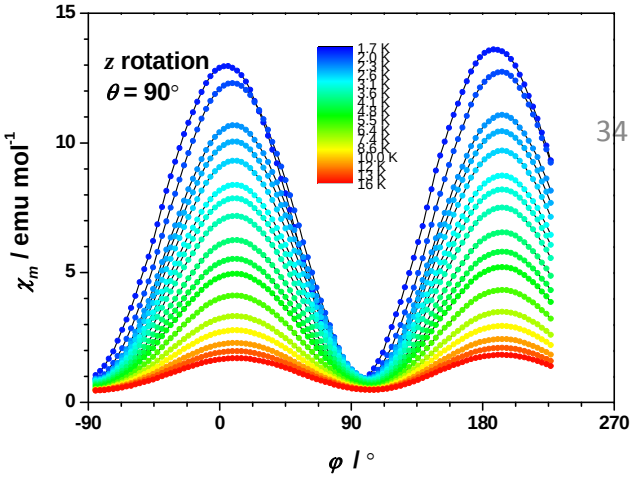


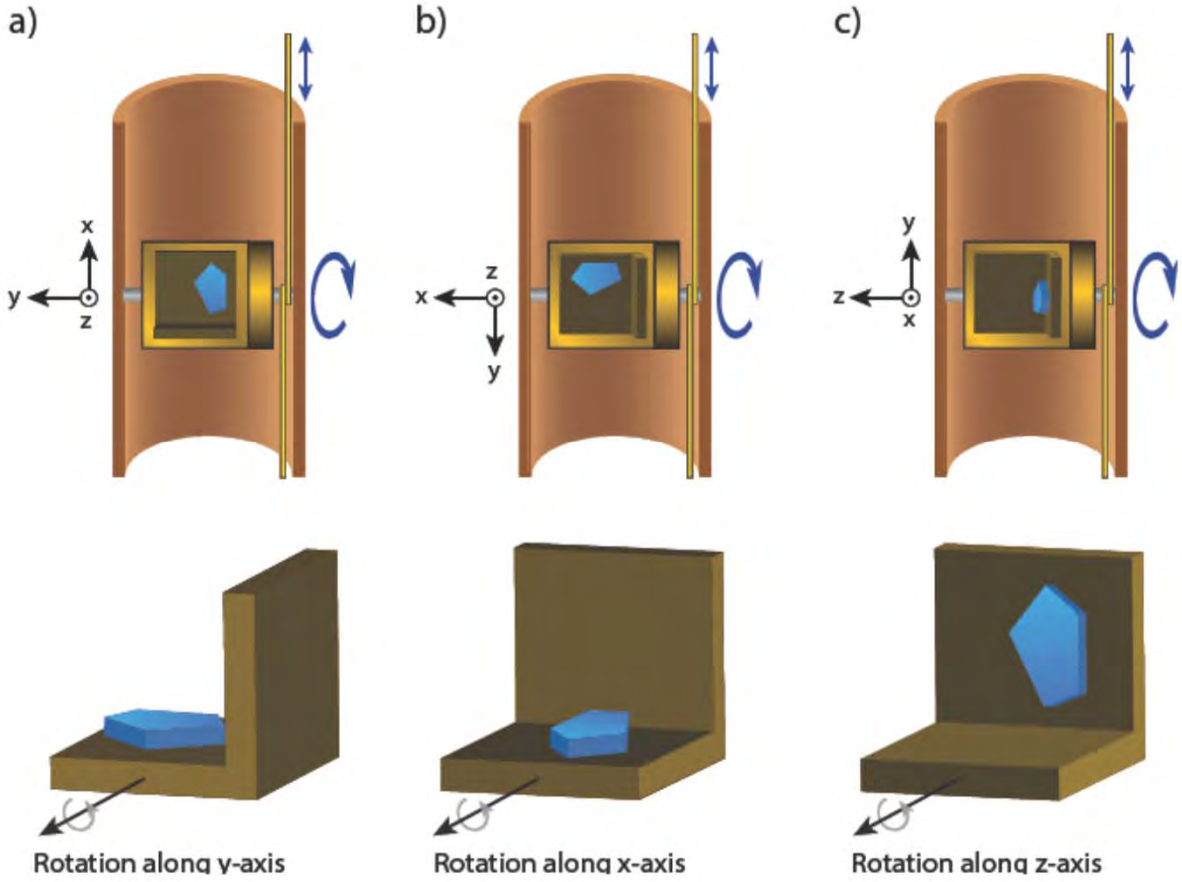

# Ch. 2. Single Crystal Magnetometry

Section 2.3 Determination



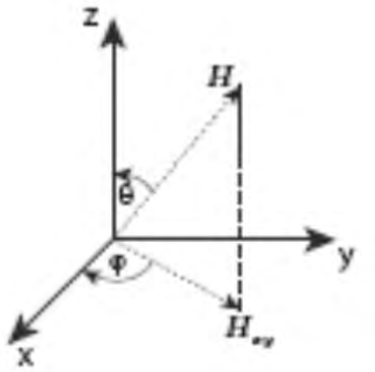


## (6) Fitting the $\chi$ tensor elements

$$M = H_0 \begin{pmatrix} \sin\theta\cos\varphi \\ \sin\theta\sin\varphi \\ \cos\theta \end{pmatrix}^T \begin{pmatrix} \chi_{xx} & \chi_{xy} & \chi_{xz} \\ \chi_{yx} & \chi_{yy} & \chi_{yz} \\ \chi_{zx} & \chi_{zy} & \chi_{zz} \end{pmatrix} \begin{pmatrix} \sin\theta\cos\varphi \\ \sin\theta\sin\varphi \\ \cos\theta \end{pmatrix}$$

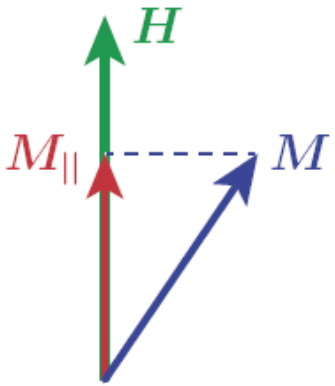


Surface fitting with two variables

$$\begin{aligned} \chi = \frac{M}{H_0} = {} & \chi_{xx}\sin^2\theta\cos^2\varphi + \chi_{yy}\sin^2\theta\sin^2\varphi + \chi_{zz}\cos^2\theta \\ & + 2\chi_{xy}\sin^2\theta\cos\varphi\sin\varphi + 2\chi_{xz}\cos\theta\sin\theta\cos\varphi \\ & + 2\chi_{yz}\cos\theta\sin\theta\sin\varphi\,. \end{aligned}$$

$$\begin{aligned} \chi_x(\delta) &= \chi_{yy}\cos^2(\delta) + \chi_{zz}\sin^2(\delta) + 2\chi_{yz}\sin(\delta)\cos(\delta)\,, \\ \chi_y(\delta) &= \chi_{xx}\sin^2(\delta) + \chi_{zz}\cos^2(\delta) - 2\chi_{xz}\sin(\delta)\cos(\delta)\,, \\ \chi_z(\delta) &= \chi_{xx}\sin^2(\delta) + \chi_{yy}\cos^2(\delta) + 2\chi_{xy}\sin(\delta)\cos(\delta)\,. \end{aligned}$$

Curve fitting with one variables (three functions parallelly)

# Ch. 2. Single Crystal Magnetometry

Section 2.3 Determination



**(7) Symmetry and equivalent considerations**

- Neuman's principle: ***b*** of monoclinic system is always one of the principal axes
- **equivalent positions**

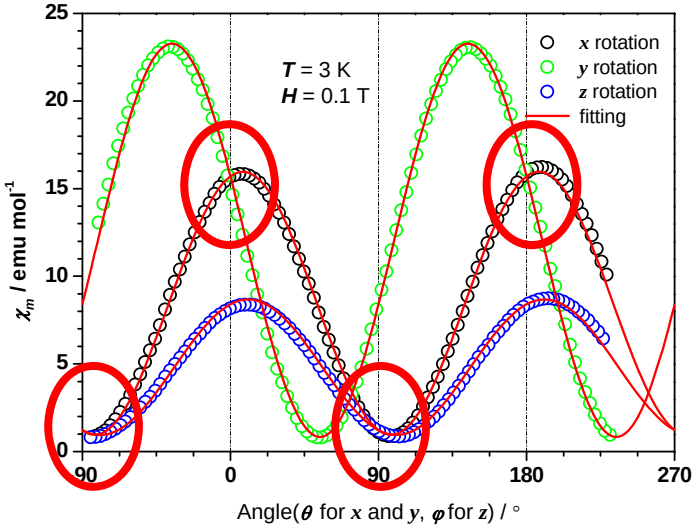


$$\begin{pmatrix} 8.40 & 1.43 & -10.61 \\ 1.43 & 1.22 & -1.96 \\ -10.61 & -1.96 & 15.7019 \end{pmatrix}$$

$\chi$ tensor in XYZ space

# Ch. 2. Single Crystal Magnetometry

## Section 2.3 Determination



### (8) Diagonalization

Fitting results $\begin{pmatrix} 8.40 & 1.43 & -10.61 \\ 1.43 & 1.22 & -1.96 \\ -10.61 & -1.96 & 15.7019 \end{pmatrix}$

Diagonalization

$\begin{pmatrix} 23.54 & & \\ & 0.96 & \\ & & 0.82 \end{pmatrix}$

eigenvalues

{-0.577552,-0.108217,0.809149}

{-0.104866,-0.973128,-0.204999}

{-0.80959,0.20325,-0.550684}

eigenvectors in XYZ

Eigenvectors in abc

{-0.0164857,-0.0593218,0.0664437}

{-0.102119,0.00984252,-0.0168336}

{0.0249881,-0.0625164,-0.0452197}

$$\begin{pmatrix} \vec{a} \\ \vec{b} \\ \vec{c} \end{pmatrix} = \begin{pmatrix} 1.78 & 9.41 & 0 \\ 11.93 & 0 & 0 \\ 2.40 & 0.71 & 12.18 \end{pmatrix} \begin{pmatrix} \vec{X} \\ \vec{Y} \\ \vec{Z} \end{pmatrix}$$

# Ch. 2. Single Crystal Magnetometry

Section 2.3 Determination



**(9) expressed in abc space**

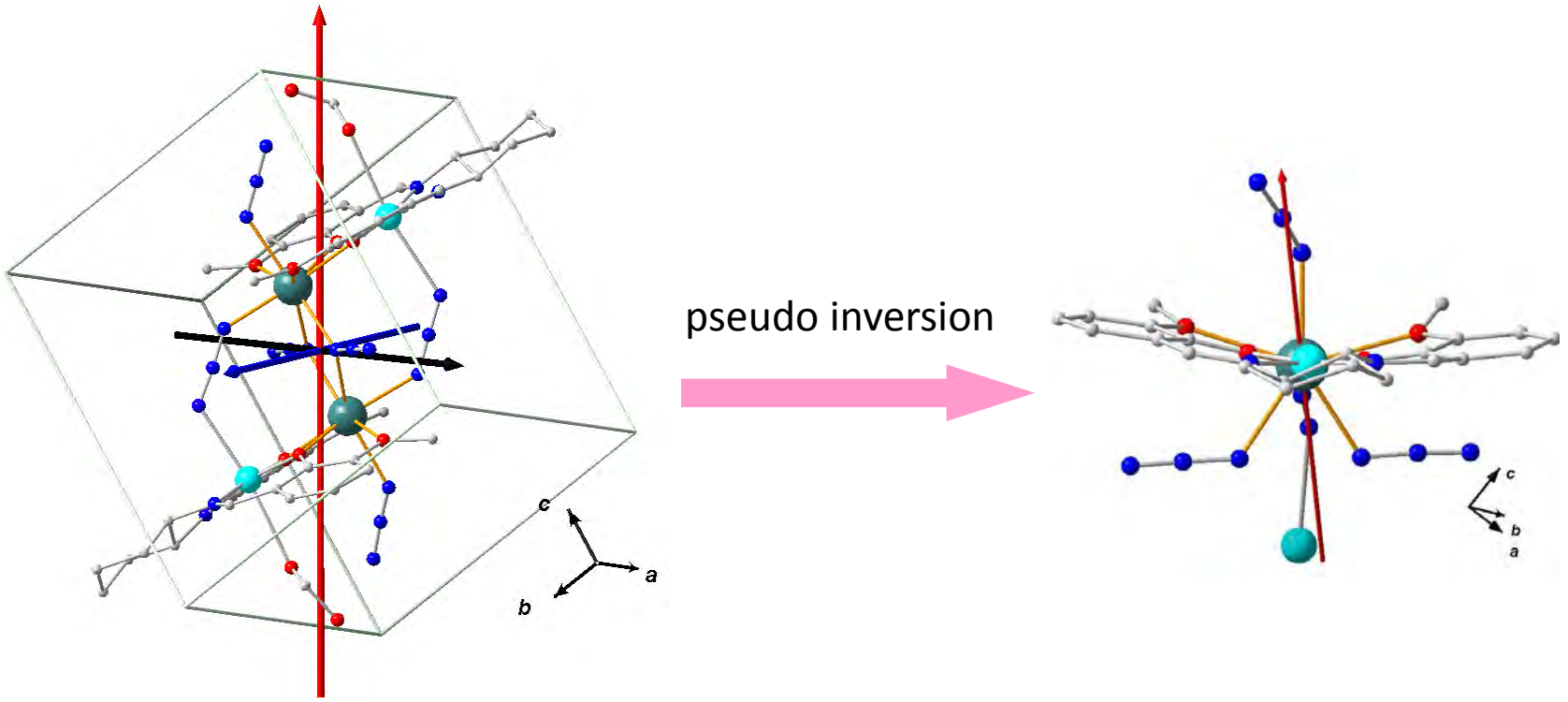

# Ch. 2. Single Crystal Magnetometry

Section 2.3 Determination



**(10) Ground state determination**

- Curie Law: Population is not changed a lot in the temperature range
- The first excited state is high enough.

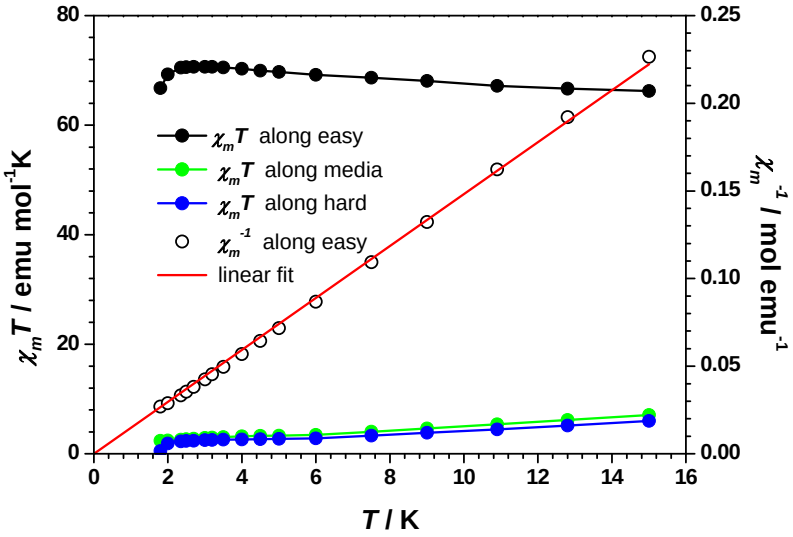


$$\chi T = \frac{1}{8} g^2 S(S+1)$$

$$g_{//}^{eff} = 2 g_J \left\langle \pm J_z \left| \hat{J}_z \right| \pm J_z \right\rangle$$

# Ch. 1. Introduction



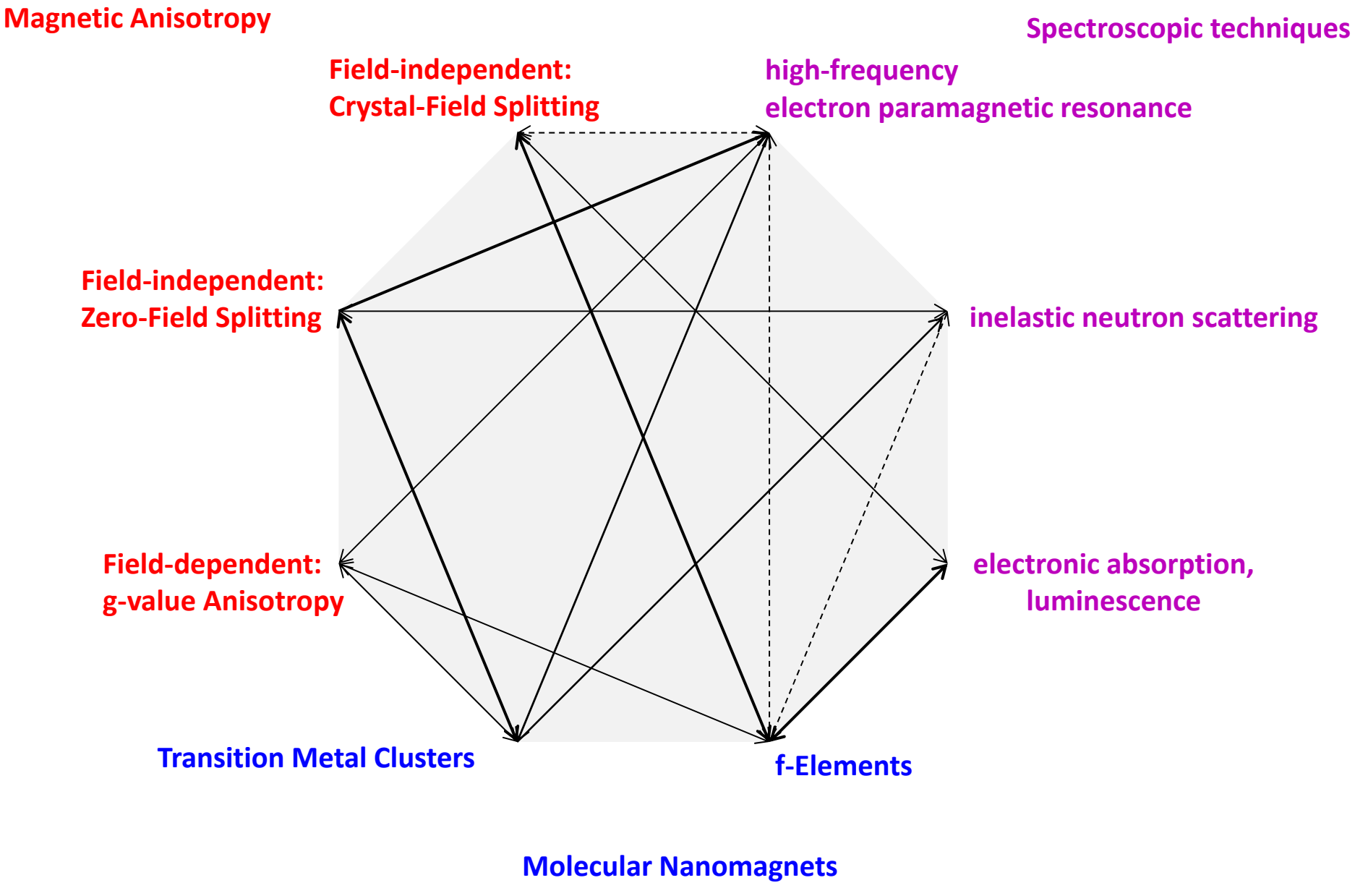

1. Introduction
2. Single Crystal Magnetometry
3. High-Frequency EPR Spectroscopy
4. Inelastic Neutron Scattering
5. Electronic Absorption and Luminescence

# Ch. 3. High-Frequency EPR

## Section 3.1 Theoretical Background and Experimental Considerations



**Basics of EPR**

- The **Zeeman term** describes the interaction of the spin with a magnetic field.
- In the absence of other interactions the field is chosen along the z-axis.
- The electronic Zeeman term then has the form: $\hat{\mathcal{H}}^{\text{Zeeman}} = g\mu_B B\hat{S}_z$
- Accordingly, the energies of the spin states depend on $m_S$ : $E = g\mu_B B m_S$

  *Note: remember* $\hat{S}_z\,|S\ m_s\ I\ m_I\rangle = m_s\,|S\ m_s\ I\ m_I\rangle$.

- $g$ = 2.00235… for a free electron.

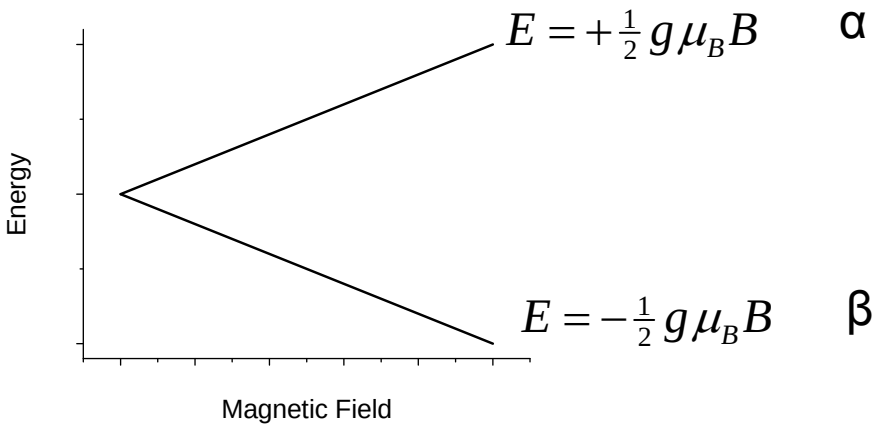


For $S$ = 1/2

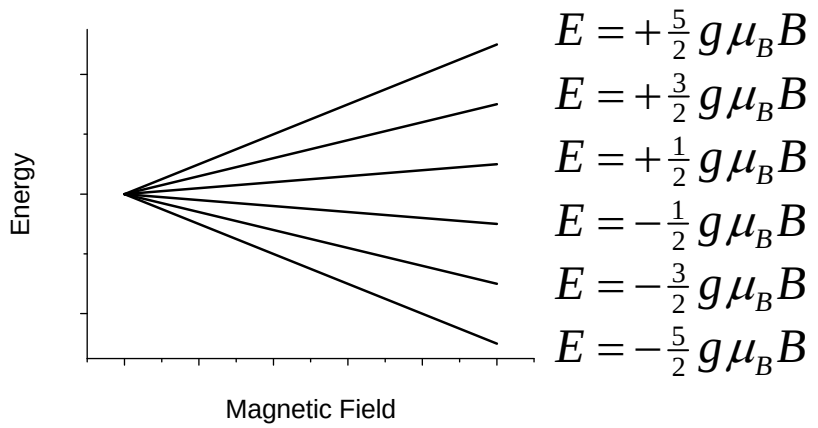


For $S$ = 5/2

# Ch. 3. High-Frequency EPR

## Section 3.1 Theoretical Background and Experimental Considerations



**Basics of EPR**

- For $S$ = 1/2, the energy difference between the two $m_S$ levels is: $\Delta E = g\mu_B B$
- If the energy of the electromagnetic radiation matches the energy difference, radiation can be absorbed. The spin interacts with the magnetic field of the electromagnetic radiation.
- This is called the **resonance condition**: $h\nu = g\mu_B B$
- For technical reasons, in EPR conventionally the frequency is kept constant, while the field is swept.
- The EPR selection rule is therefore $\Delta S = 0$, $\Delta m_S = \pm 1$ (perpendicular mode)

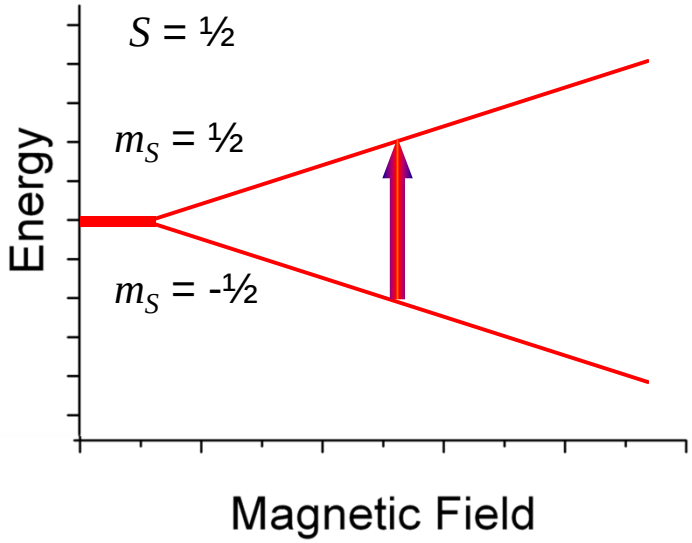


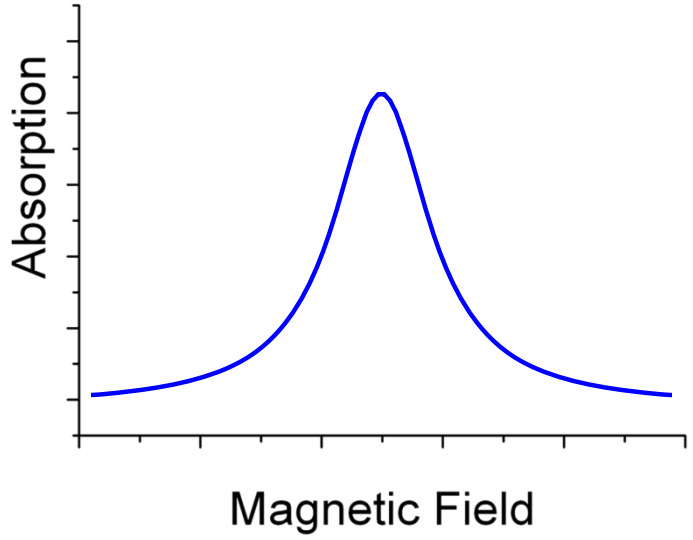

# Ch. 3. High-Frequency EPR

## Section 3.1 Theoretical Background and Experimental Considerations



**Basics of EPR – Selection rules.**

- Which transitions can be observed?
- Typically microwave magnetic field $\mathbf{b}_1 \perp$ external magnetic field $\mathbf{B}_0$.
- What about the Zeeman interaction of $\mathbf{b}_1$ with the spin?

$$\hat{\mathcal{H}}^{\text{Zeeman}} = g\mu_B b_1 \hat{S}_{x,y}$$

- What is the action of $\hat{S}_x$ and $\hat{S}_y$ on the spin state $|S\ m_s\ I\ m_I\rangle$ ?
- It is useful to make combinations of $\hat{S}_x$ and $\hat{S}_y$, called shift operators:

$$\hat{S}_+ = \hat{S}_x + i\hat{S}_y \quad \hat{S}_- = \hat{S}_x - i\hat{S}_y$$

- The shift operators change the $m_S$ quantum number by ±1:

$$\hat{S}_+ |S\ m_s\rangle = \sqrt{S(S+1) - m_s(m_s+1)}\ |S\ m_s+1\rangle$$

$$\hat{S}_- |S\ m_s\rangle = \sqrt{S(S+1) - m_s(m_s-1)}\ |S\ m_s-1\rangle$$

- The EPR selection rule is therefore $\Delta m_S = \pm 1$
- In addition $\Delta S = 0$.

# Ch. 3. High-Frequency EPR

## Section 3.1 Theoretical Background and Experimental Considerations



**Basics of EPR – High-frequency EPR**

- Conventional EPR uses 9 GHz radiation frequency.
- High-frequency EPR with frequencies up to 1000 GHz possible.
- High-frequency means high field, which gives increased g-value resolution.
- This is usually not of interest in molecular magnetism

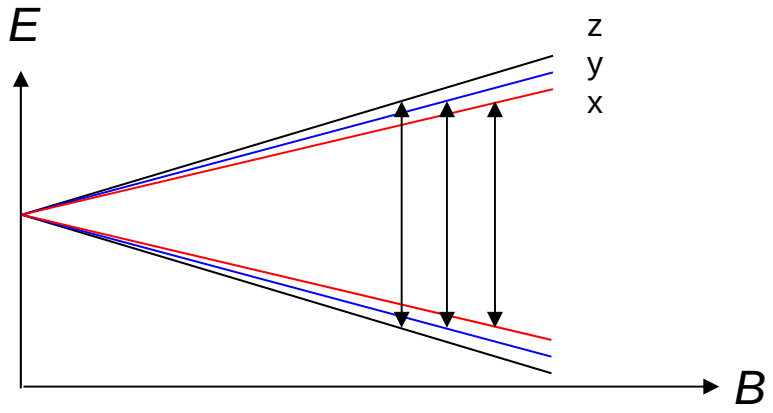


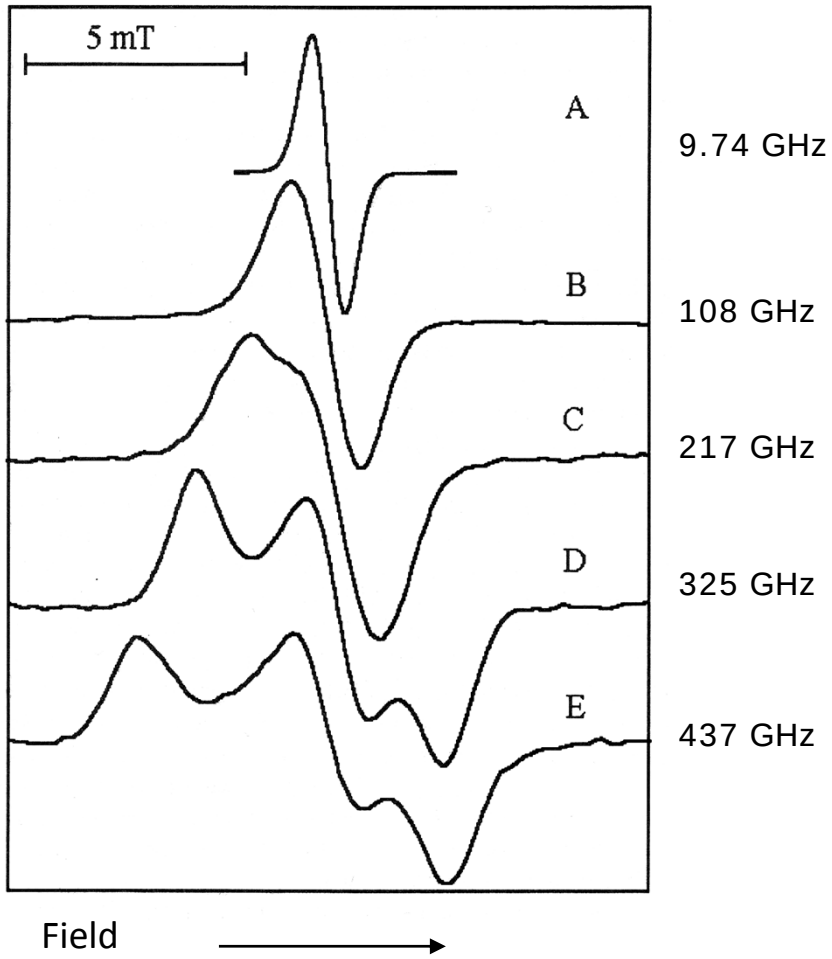


Photosystem I, light-induced $P700^{+\bullet}$, A. Angerhofer in O.Y. Grinberg (Ed.), Very High Frequency EPR

# Ch. 3. High-Frequency EPR

## Section 3.1 Theoretical Background and Experimental Considerations



**Zero-Field Splittings: Axial ZFS**

- Spin Hamiltonian $\hat{\mathcal{H}}_{\mathrm{ZFS}} = D\hat{S}_z^2 + E(\hat{S}_x^2 - \hat{S}_y^2) = D\hat{S}_z^2 + \frac{1}{2}E(\hat{S}_+^2 + \hat{S}_-^2)$
- The *D* parameter lifts the degeneracy of the $m_S$ levels.
- For $D < 0$, the $m_S = \pm S$ levels are lowest in energy.
- For $D > 0$, the $m_S = 0$ or $m_S = \pm ½$ are lowest in energy.
- *D* can be 0-$10^2$ $cm^{-1}$.

- For $S = 1$, energy gap between $m_S = 0$ or $m_S = \pm 1$ equals *D*.

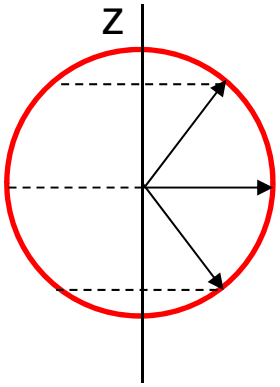


$S = 1$

$m_S = +1$

$m_S = 0$

$m_S = -1$



$m_S = 0$



$m_S = \pm 1$

$D < 0$

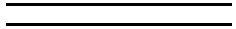

$m_S = \pm 1$



$m_S = 0$

$D > 0$

# Ch. 3. High-Frequency EPR

## Section 3.1 Theoretical Background and Experimental Considerations



**Large Zero-Field Splittings.**

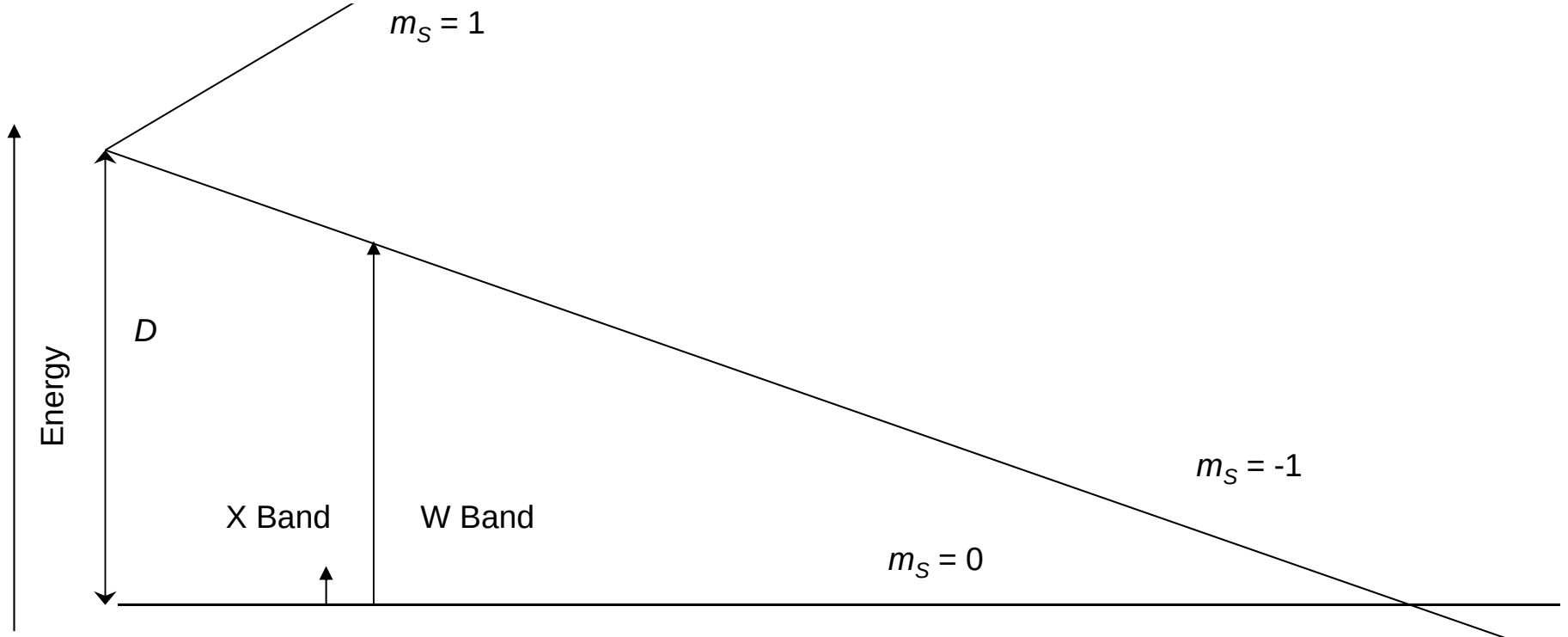


- Only $\Delta M_S = \pm 1$ allowed.
- At X-band microwave quantum too small.
- At higher frequencies transitions can be observed.
- Large ZFS ions with integer spin are therefore traditionally called EPR silent

# Ch. 3. High-Frequency EPR

## Section 3.1 Theoretical Background and Experimental Considerations



**High-Field limit**

$S = 1$, $D = -1\ \text{cm}^{-1} = -30$ GHz, $\nu = 150$ GHz, $T = 300$ K

$\vartheta = 0$: $B_0 \,||\, z$

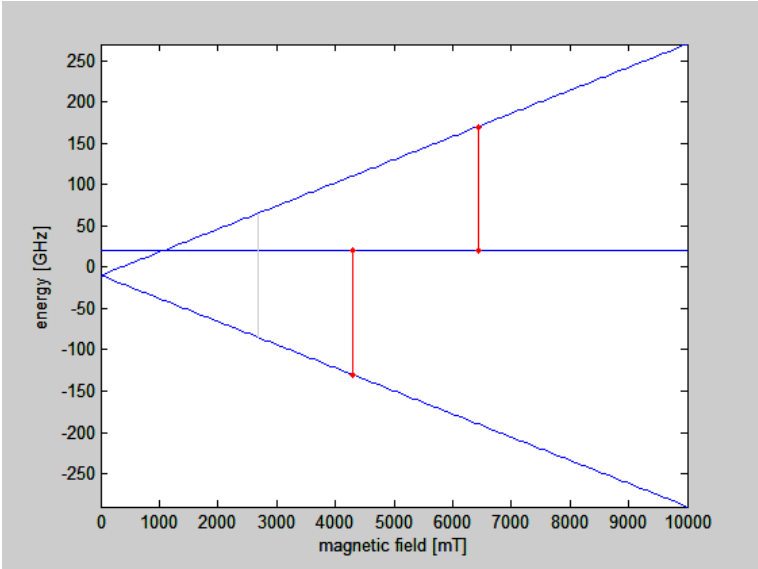


$\vartheta = 90$: $B_0 \,||\, z$

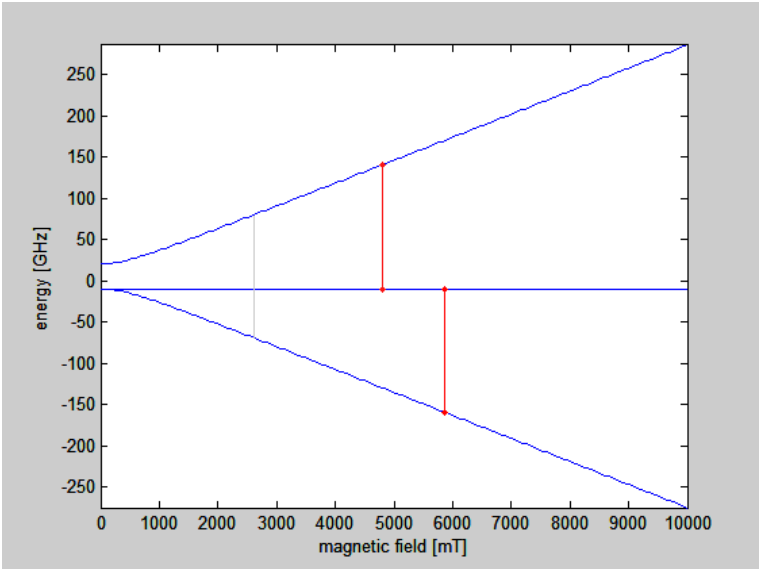

# Ch. 3. High-Frequency EPR

## Section 3.1 Theoretical Background and Experimental



**High-Field limit**

$S = 1$, $D = -1\ cm^{-1} = -30$ GHz, $\nu = 150$ GHz, $T = 300$ K

Absorption

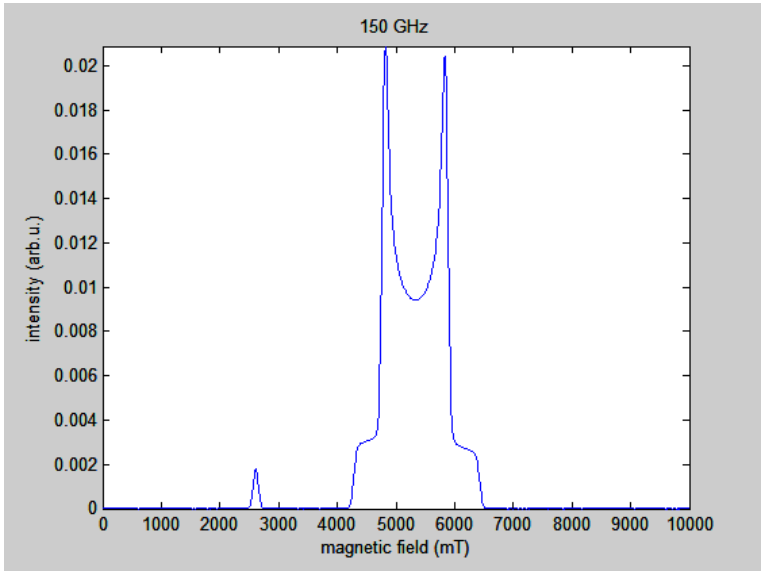


First derivative

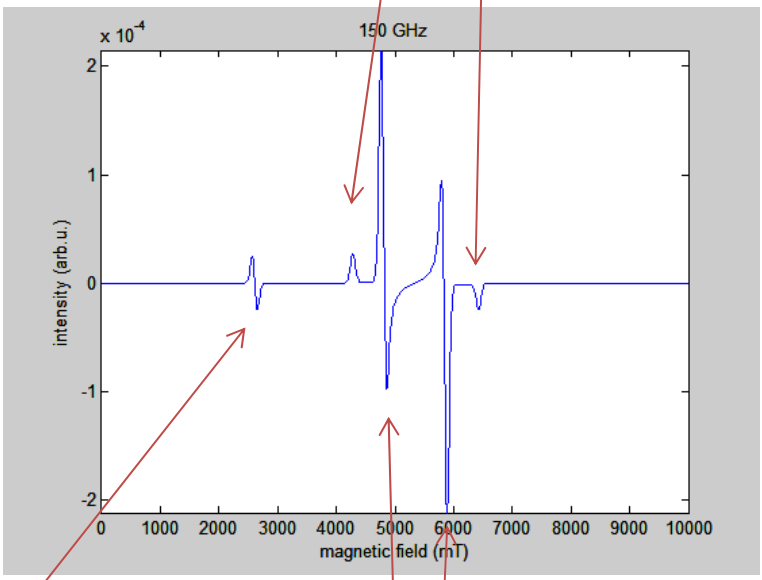


Forbidden transition

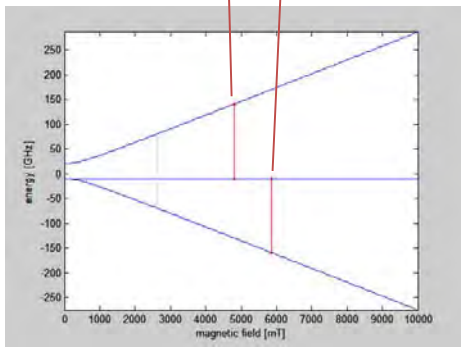

# Ch. 3. High-Frequency EPR

## Section 3.1 Theoretical Background and Experimental Considerations



**High-Field limit**

- $[Ni(5\text{-methylpyrazole})_6](ClO_4)_2$
- $S = 1$, $D = 0.72\ cm^{-1} = 21.6$ GHz, $T = 100$ K

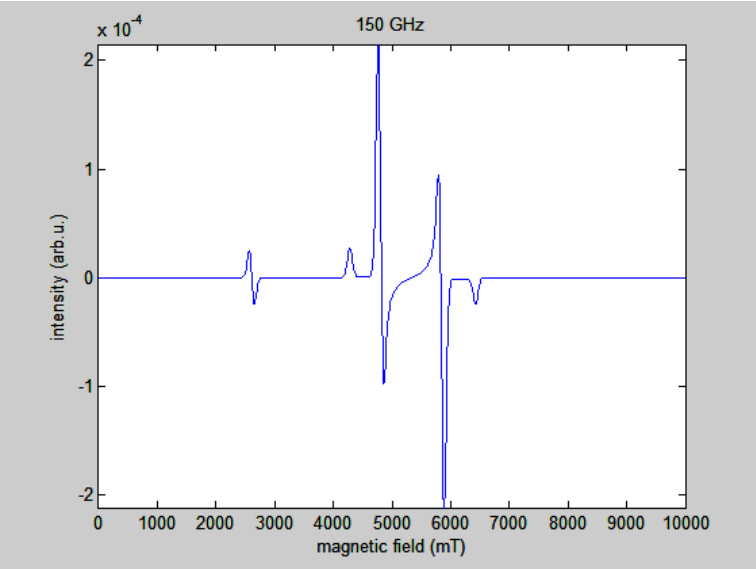


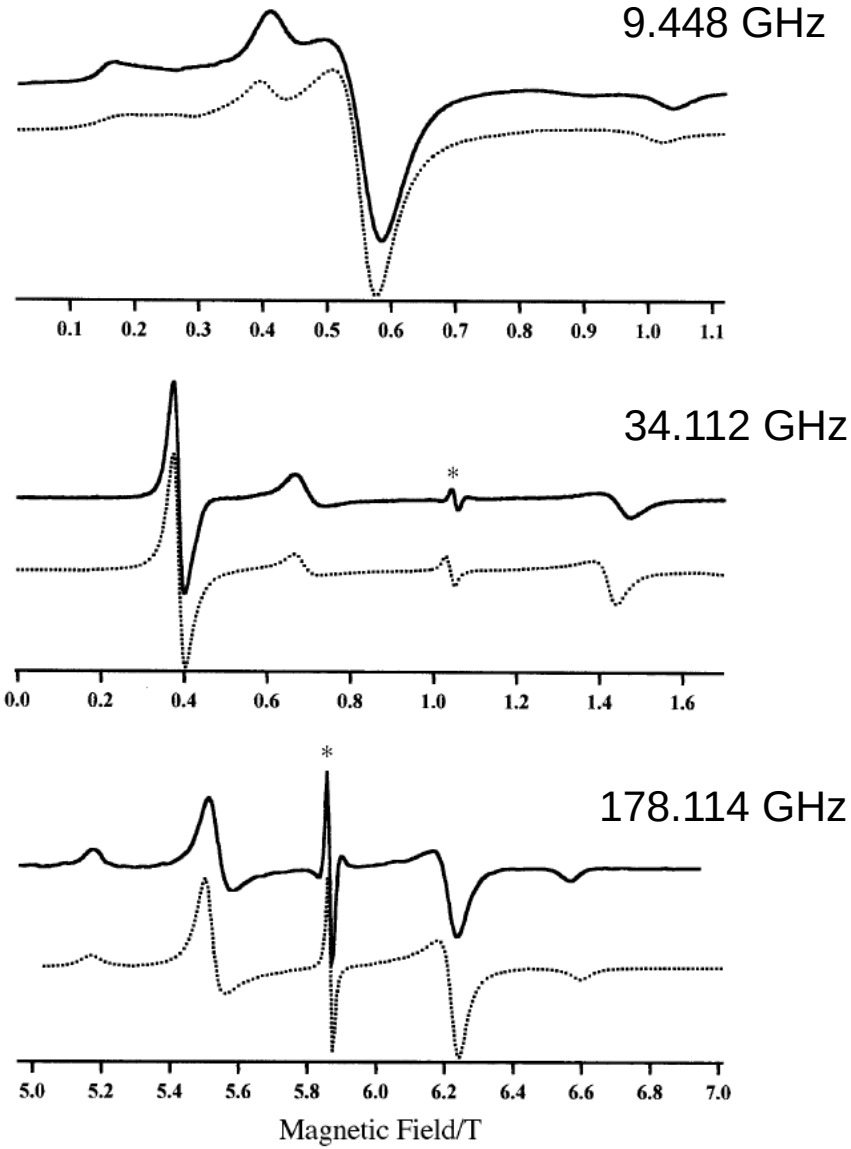


Collison, J. Chem. Soc., Faraday Trans., 1998, 3019

# Ch. 3. High-Frequency EPR

## Section 3.1 Theoretical Background and Experimental Considerations



**High-Field limit**

- HFEPR allows the determination of the sign of D

At low temperature, and $B_0$ // $z$:

- For D < 0 the low field line remains.
- For D > 0, the high field line remains.

$B_0//z$, $S = 3$, $D < 0$

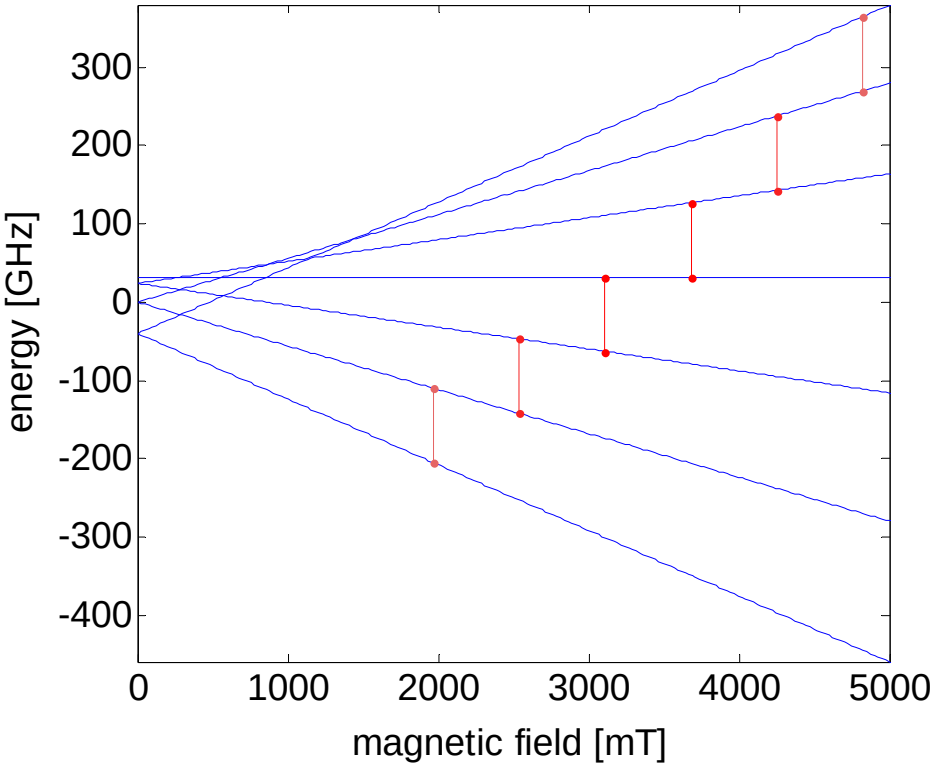


$S = 3$, $D > 0$

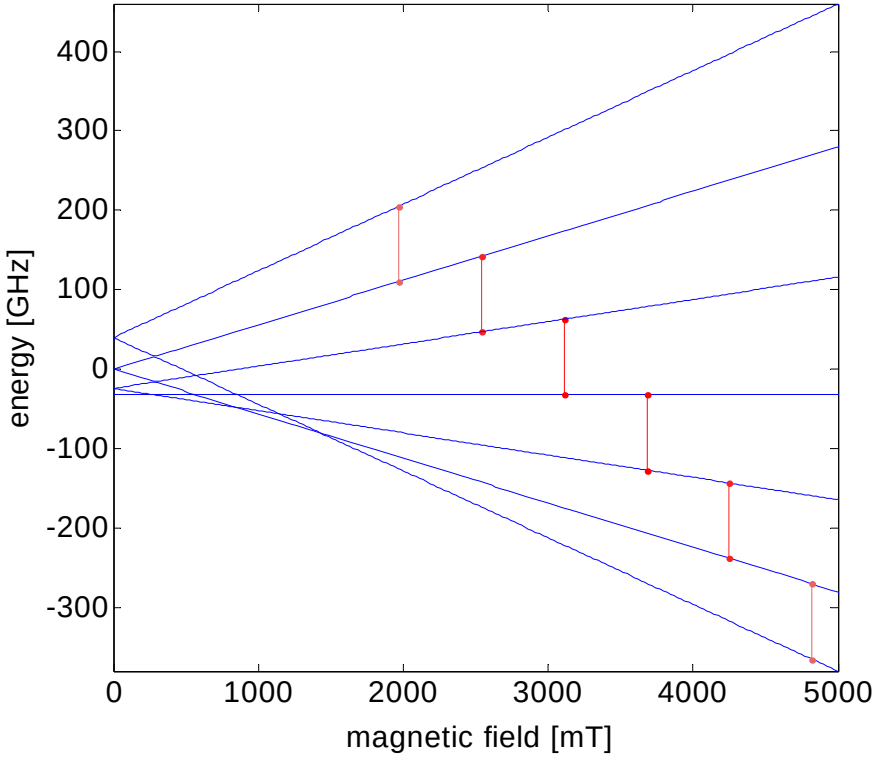

# Ch. 3. High-Frequency EPR

## Section 3.1 Theoretical Background and Experimental Considerations



**High-Field limit**

- For $g\, m_B\, H >> D$ and uniaxial anisotropy there are $2S$ resonance lines.
- The resonance fields are given by:
- $B_{//} = (g_e/g_{//})[B_0+(2M_S-1)D]$ $B_{\perp} = (g_e/g_{\perp})[B_0-(2M_S-1)D/2]$
- Spacing: $2D/g\mu_B$ for $B//z$ $D/g\mu_B$ for $B\perp z$
- Example: $D$ negative

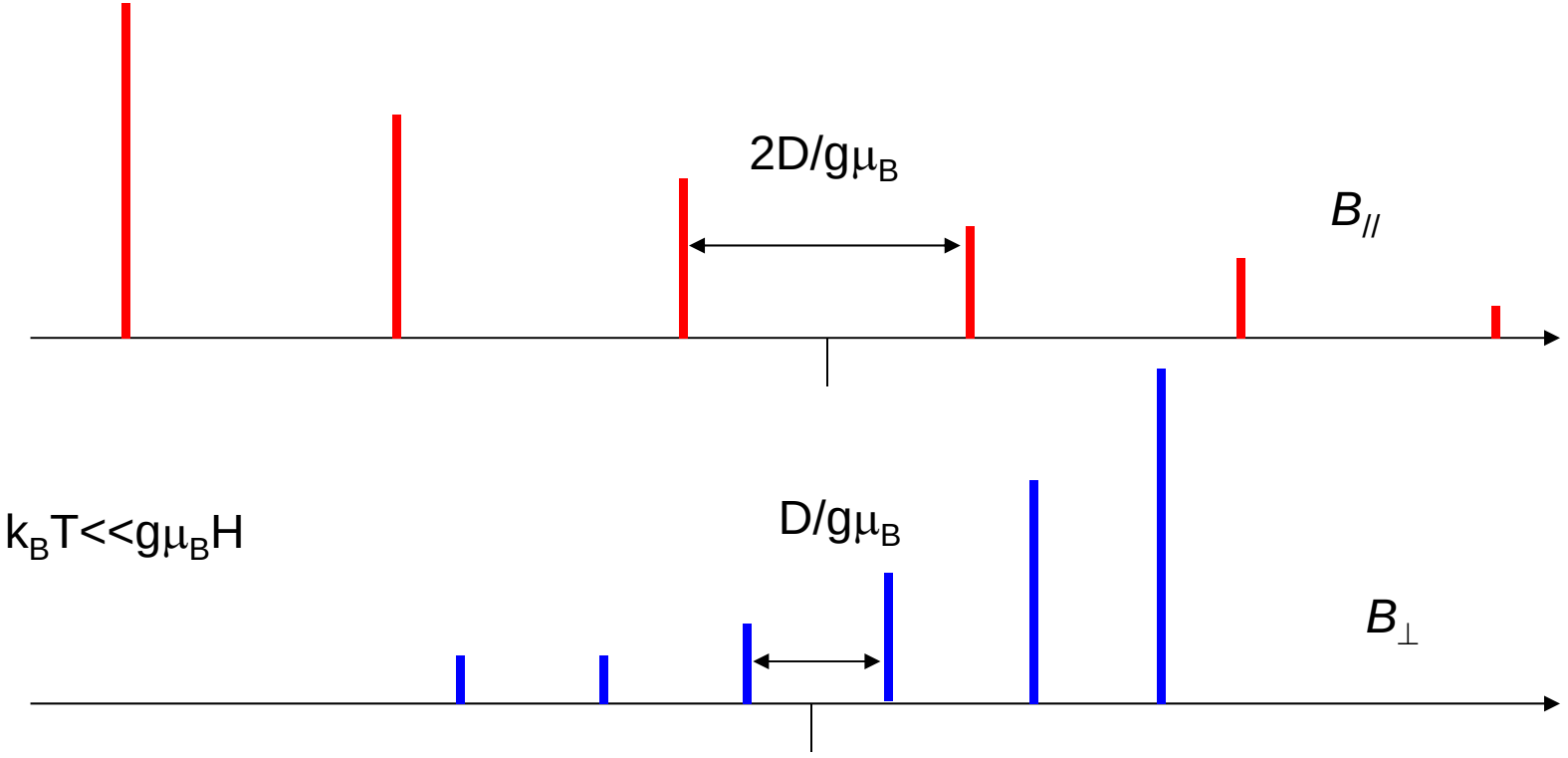

# Ch. 3. High-Frequency EPR

## Section 3.2 Examples



**Example $[Fe_4(L)_2(dpm)_6]$**

- L = 2-(bromomethyl)-2-(hydroxymethyl)-1,3-propanediol.
- Antiferromagnetic exchange coupling leads to $S = 5$ ground state. $M_S = -5, -4, \ldots, 4, 5$.
- Lines with large spacing at low fields, lines with small spacing at high field.
- That means that $D < 0$.
- From fit (black): $D = -0.432\ cm^{-1}$, $B_4^0 = 2 \times 10^{-5}\ cm^{-1}$.
- $B_4^0$ is a higher order ZFS term. $H_{ZFS} = D\,\hat{S}_z^2 + B_4^0 \hat{O}_4^0$.

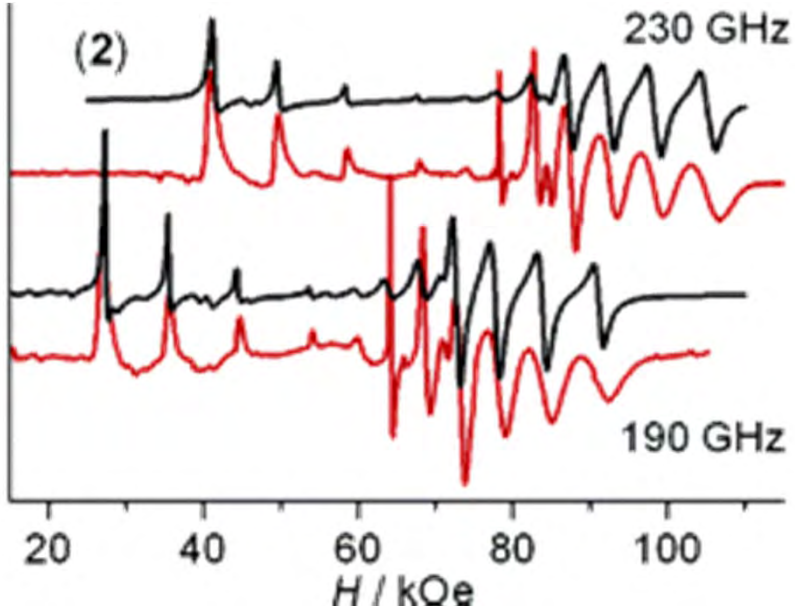


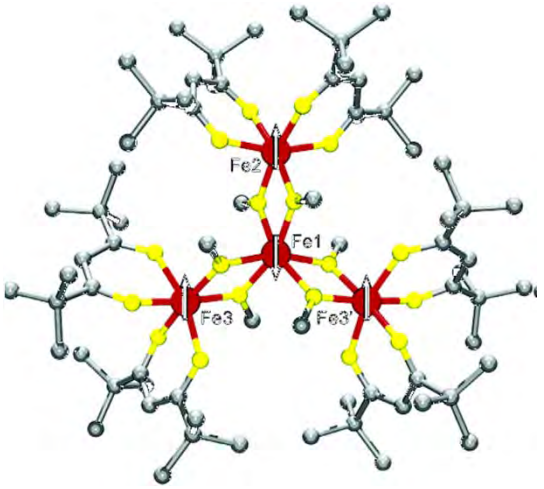


[Accorsi, JACS, 2006]

# Ch. 3. High-Frequency EPR

## Section 3.2 Examples



**Example $Ni(PPh_3)_2Cl_2$**

$S = 1$, $D = +13.20\ cm^{-1} = 396$ GHz, $E = 1.85\ cm^{-1}$, $g = 2.20$ (isotropic), $T = 4.5$ K

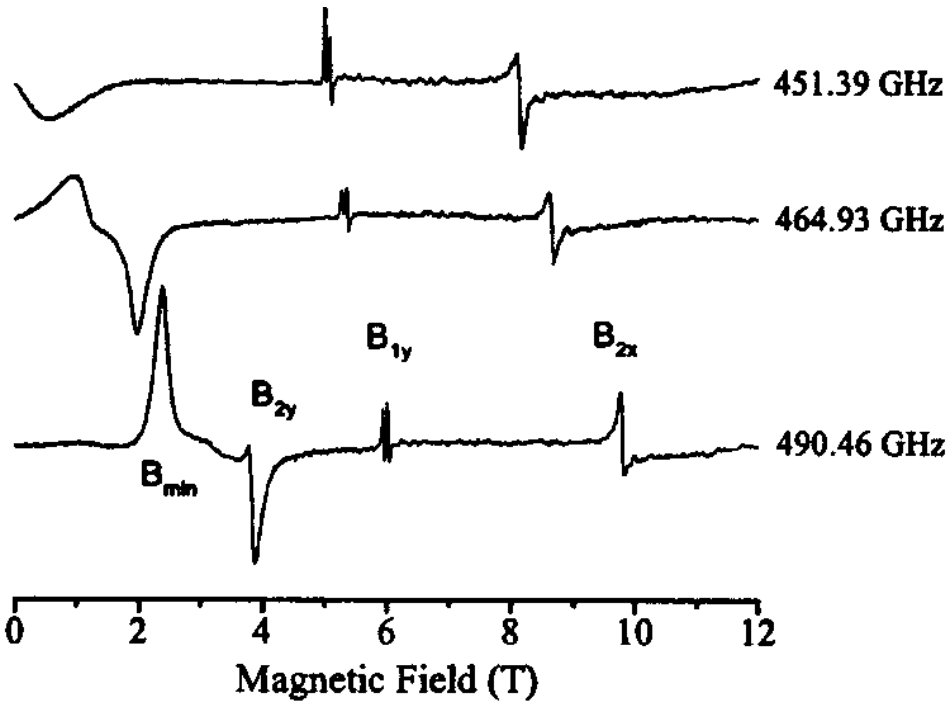


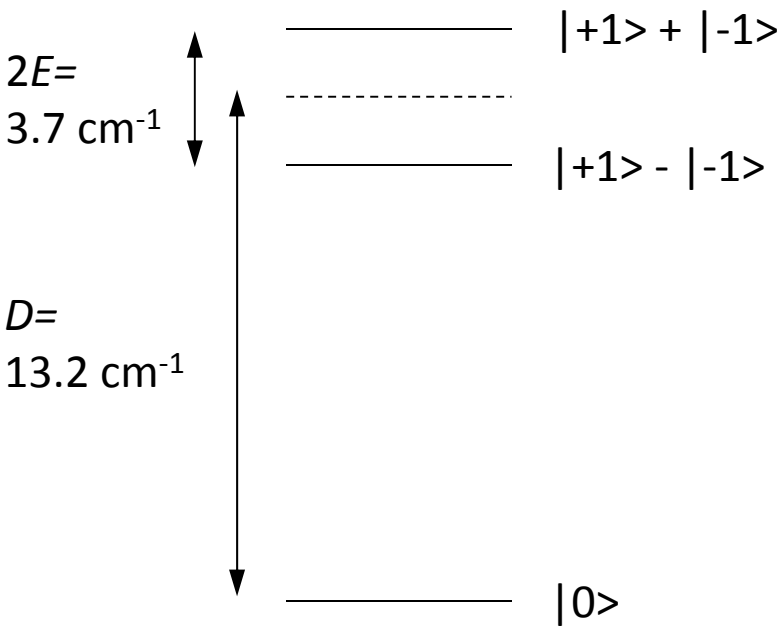


J. Krzystek, Inorg. Chem., 41, 4478 (2002)

# Ch. 3. High-Frequency EPR

## Section 3.2 Examples



**Example $Ni(PPh_3)_2Cl_2$**

$S = 1$, $D = +13.20\ cm^{-1} = 396$ GHz, $E = 1.85\ cm^{-1}$, $g = 2.20$ (isotropic), $T = 4.5$ K

Rhombic anisotropy: x- and y-axis different, $\vartheta$ and $\varphi$ both important.

$\vartheta = 0$, $\varphi = 0$: $B_0 \,||\, z$ $\vartheta = 90$, $\varphi = 90$: $B_0 \,||\, y$ $\vartheta = 90$, $\varphi = 0$: $B_0 \,||\, x$

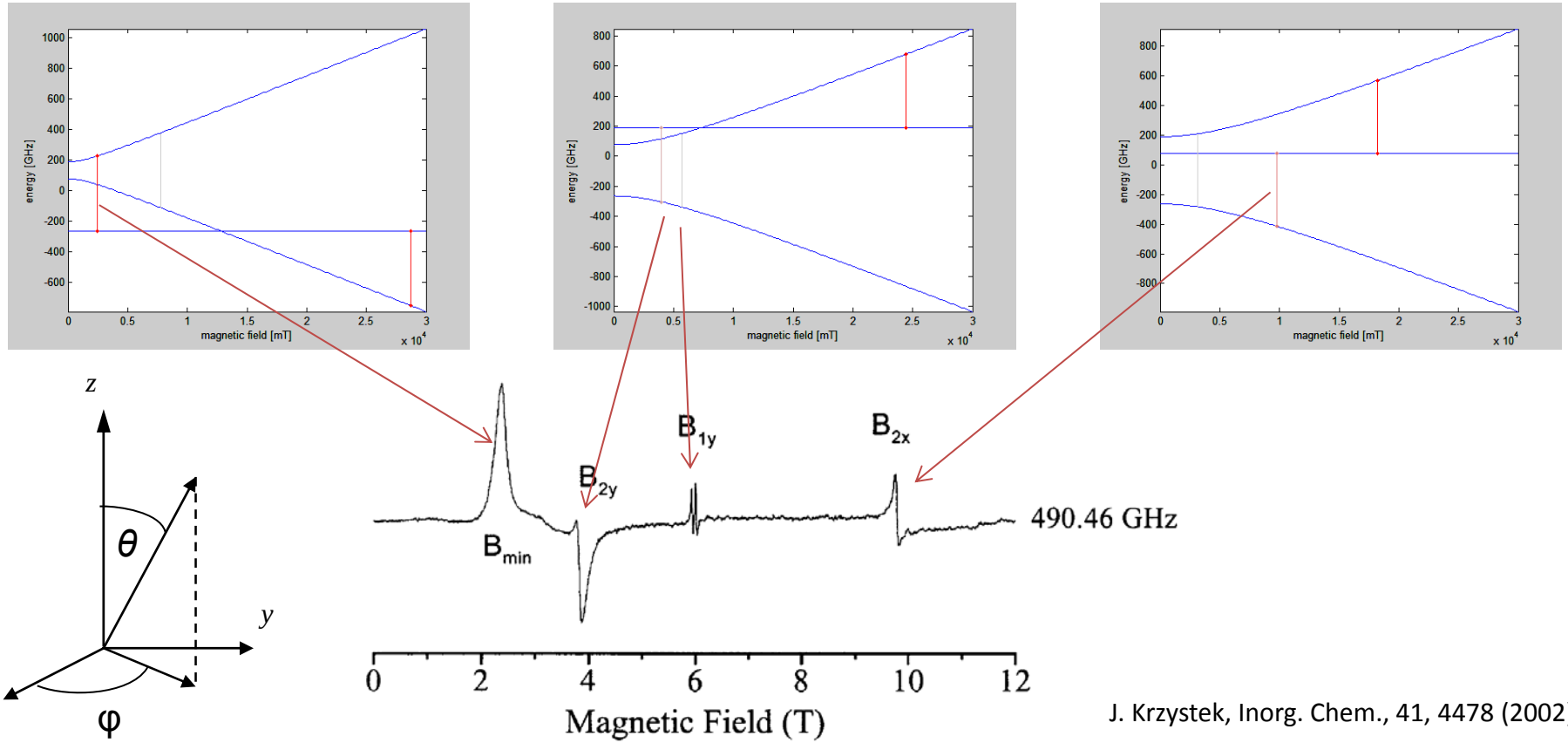


J. Krzystek, Inorg. Chem., 41, 4478 (2002)

# Ch. 3. High-Frequency EPR

## Section 3.2 Examples



**Example $Ni(PPh_3)_2Cl_2$**

$S = 1$, $D = +13.20\ cm^{-1} = 396$ GHz, $E = 1.85\ cm^{-1}$, $g = 2.20$ (isotropic), $T = 4.5$ K

Rhombic anisotropy: x- and y-axis different, $\vartheta$ and $\varphi$ both important.

yz-plane

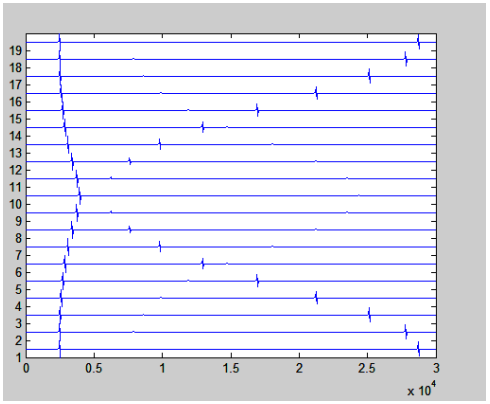

xz-plane

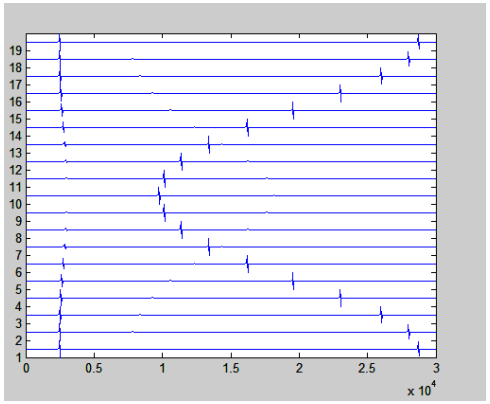

xy-plane

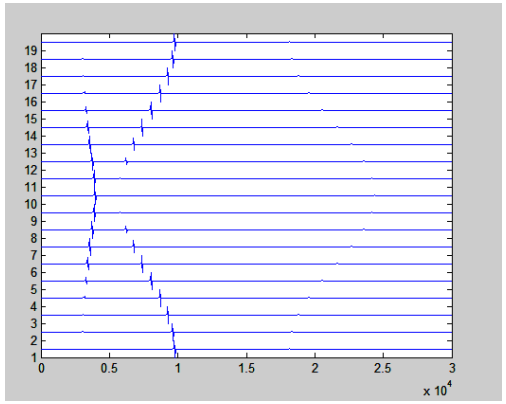

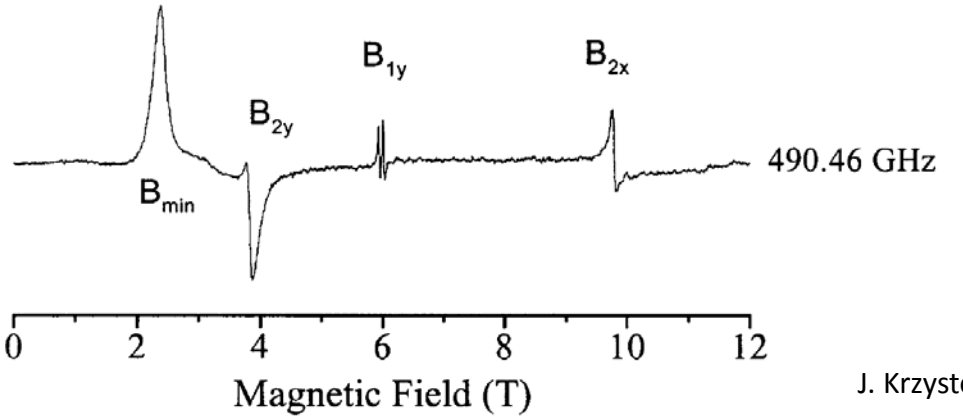


J. Krzystek, Inorg. Chem., 41, 4478 (2002)

# Ch. 3. High-Frequency EPR

## Section 3.2 Examples



**Example $Ni(PPh_3)_2Cl_2$**

- *B* not much larger than *D*: no high-field simplification.
- Fictitious 2000 GHz spectrum goes up to 80 T.

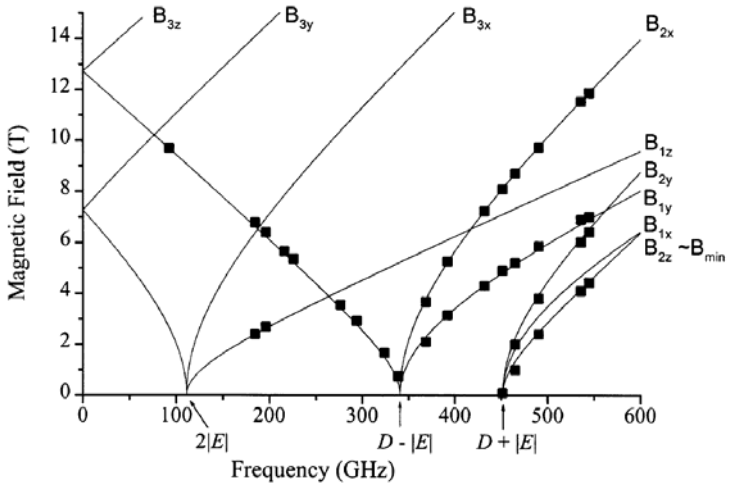


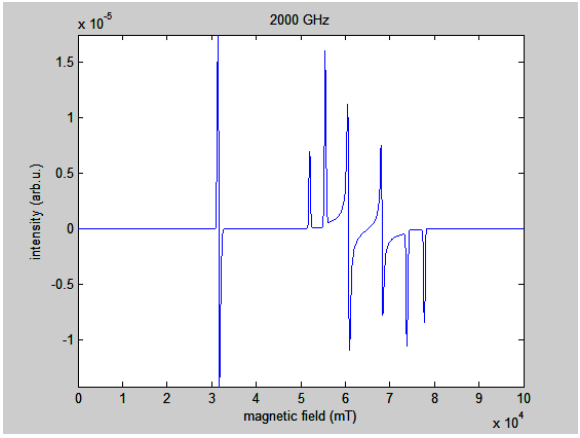


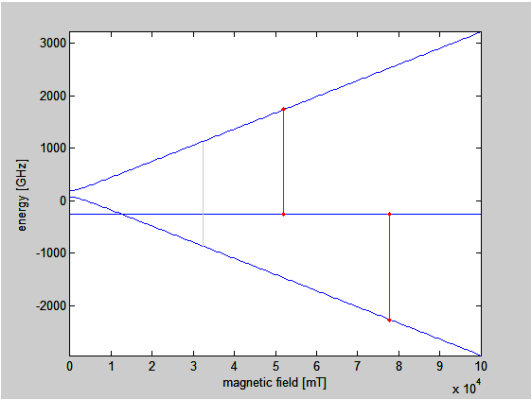


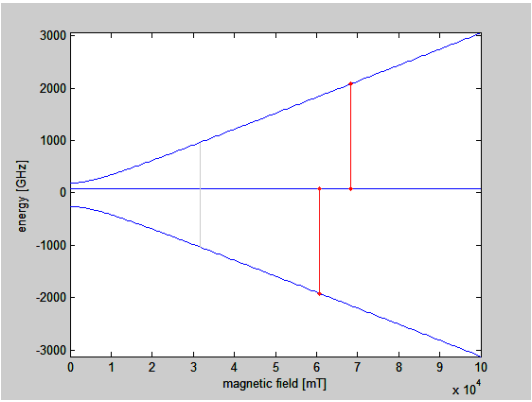


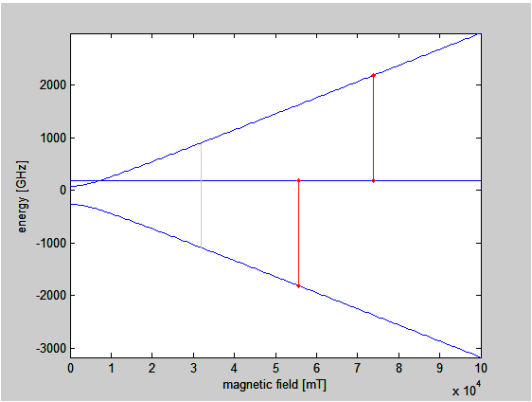

# Ch. 3. High-Frequency EPR

## Section 3.2 Examples



**Example $Ni(PPh_3)_2Cl_2$**

- *B* not much larger than *D*: no high-field simplification.
- Fictitious 2000 GHz spectrum goes up to 80 T.

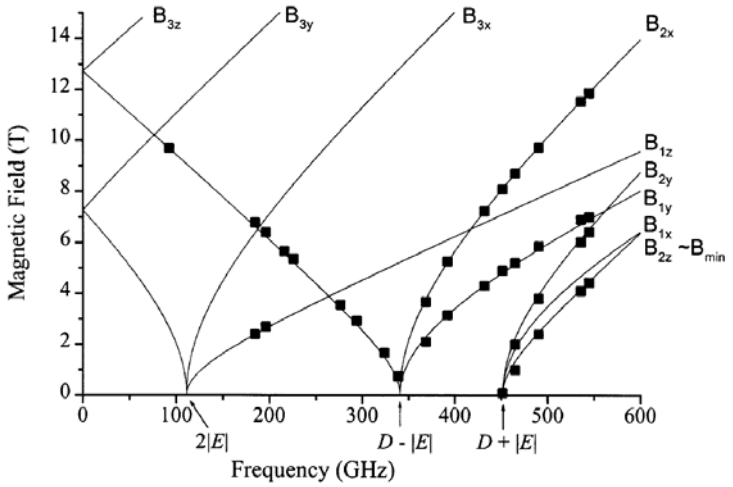


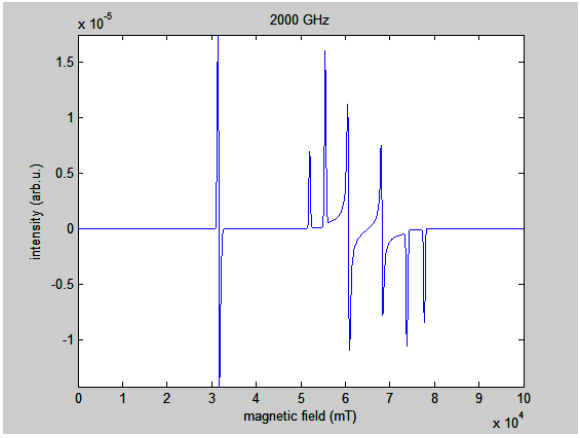


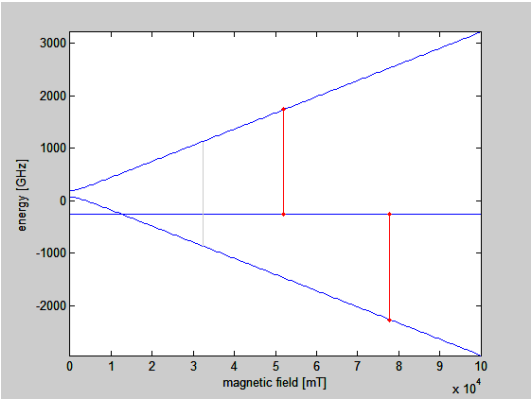


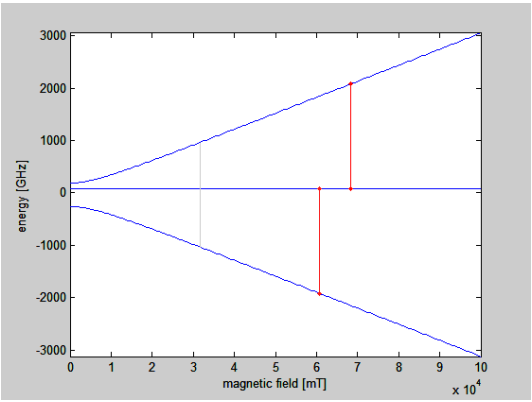


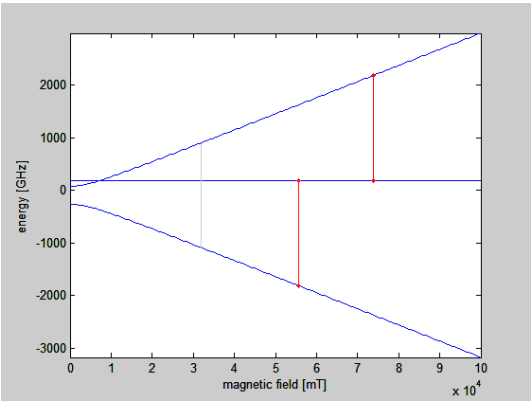

# Ch. 3. High-Frequency EPR

## Section 3.1 Theoretical Background and Experimental Considerations



**Where can I do high-frequency (ν > 95 GHz) EPR on molecular nanomagnets?**

- France: LNCMI Grenoble (Barra)
- Germany: IFW Dresden (Kataev)
- Germany: HLD Dresden (Zvyagin)
- Germany: Uni Stuttgart (Van Slageren)
- Italy: CNR Pisa (Pardi)
- USA: HMFL Tallahassee (Hill, Krzystek, Ozarowski).
- Japan: Kobe (Nojiri)

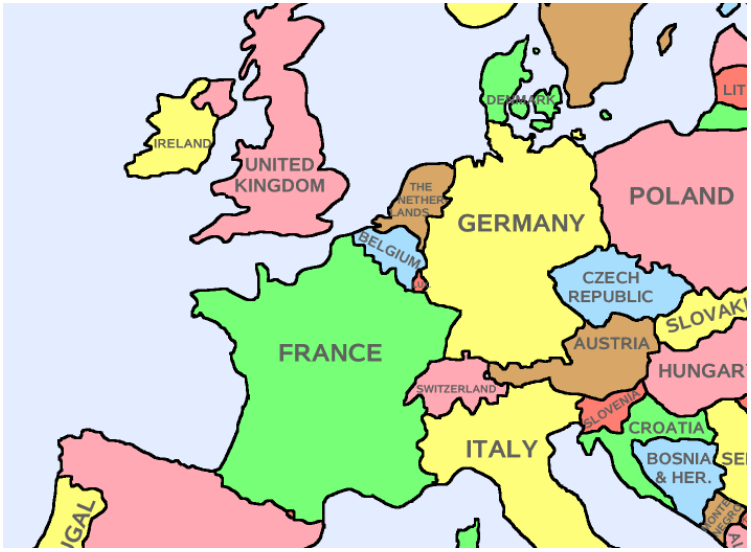



# Ch. 3. High-Frequency EPR

## Section 3.3 Frequency domain methods



### Frequency Domain Magnetic Resonance

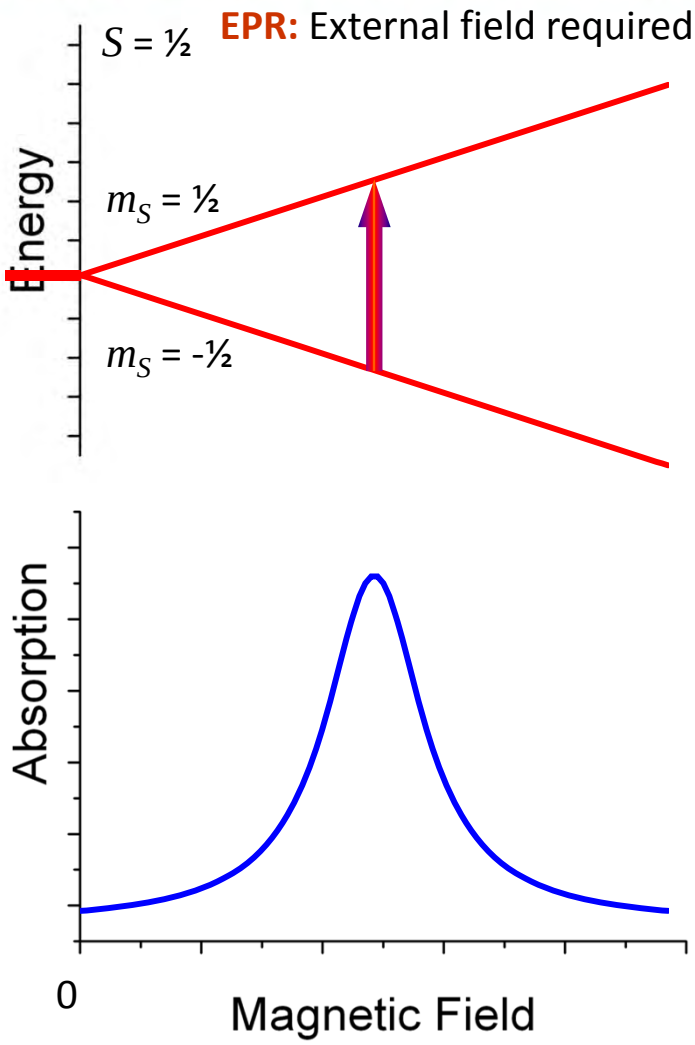


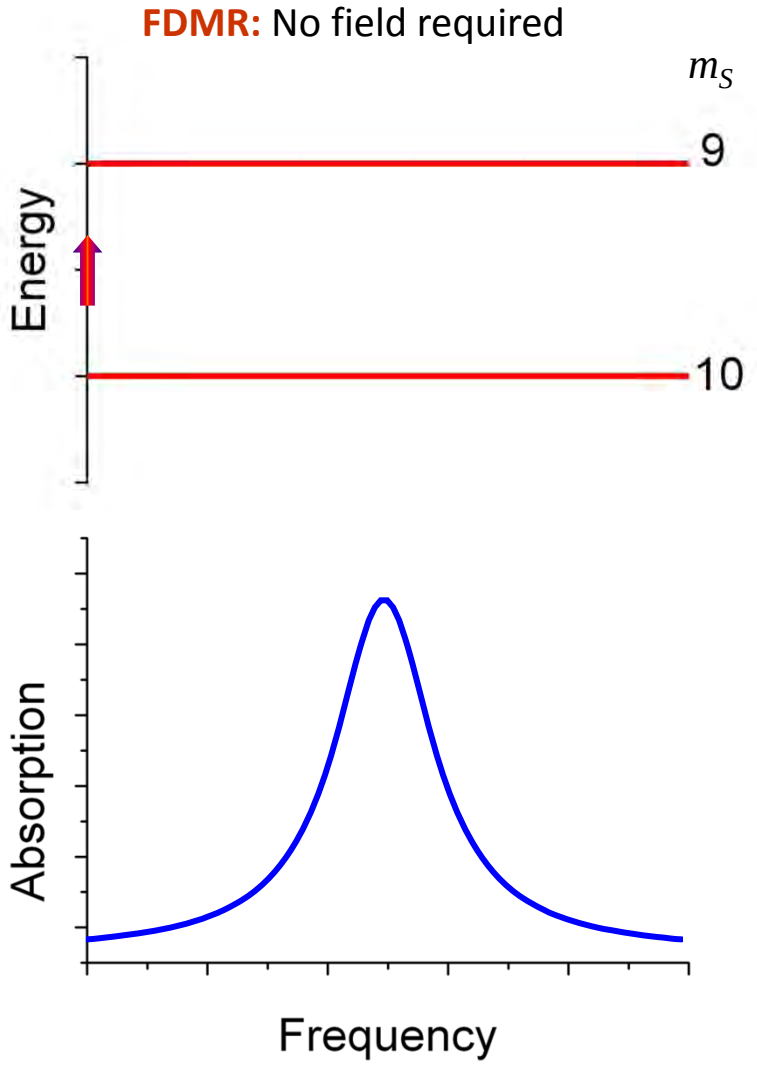


Van Slageren, Top. Curr. Chem. 2012

# Ch. 3. High-Frequency EPR

## Section 3.3 Frequency domain methods



**Monochromatic sweepable sources vs interferometer (FTIR) based methods**

**Monochromatic sweepable sources**

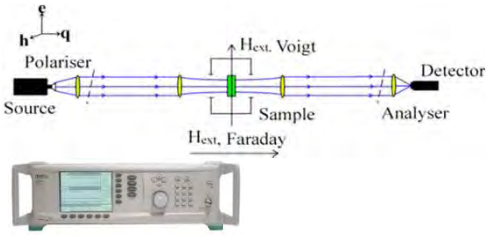


- synthesizer + multipliers or backward-wave oscillators (+ multipliers)

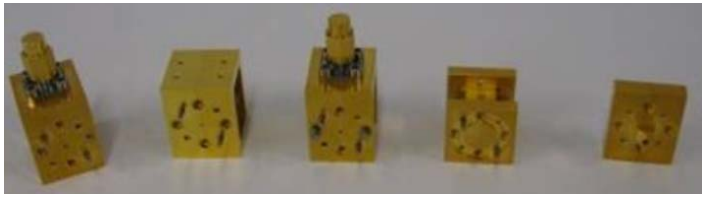

\+ high resolution, easier below 10 $cm^{-1}$.

– limited range

**Interferometer**

- Mercury lamp or synchrotron

\+ easy to obtain ultra broad band spectrum, easier at higher frequencies > 25 $cm^{-1}$

– field/frequency not independent.

$Mn_{12}ac$

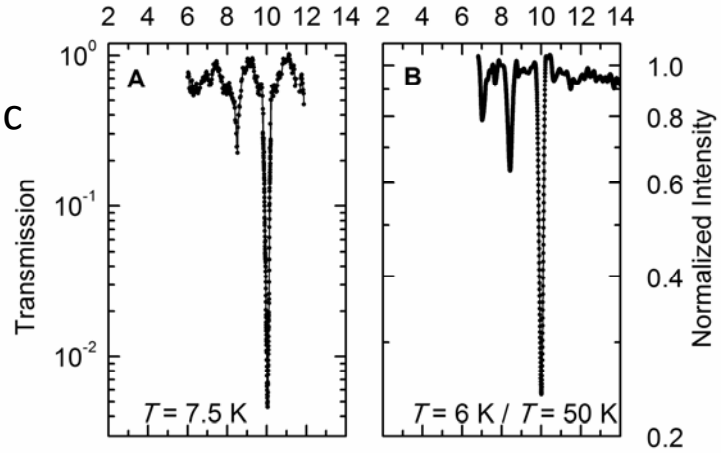


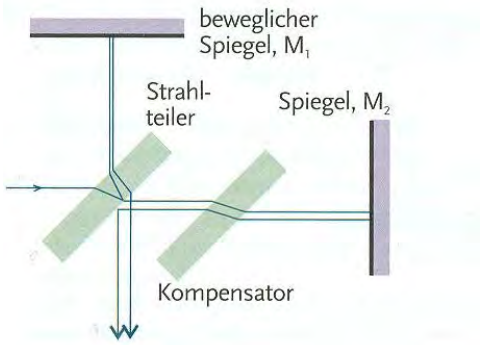


Van Slageren, Top. Curr. Chem. 2012; Schnegg, HZB Berlin

# Ch. 3. High-Frequency EPR

## Section 3.3 Frequency domain methods



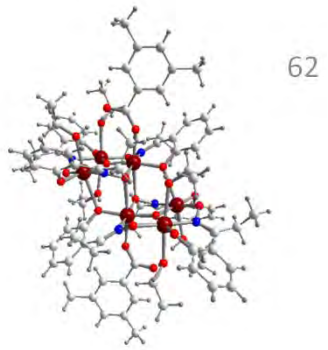

**Example 1. $[Mn^{III}_6O_2(Me_2Bz)_2(Et\text{-}sao)_6(EtOH)_4]$ ($\Delta E$ = 84 K)**

- S = 12. $D$ = –0.43 $cm^{-1}$ from magnetisation. $\Delta E$ = 84 K (record).
- Powder pellet sample. 6 sharp magnetic resonance lines
- Oscillating baseline due to interference within pellet
- Single scan takes ca. 30 seconds

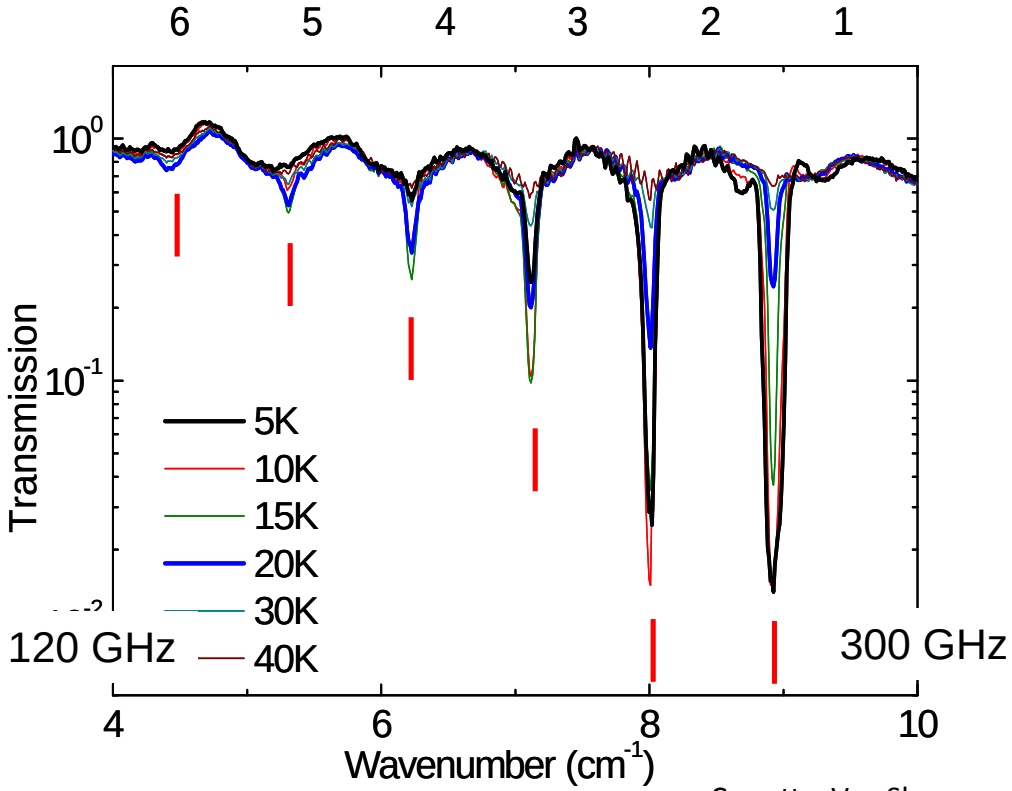


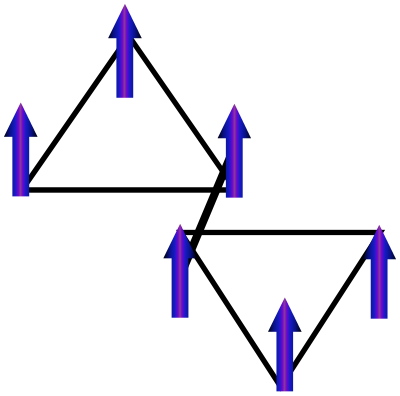

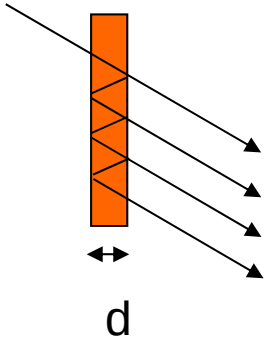


Carretta, Van Slageren et al., PRL 2008, Pieper, Van Slageren et al. PRB 2010

# Ch. 3. High-Frequency EPR

## Section 3.3 Frequency domain methods



**Example 1. $[Mn^{III}_6O_2(Me_2Bz)_2(Et\text{-}sao)_6(EtOH)_4]$ ($\Delta E$ = 84 K)**

- Giant spin model (ground state only).
- $\mathcal{H} = D\hat{S}_z^2 + B_4^0 \hat{O}_4^0$
- $D$ = -0.362 $cm^{-1}$
- $B_4^0$ = -6.08 x $10^{-6}$ $cm^{-1}$

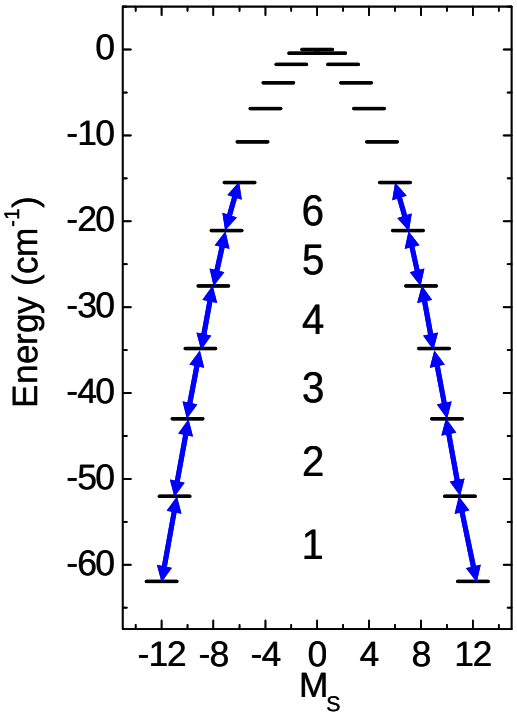


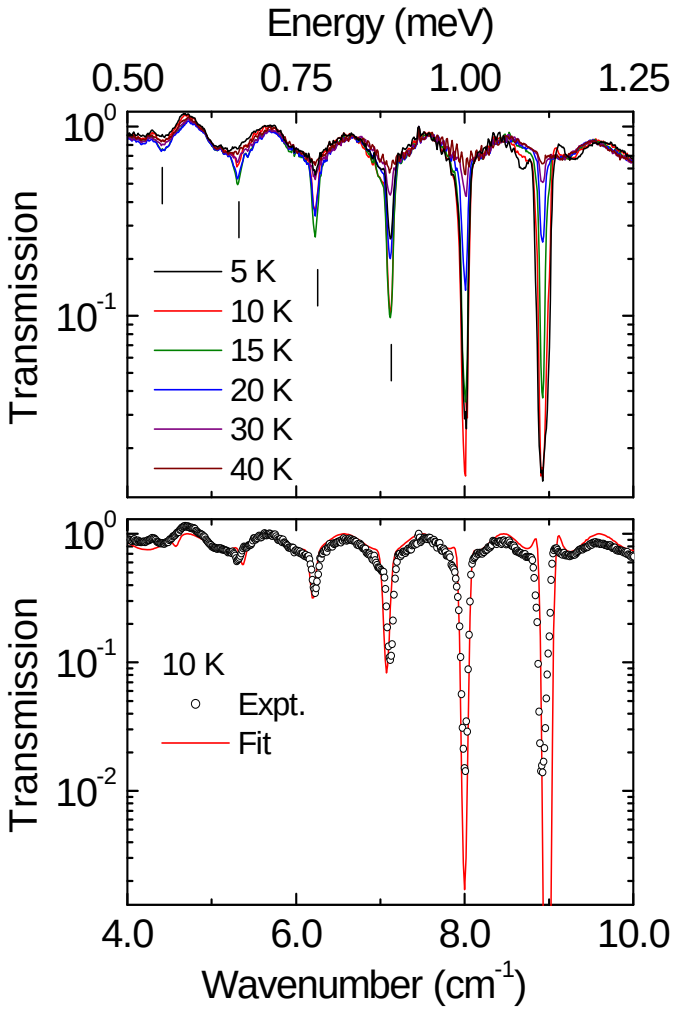


Carretta, Van Slageren et al., PRL 2008, Pieper, Van Slageren et al. PRB 2010

# Ch. 3. High-Frequency EPR

## Section 3.3 Frequency domain methods



**Example 1. $[Mn^{III}_6O_2(Me_2Bz)_2(Et\text{-}sao)_6(EtOH)_4]$ ($\Delta E$ = 84 K)**

- Comparison with HFEPR
- Single crystal.
- $D$ = –0.360(5) $cm^{-1}$
- $B_4^0$ = –5.7(5) $10^{-6}$ $cm^{-1}$
- 7 Frequencies x 7 T sweep....

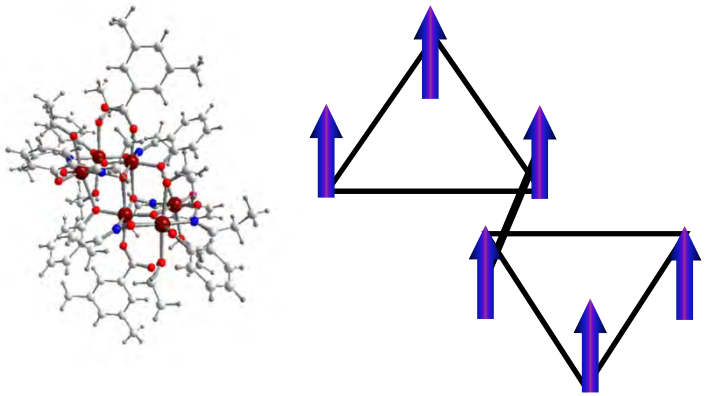

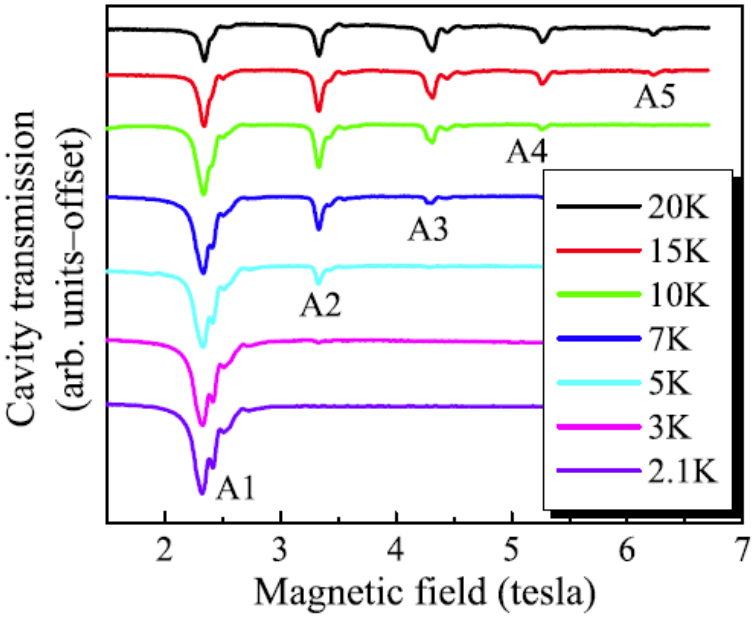


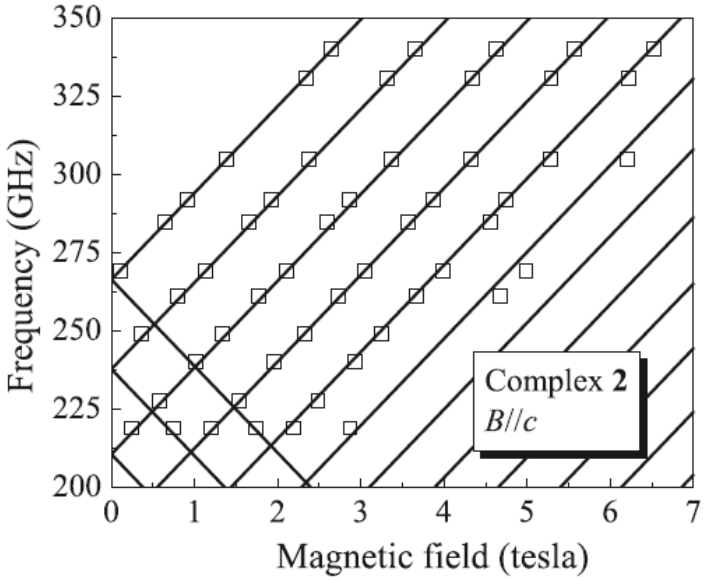


Datta, Dalton Trans. 2009

# Ch. 3. High-Frequency EPR

## Section 3.3 Frequency domain methods



**Example 2. $[Ni(PPh_3)_2Cl_2]$**

- Read off D and E from single scan.

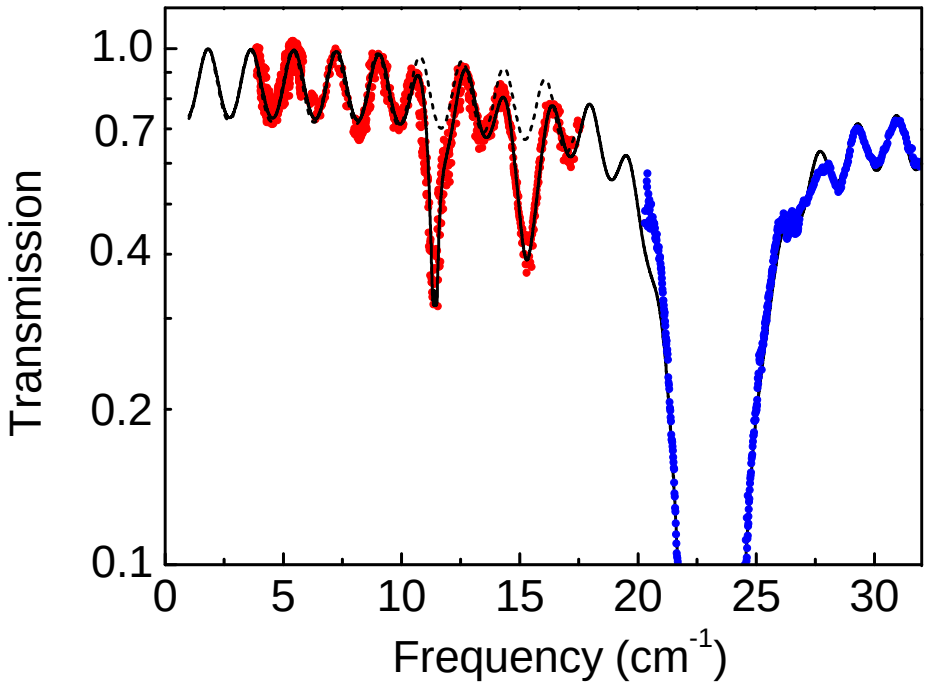


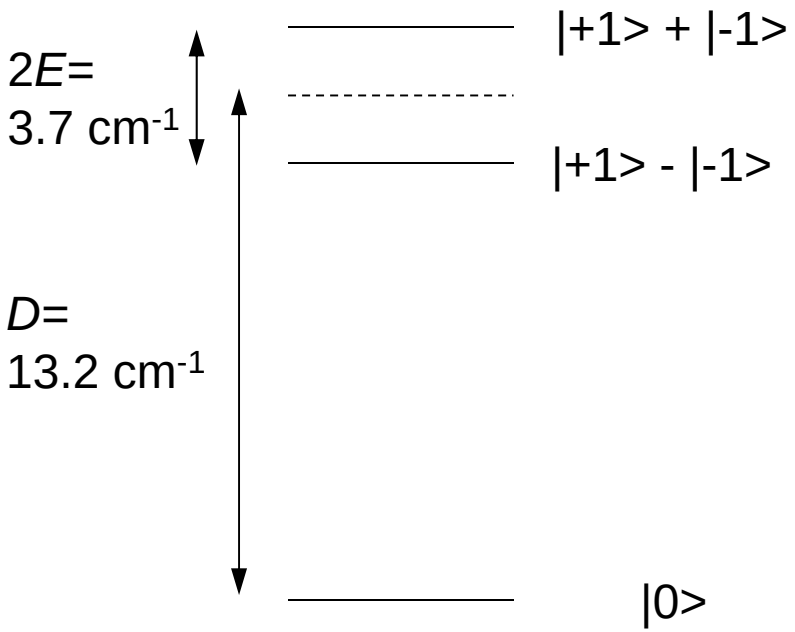


Vongtragool, IC, 2003

# Ch. 3. High-Frequency EPR

## Section 3.3 Frequency domain methods



**Example 3. $(NBu_4)^+[Ln(Pc)_2]^-$**

- Bruker 113v FTIR, Ln = Ho.

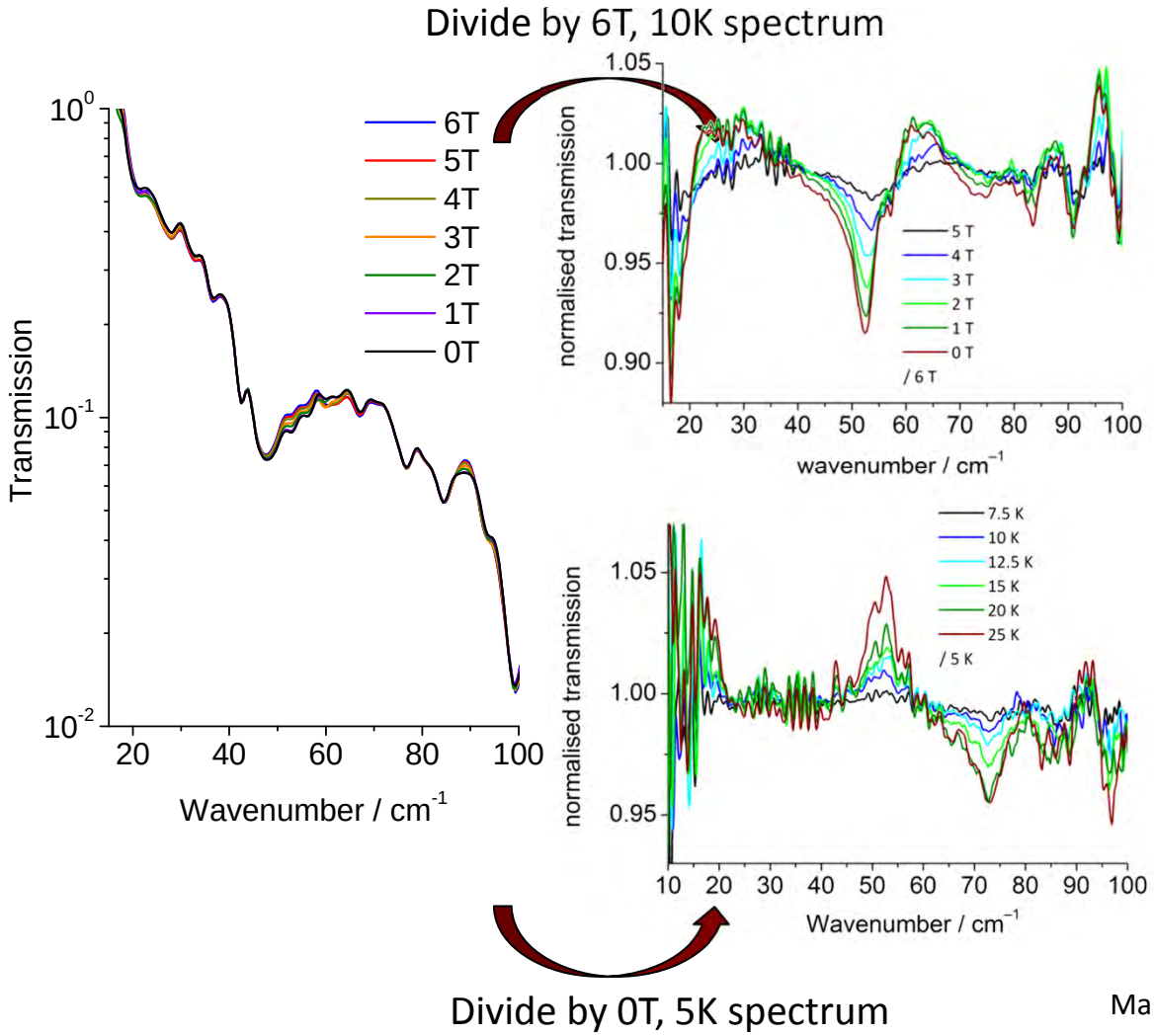


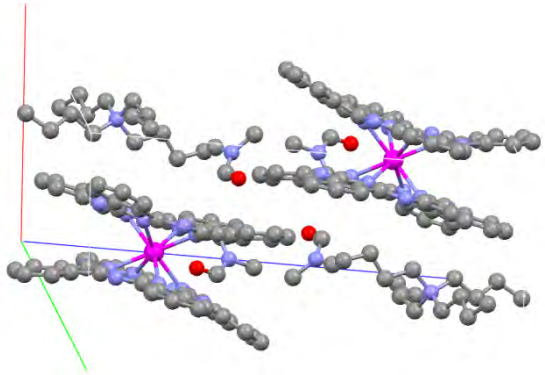

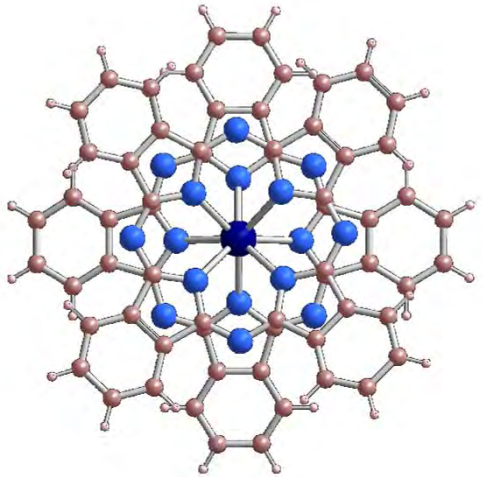

Marx, Dörfel, Moro, Waters, Van Slageren, unpublished

1. Introduction
2. Single Crystal Magnetometry
3. High-Frequency EPR Spectroscopy
4. Inelastic Neutron Scattering
5. Electronic Absorption and Luminescence

# Ch. 4. Inelastic Neutron Scattering

## Section 4.1 Theoretical background and experimental considerations



**Introduction**

- Neutrons can have energies in the same range as the microwave/THz electromagnetic radiation used in EPR.
- However, the neutron wavelength is much shorter, and can be of the order of bond distances.
- Some data on the neutron:
- Mass m = 1.674927351(74)×$10^{-27}$ kg
- Magnetic moment $\mu$ = –1.04187563(25)×$10^{-3}$ $\mu_B$.
- Spin s = ½.
- De Broglie wavelength : $\lambda = \frac{h}{p} = \frac{h}{\sqrt{2mE}} = \frac{9.044605}{\sqrt{E}[\mathrm{meV}]}[\mathrm{Å}]$

- For an energy of $E$ = 25 $cm^{-1}$ ≈ 3 meV, $\lambda$ = 5 Å
- Rather than the wavelength, we can deal with the wave vector $\vec{k} = \frac{2\pi}{\lambda}$

# Ch. 4. Inelastic Neutron Scattering

## Section 4.1 Theoretical background and experimental considerations



**Introduction**

- Because the wavelength is much shorter than for photons of the same energy, we have to consider momentum conservation in addition to energy conservation.
- Energy conservation: the energy change of the neutron is taken up by the sample: $\Delta E = \hbar\omega = E_f - E_i$.
- Momentum conservation: $\Delta \boldsymbol{k} = \hbar \boldsymbol{Q} = \hbar(\boldsymbol{k}_i - \boldsymbol{k}_f)$
- Neutrons are detected at different angles.
- Time of arrival corresponds to kinetic energy
- Plot of S(Q,ω).
- Selection rules $\Delta S = 0, \pm 1$; $\Delta m_S = 0, \pm 1$

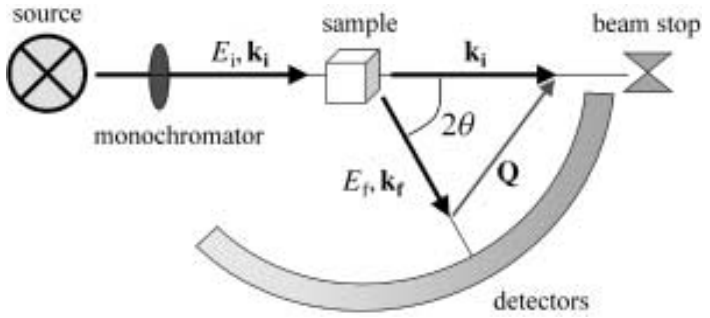


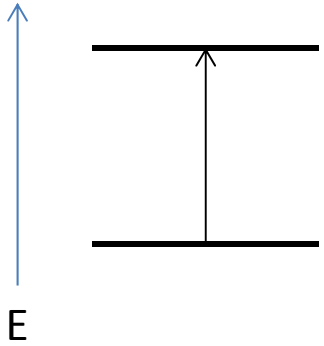


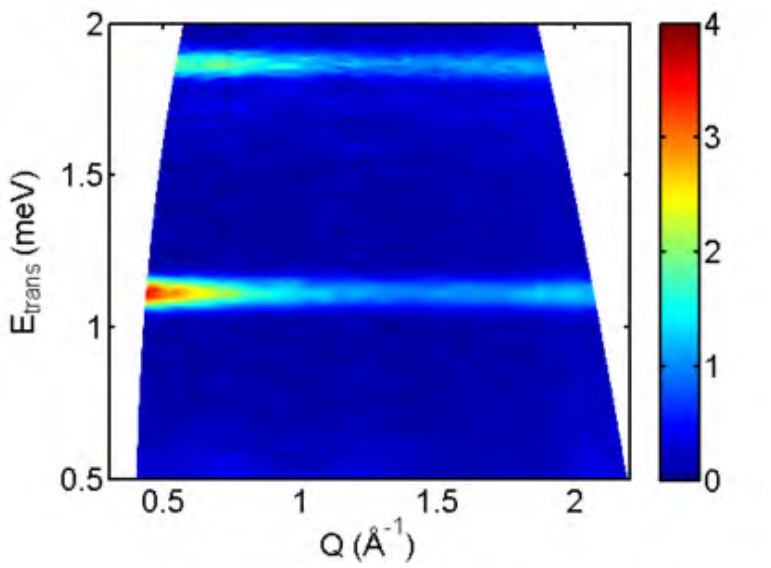

# Ch. 4. Inelastic Neutron Scattering

## Section 4.1 Theoretical background and experimental considerations



**Introduction**

- Determining the nature of the excitaton from the Q-dependence.
- Magnetic excitation:

$\Delta S = \pm 1$: $I_{i\to f}(\boldsymbol{Q},\omega) \to 0$

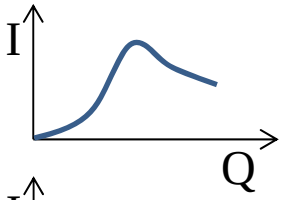


$\Delta S = 0$: $I_{i\to f}(\boldsymbol{Q},\omega) \to max$

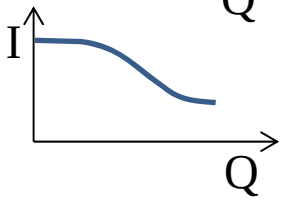


- Phonons:

$$I(Q,\omega,T) \propto Q^2 \times \frac{1}{1-e^{\hbar\omega/k_B T}}$$

- Generally confine to low Q to focus on magnetic transitions

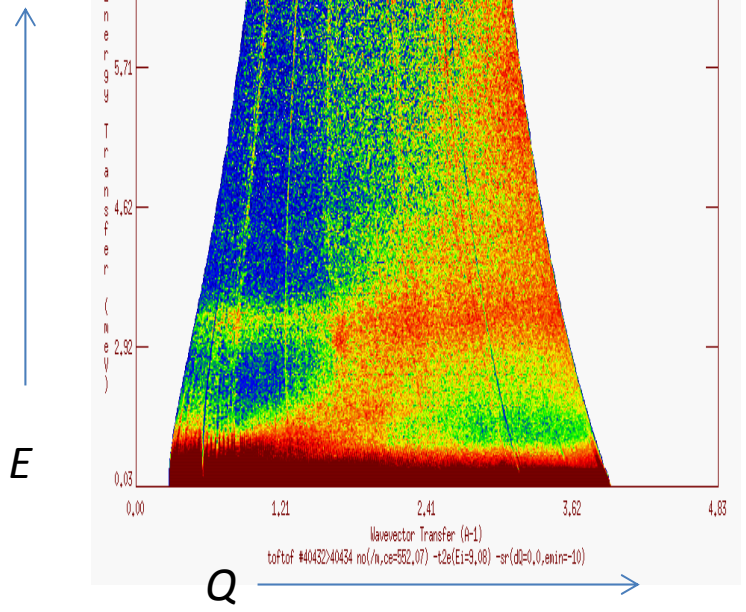

# Ch. 4. Inelastic Neutron Scattering

## Section 4.1 Theoretical background and experimental considerations



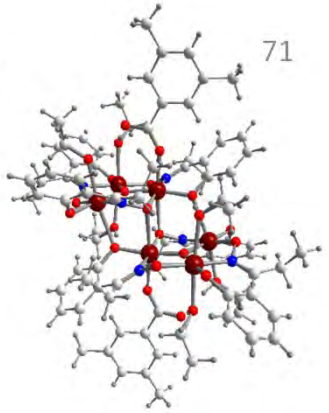

**Example: Mn6**

- Compare INS with FDMR

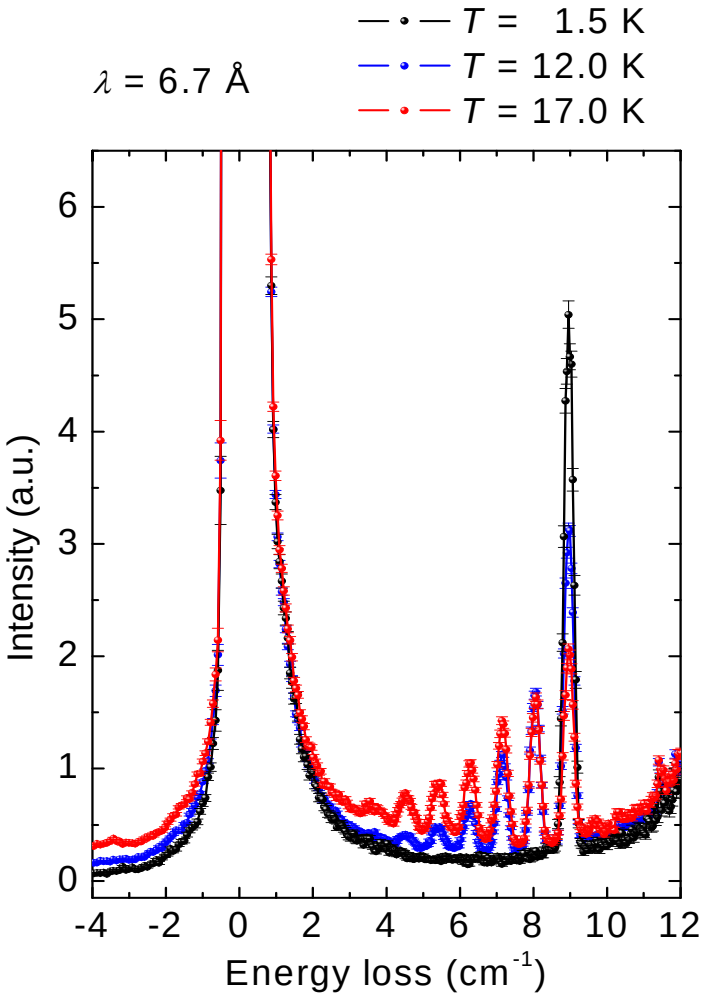


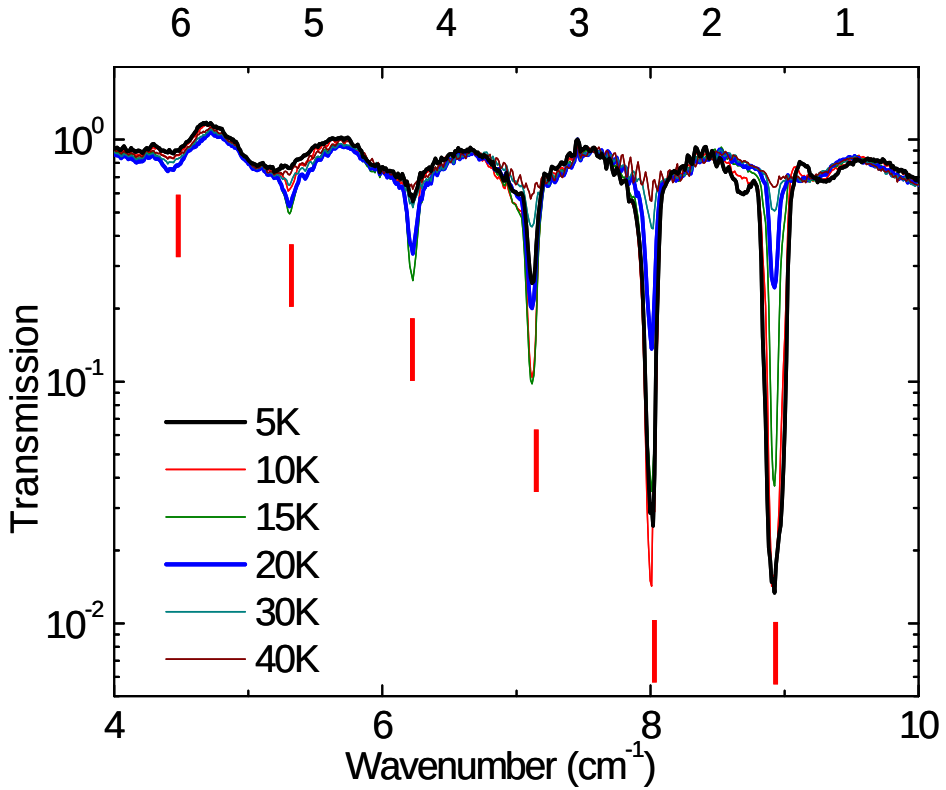


Pieper, PRB, 2010

# Ch. 4. Inelastic Neutron Scattering

## Section 4.1 Theoretical background and experimental considerations



**FDMR vs HFEPR vs INS**

| | HF Cavity EPR | HFEPR/FDMRS | INS |
|---|---|---|---|
| **Selection rules** | $\Delta M_S = \pm 1, \Delta S = 0$ | $\Delta M_S = \pm 1, \Delta S = 0$ | $\Delta M_S = 0, \pm 1, \Delta S = 0, \pm 1$ |
| **Sample quantity** | **Few mg** | **50 – 200 mg** | **1 g** |
| **Resolution** | **$10^{-2}$ cm$^{-1}$** | **$10^{-2}$ cm$^{-1}$** | **0.5 cm$^{-1}$** |

**Intensity**

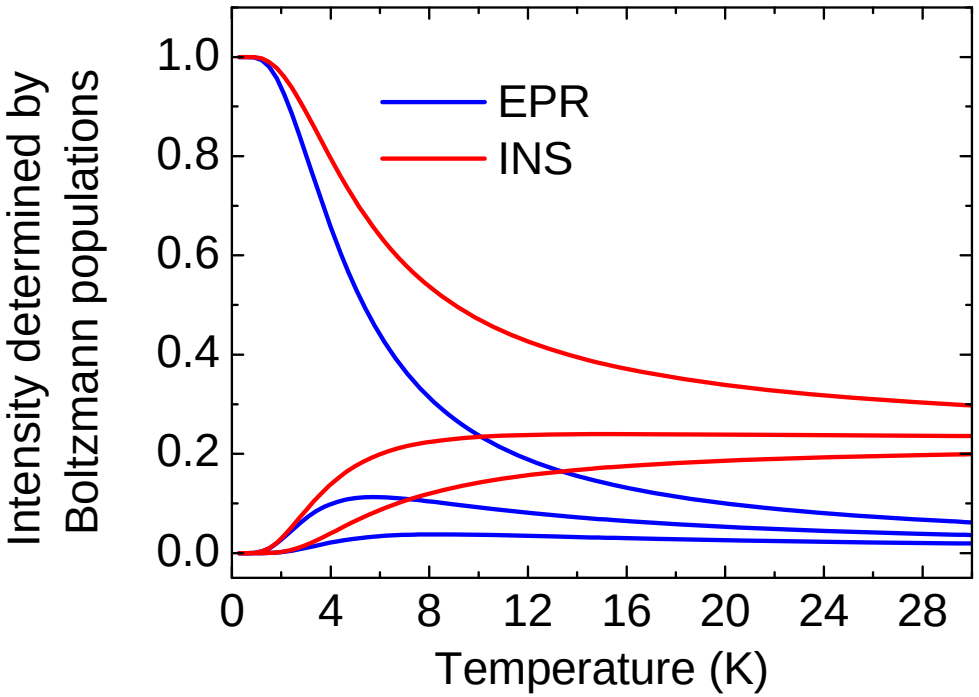

# Ch. 4. Inelastic Neutron Scattering

## Section 4.1 Theoretical background and experimental considerations



**Example: Mn6**

- Take advantage of the ΔS = 0, ±1 selection rule of INS

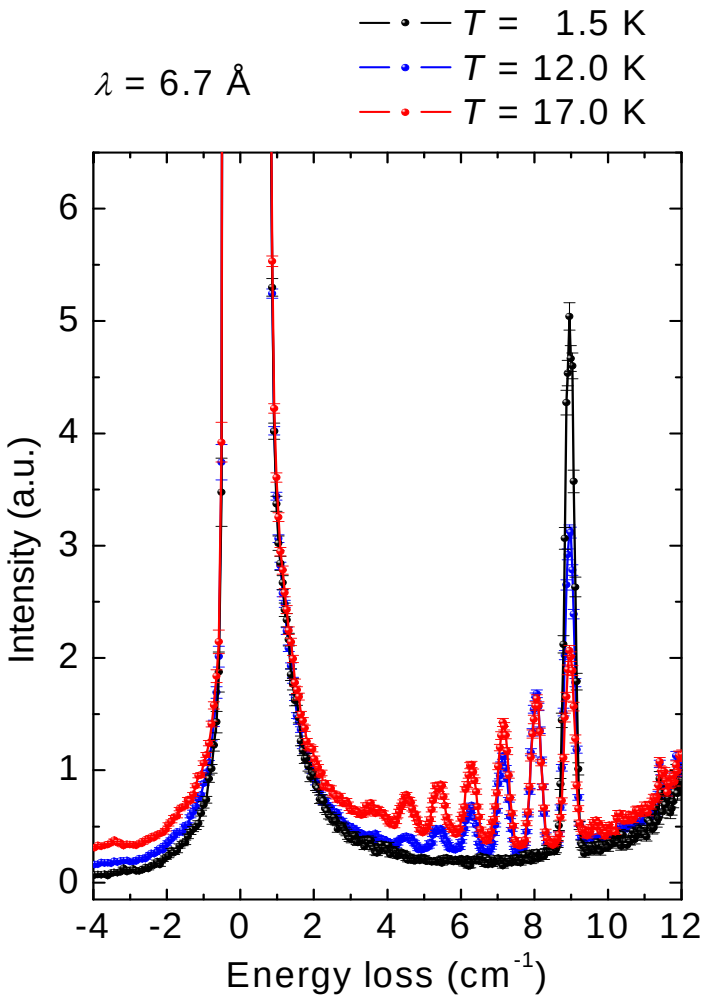


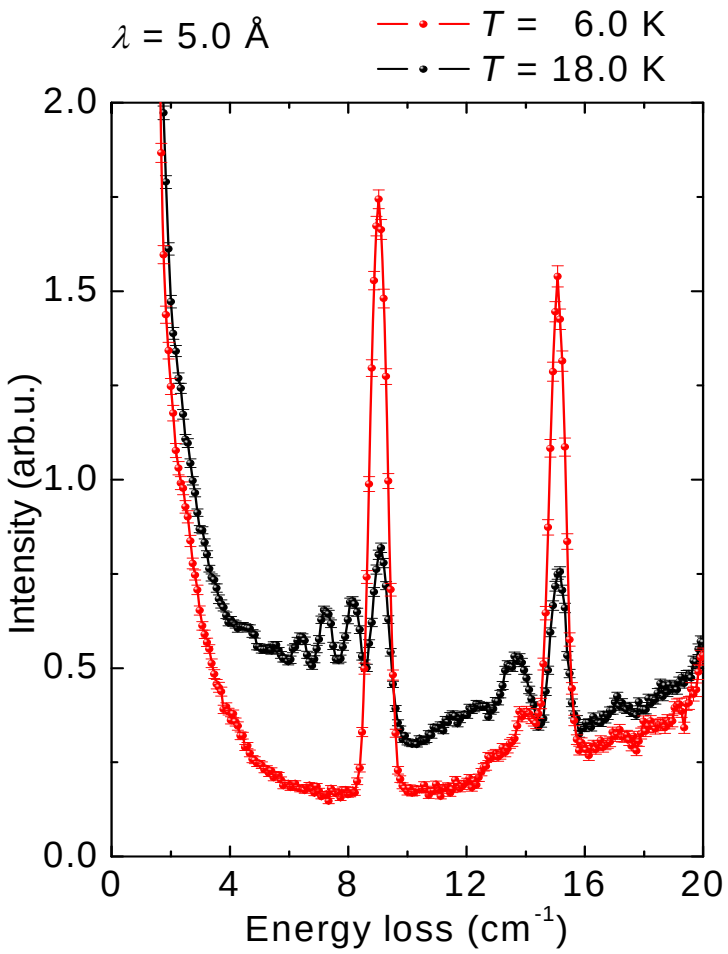


Pieper, PRB, 2010

# Ch. 4. Inelastic Neutron Scattering

## Section 4.1 Theoretical background and experimental considerations



**Example: Mn6**

- The Q dependence reveals the nature of the spin excitation

$\Delta S = \pm 1$: $I_{i\to f}(\boldsymbol{Q},\omega) \to 0$

$\Delta S = 0$: $I_{i\to f}(\boldsymbol{Q},\omega) \to max$

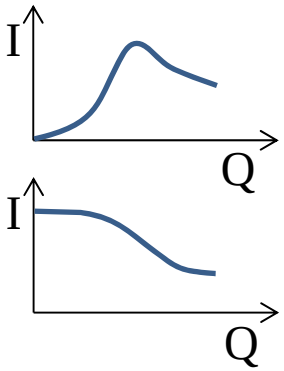


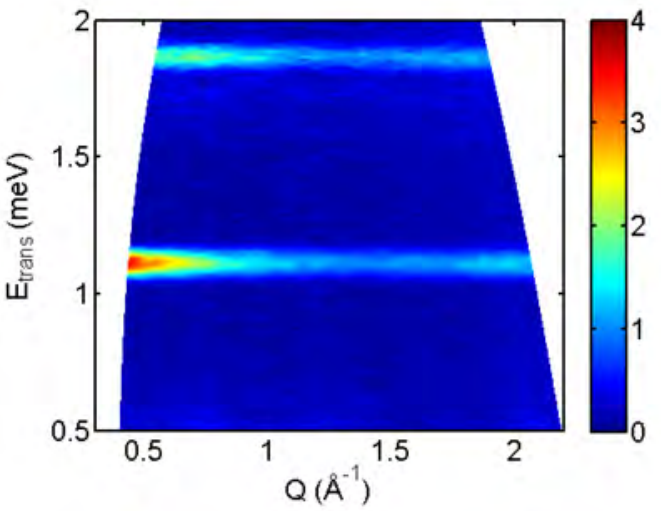


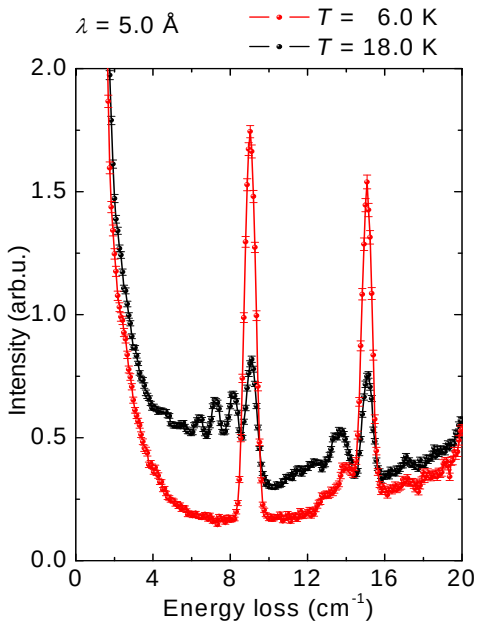


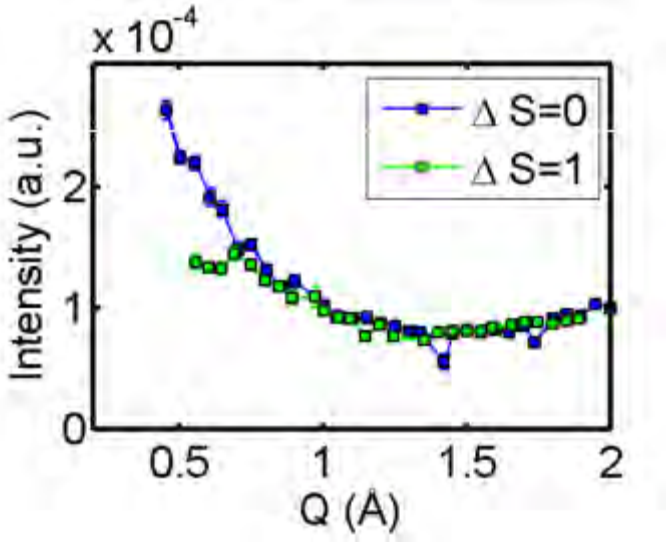


Pieper, PRB, 2010

1. Introduction
2. Single Crystal Magnetometry
3. High-Frequency EPR Spectroscopy
4. Inelastic Neutron Scattering
5. Electronic Absorption and Luminescence

# Ch. 5. Electronic Absorption and Luminescence

## Section 5.1 Electronic Absorption



**Lanthanides**

- f-Orbitals are buried deep within the electron cloud
- ff-transitions are Laporte-forbidden (u ↔ u)
- Hence, the extinction coefficients are very small ($\varepsilon \sim 1\ M^{-1}\ cm^{-1}$), cf. dd $10^2$, CT $10^4$.
- On the other hand, the absorption bands are very narrow, and split due to the CF splitting of the **excited** state.

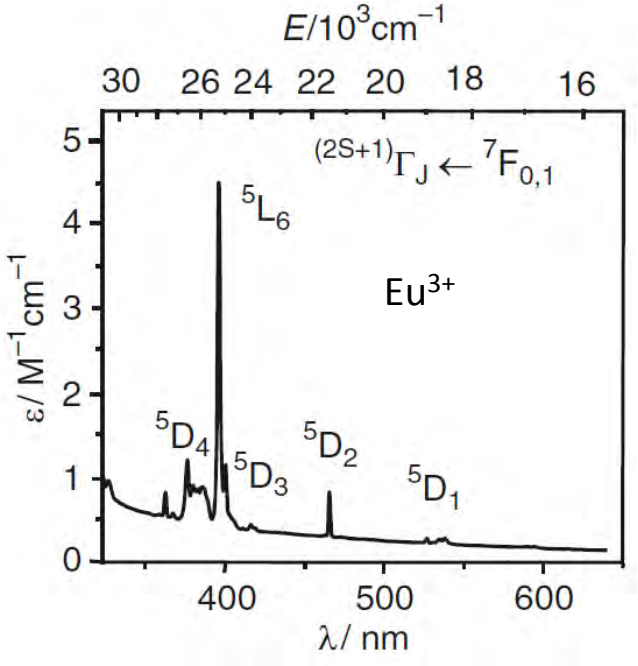


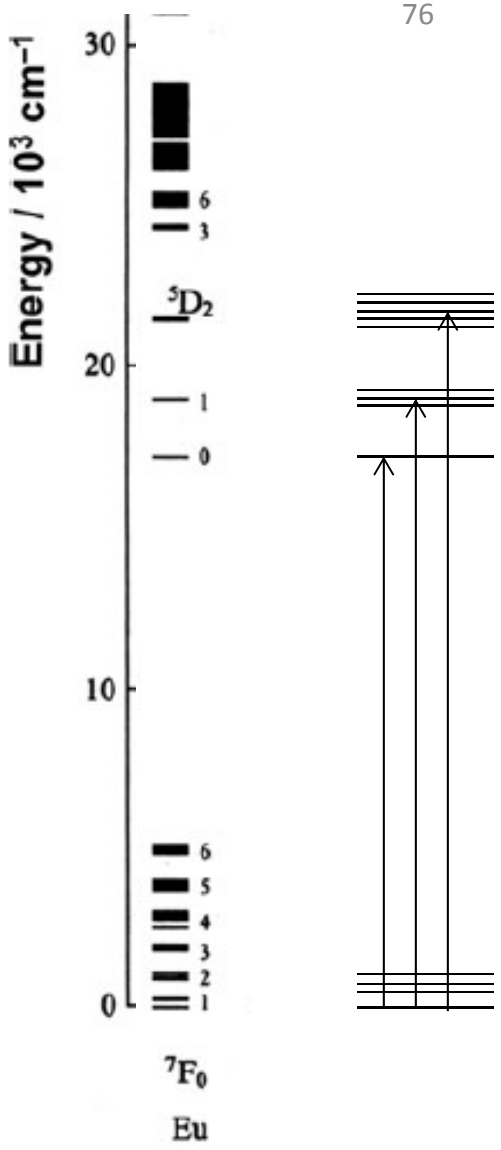


Bünzli in Lanthanide Luminescence: Photophysical, Analytical and Biological Aspects, Springer Ser Fluoresc (2010), DOI 0.1007/4243_2010_3

# Ch. 5. Electronic Absorption and Luminescence

## Section 5.1 Electronic Absorption



**Lanthanides**

- Excitations can be electric dipole, magnetic dipole, or electric quadrupole
- In actinides, extinction coefficients are larger.
- Judd-Ofelt theory describes the absorption intensity of ED transitions.

$$D_{\mathrm{ED}} = e^2 \sum_{\lambda=2,4,6} \Omega_\lambda \left| \langle \Psi \| U^\lambda \| \Psi' \rangle \right|^2,$$

- Parameters Ω are phenomenological.

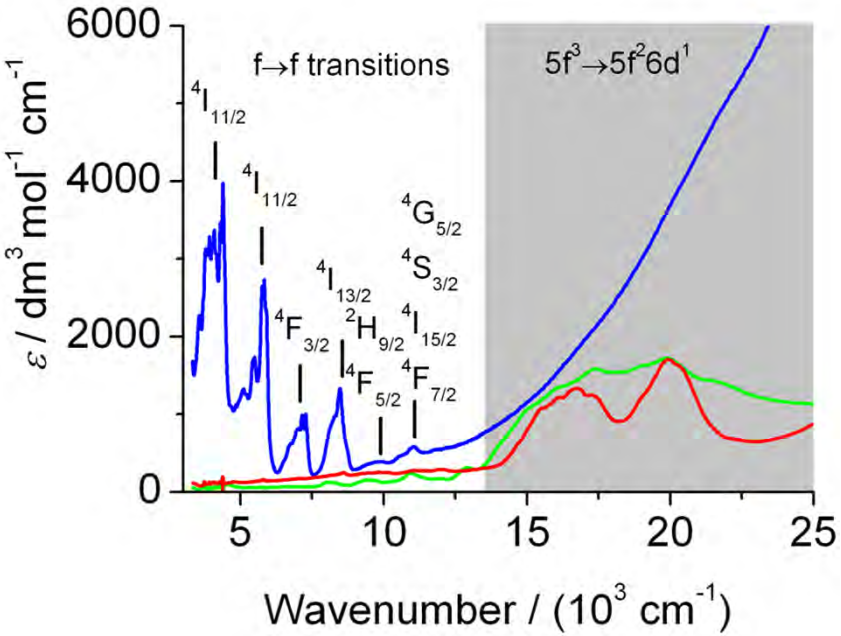


**Table 5** Selection rules for intra-configurational f–f transitions

| Operator | Parity | $\Delta S$ | $\Delta L$ | $\Delta J$[a] |
|---|---|---|---|---|
| ED | Opposite | 0 | $\leq 6$ | $\leq 6$ (2,4,6 if $J$ or $J' = 0$) |
| MD | Same | 0 | 0 | $0, \pm 1$ |
| EQ | Same | 0 | $0, \pm 1, \pm 2$ | $0, \pm 1, \pm 2$ |

[a] $J = 0$ to $J' = 0$ transitions are always forbidden

Bünzli in Lanthanide Luminescence: Photophysical, Analytical and Biological Aspects, Springer Ser Fluoresc (2010), DOI 0.1007/4243_2010_3
Mills, Nature Chem. 2011

# Ch. 5. Electronic Absorption and Luminescence

## Section 5.2 Luminescence

**Lanthanides**

- Many lanthanides are strongly luminescent.


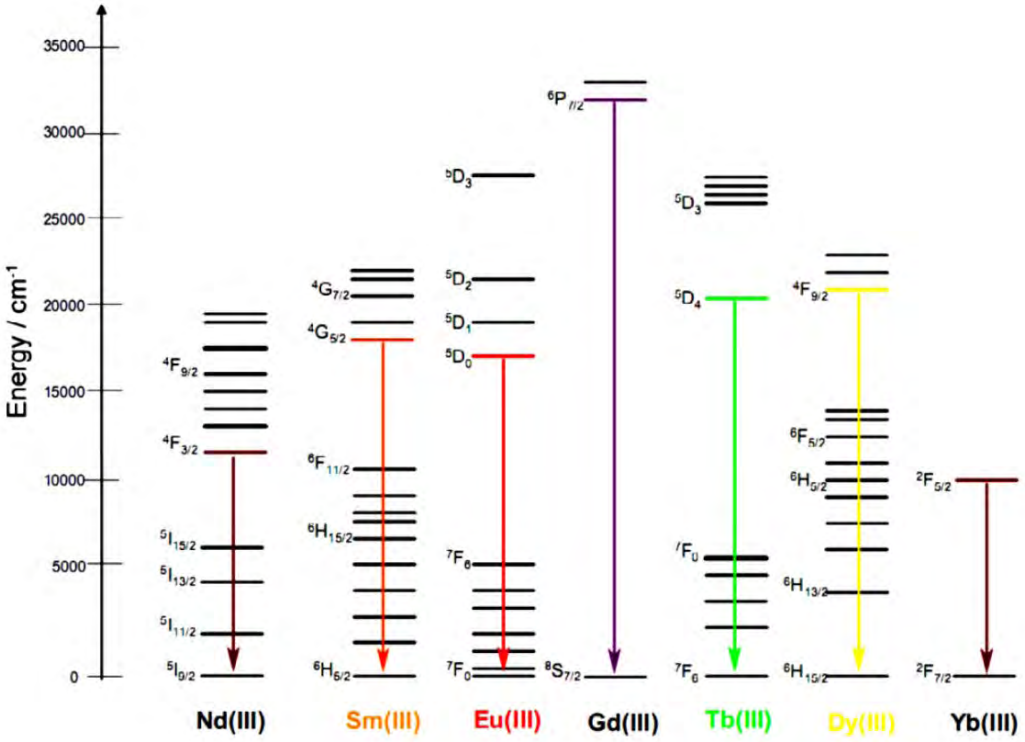


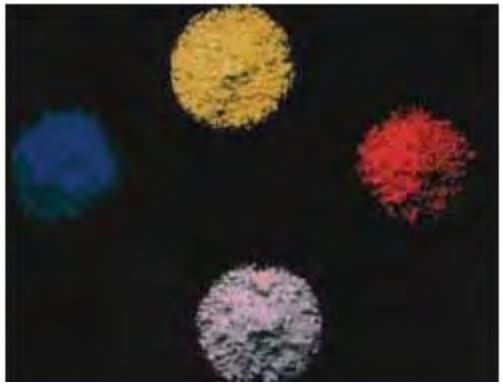

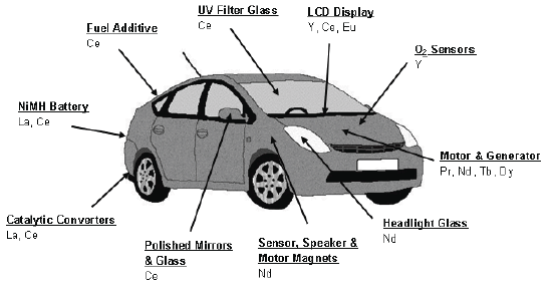


Natrajan, EUFEN2, COST CM 1006, Dublin 2013

# Ch. 5. Electronic Absorption and Luminescence

## Section 5.2 Luminescence



**Lanthanides**

- The splitting of the luminescence band yields information on the crystal field splitting of the ground state.

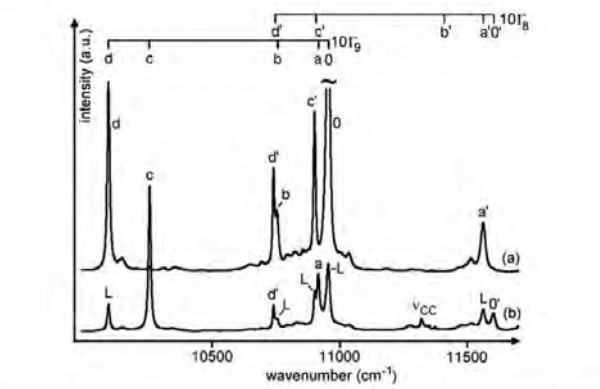


Fig. 1. Luminescence spectra of $NdCp^*_3$ in the range 10000–11700 cm$^{-1}$: (a) σ spectrum; (b) π spectrum. 0, a, b, c, d resp. 0′, a′, b′, c′, d′ signify transitions initiating at $10\Gamma_9$ and $10\Gamma_8$, respectively, and terminating at the states $1\Gamma_7$ (ground state), $1\Gamma_9$, $1\Gamma_8$, $2\Gamma_9$ and $2\Gamma_7$ of the ground multiplet $^4I_{9/2}$. L denotes polarization leaks.

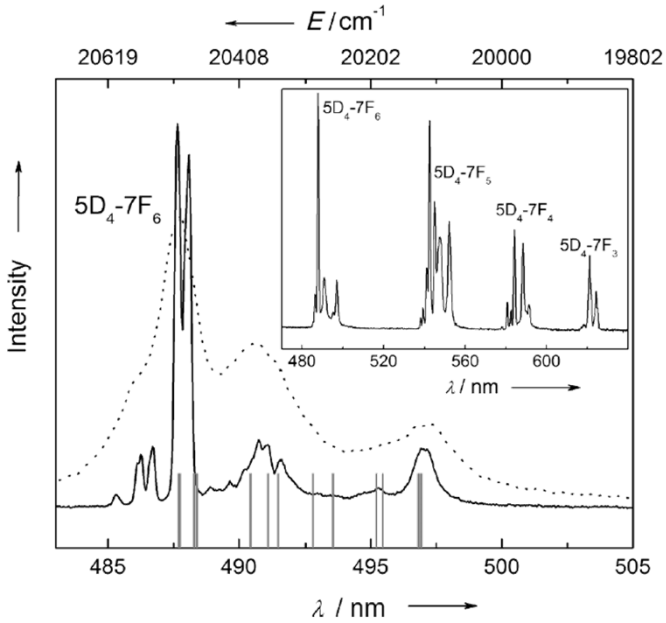


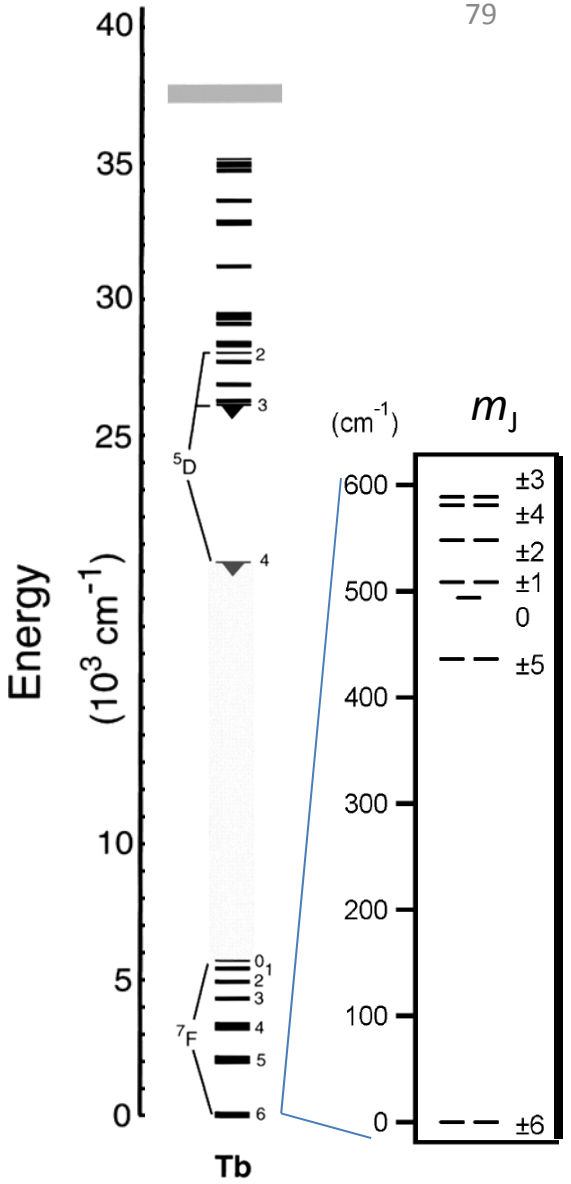


H.-D. Amberger, many publications; Görller-Wallrand, many publications; Boulon, ACIE, 2013

# Ch. 5. Electronic Absorption and Luminescence

## Section 5.3 Magnetic Circular Dichroism



**Magnetic Circular Dichroism**

- The intensity of an absorption band due to an electronic transition between two states is proportional to the square of the electric dipole matrix element:

$$I \propto \left| \langle X | \varepsilon | G \rangle \right|^2$$

- In MCD, the difference in absorption between left- ($\sigma^-$)and right-($\sigma^+$)-circularly polarised light is measured:

$$\varepsilon_{MCD} = \tfrac{1}{2}\left(\varepsilon_+ - \varepsilon_-\right)$$

- No MCD without field.

**Applied magnetic field** can:

- Lift magnetic degeneracies of the ground and excited states.
- Change the population of the levels via a new Boltzmann distribution.
- Mix the levels G and X with other electronic levels.

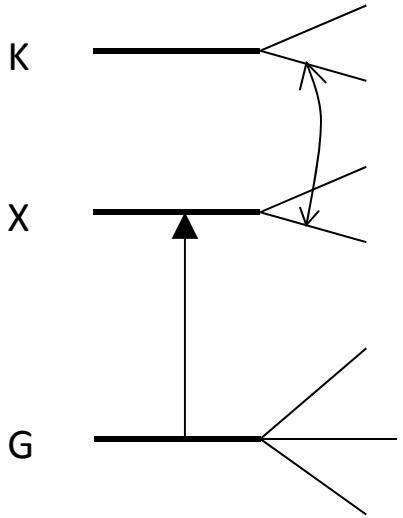

# Ch. 5. Electronic Absorption and Luminescence

## Section 5.3 Magnetic Circular Dichroism



**Magnetic Circular Dichroism**

- This leads to three contributions to the MCD spectrum:
  - the A-term, due to Zeeman splitting of the ground and/or excited degenerate states,
  - the B-term, due to field-induced mixing of states,
  - the C-term, due to a change in the population of molecules over the Zeeman sublevels of a paramagnetic ground state.

$$\frac{\Delta\varepsilon}{E} = \gamma\mu_B B\left[-A_1\frac{\partial f(E)}{\partial E} + \left(B_0 + \frac{C_0}{k_B T}\right) f(E)\right]$$

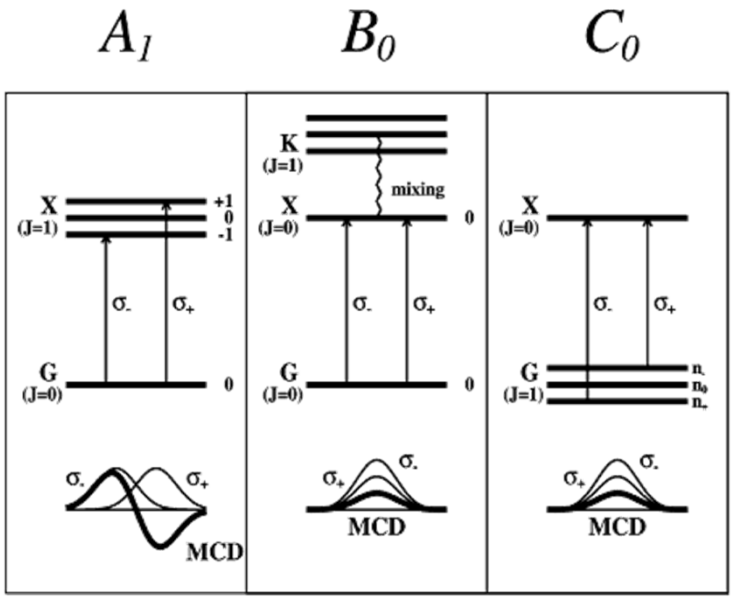


- Δε is MCD extinction coefficient.
- E = hν.
- γ is bunch of constants including dielectric permittivity.
- $\mu_B$ is Bohr magneton.
- f(E) is lineshape function.

# Ch. 5. Electronic Absorption and Luminescence

## Section 5.3 Magnetic Circular Dichroism



**Magnetic Circular Dichroism. Example 1 [$Cr_8F_8Piv_{16}$]**

- UV/Vis spectrum gives energies of excited states.
- Spin-allowed transitions stronger than spin-forbidden.
- Exchange coupling enhances intensity of spin-forbidden transitions.
- Resolution typically not enough to resolve all transitions.

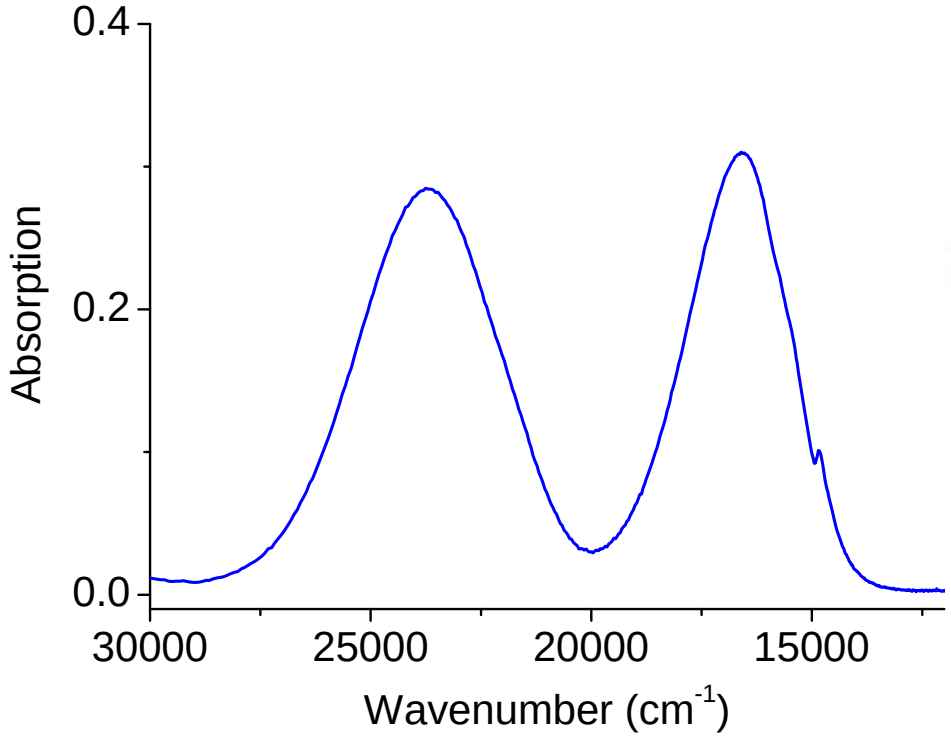


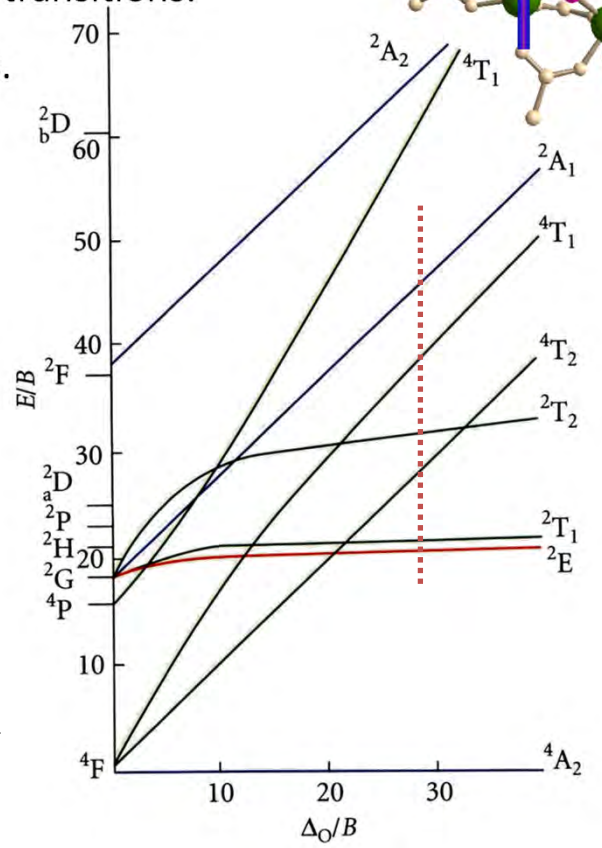


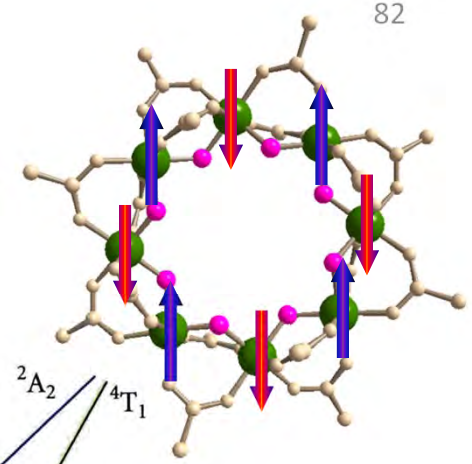

Piligkos, Van Slageren, Dalton Trans. 2010

# Ch. 5. Electronic Absorption and Luminescence

## Section 5.1 Theoretical background and experimental considerations



**Magnetic Circular Dichroism. Example 1 [$Cr_8F_8Piv_{16}$]**

- MCD signal can be both positive and negative.
- This often leads to much better resolution.
- Spin forbidden transitions are often pronounced.

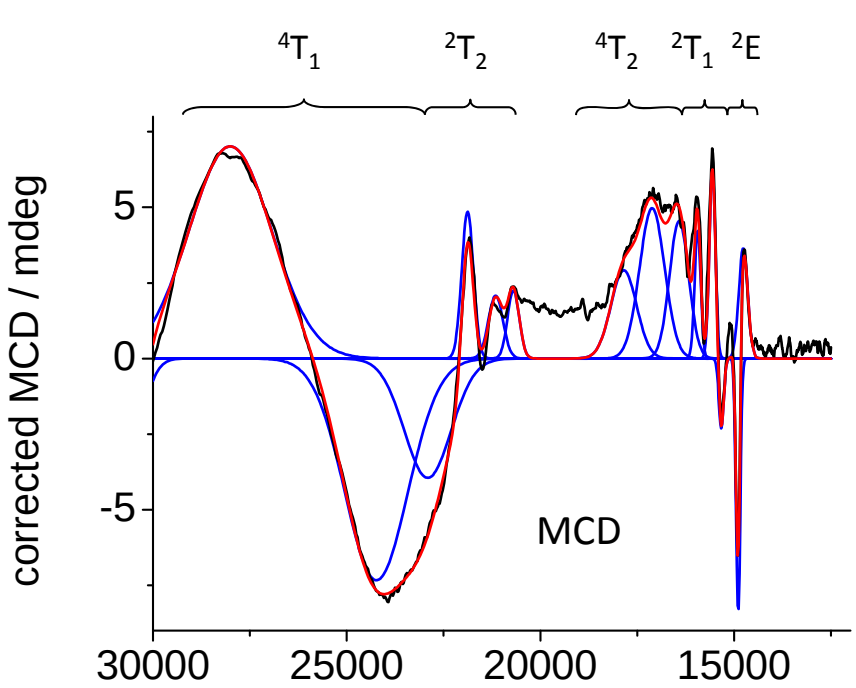


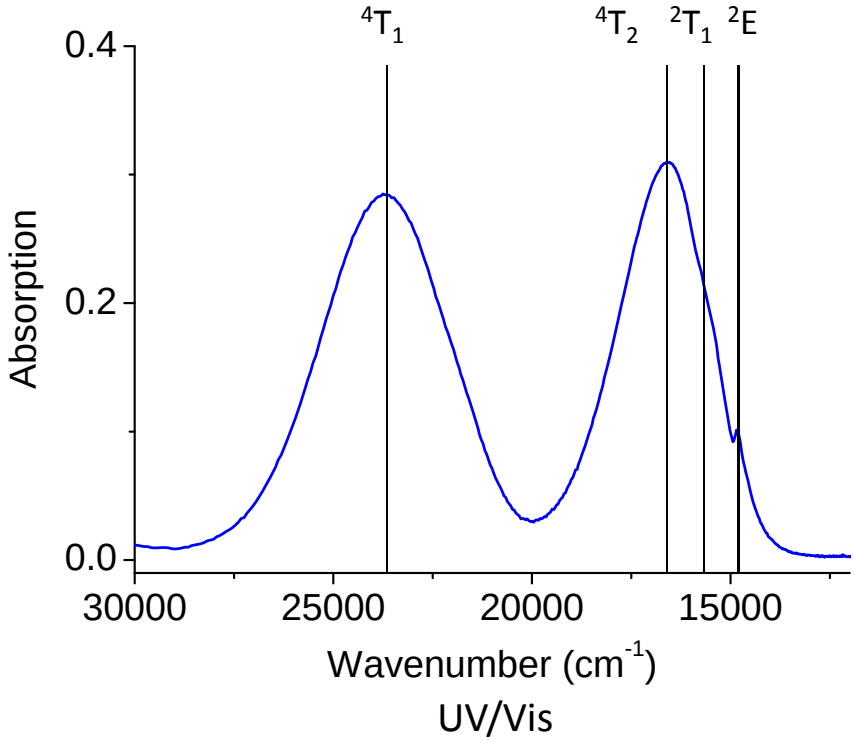


Piligkos, Van Slageren, Dalton Trans. 2010

# Ch. 5. Electronic Absorption and Luminescence

## Section 5.3 Magnetic Circular Dichroism



**Magnetic Circular Dichroism. Example 1 [$Cr_8F_8Piv_{16}$]**

- MCD splitting of absorption bands is related to ZFS.
- $\mathcal{H} = d\,\hat{S}_z^2 + e\,(\hat{S}_x^2 - \hat{S}_y^2)$.
- d = -0.364 $cm^{-1}$; e = 0.119 $cm^{-1}$.
- cf. d = -0.334 $cm^{-1}$ (strong exchange)
- cf. d = -0.24 $cm^{-1}$; e = 0.032 $cm^{-1}$ (microscopic, neglecting dipolar).

$$d_{Cr} = -\tfrac{1}{2}\zeta^2\left\{\frac{8}{3\Delta E_1} - \frac{4}{3\Delta E_2} - \frac{4}{3\Delta E_3}\right\}$$

$$e_{Cr} = -\tfrac{1}{2}\zeta^2\left\{\frac{4}{3\Delta E_2} - \frac{4}{3\Delta E_3}\right\}$$

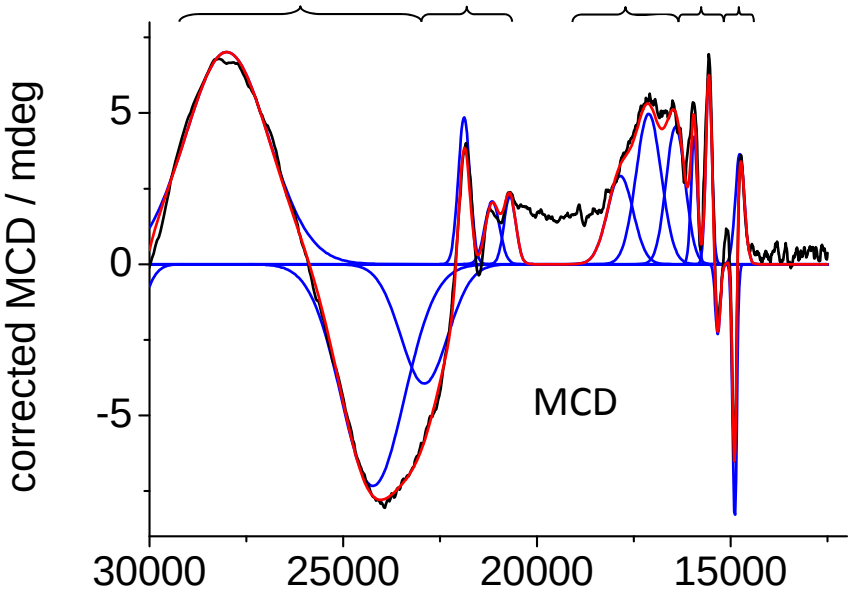


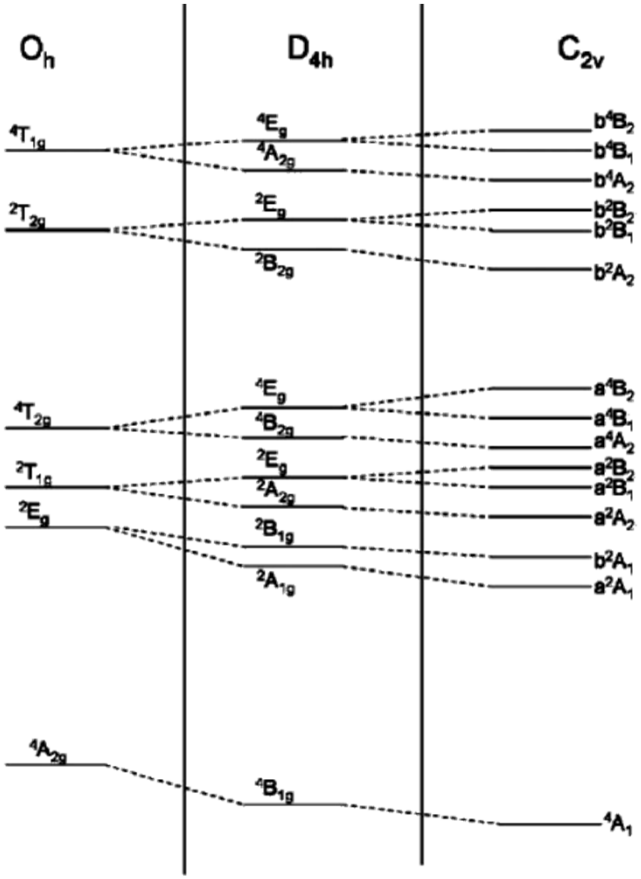


Piligkos, Van Slageren, Dalton Trans. 2010; Bradley, Dalton Trans. 2008

# Ch. 5. Electronic Absorption and Luminescence

## Section 5.3 Magnetic Circular Dichroism



**Magnetic Circular Dichroism. Example 1 [$Cr_8F_8Piv_{16}$]**

- MCD intensity is related to the magnetization of the sample.
- It gives information about the magnetic properties of the cluster.
- MCD intensity vs. B or vs. B/T shows more than just a step at the level crossing from $S = 0$ to $S = 1$.
- No MCD intensity is expected for the $S = 0$ state.

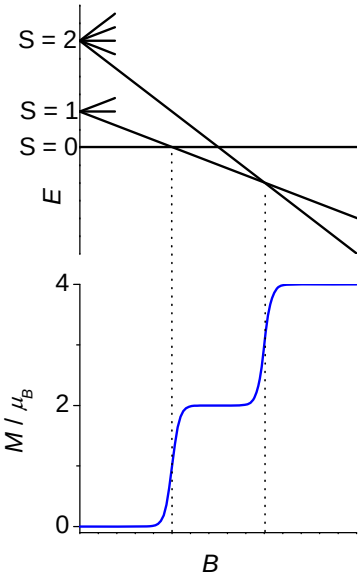


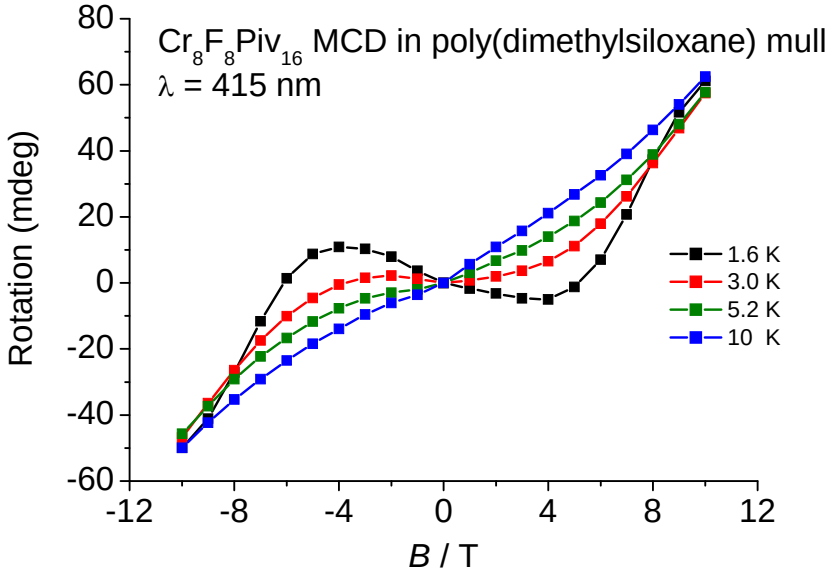


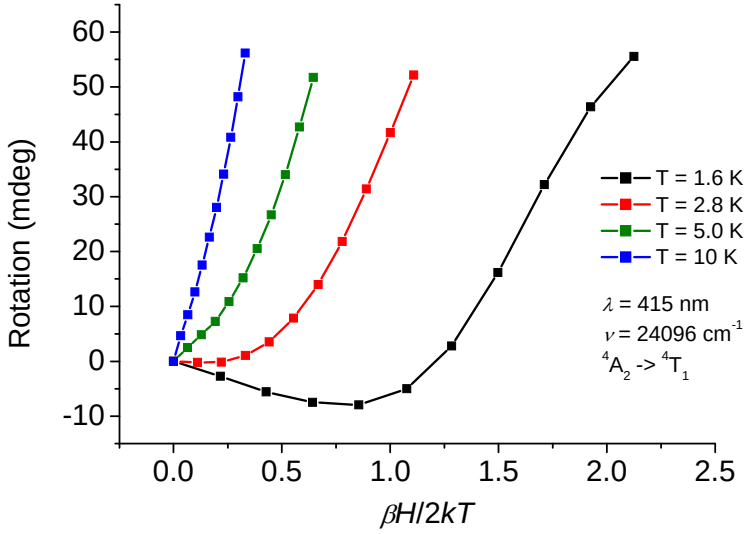


Piligkos, Van Slageren, Dalton Trans. 2010

# Ch. 5. Electronic Absorption and Luminescence

## Section 5.3 Magnetic Circular Dichroism



**Magnetic Circular Dichroism. Example 1 [$Cr_8F_8Piv_{16}$]**

- MCD curves cannot be simulated by summing contributions due to different spin states.
- Mixing between spin states occurs.
- Rhombic term (*E*) necessary.
- Spin Hamiltonian:

$$\mathcal{H} = -2J\sum_{i>j}\hat{\mathbf{S}}_i\cdot\hat{\mathbf{S}}_j + \sum_i d_i\hat{S}_z^2 + \sum_i e_i\left(\hat{S}_x^2 - \hat{S}_y^2\right) + \mu_B\mathbf{S}\cdot\mathbf{g}\cdot\mathbf{B}$$

- MCD intensity
- $$\frac{\Delta\varepsilon}{\dot{E}} = \frac{\gamma}{4\pi S}\int_0^{\pi}\int_0^{2\pi}\sum_i N_i\begin{pmatrix} l_x\left\langle\hat{S}_x\right\rangle_i M_{yz} + \\ l_y\left\langle\hat{S}_y\right\rangle_i M_{xz} + \\ l_z\left\langle\hat{S}_z\right\rangle_i M_{xy}\end{pmatrix}\sin\theta\,\mathrm{d}\theta\,\mathrm{d}\varphi$$

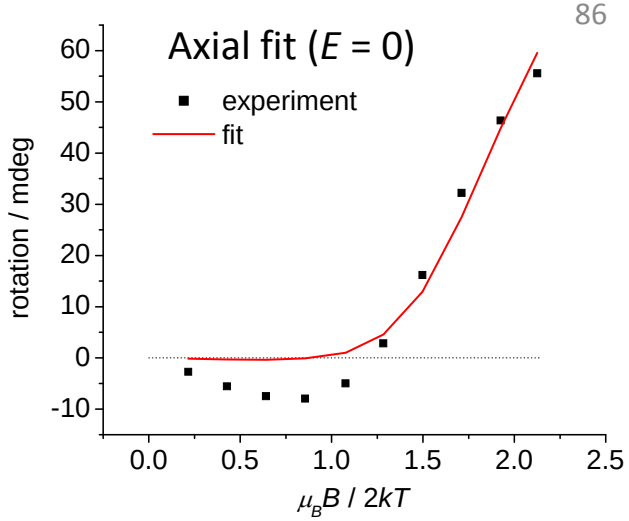


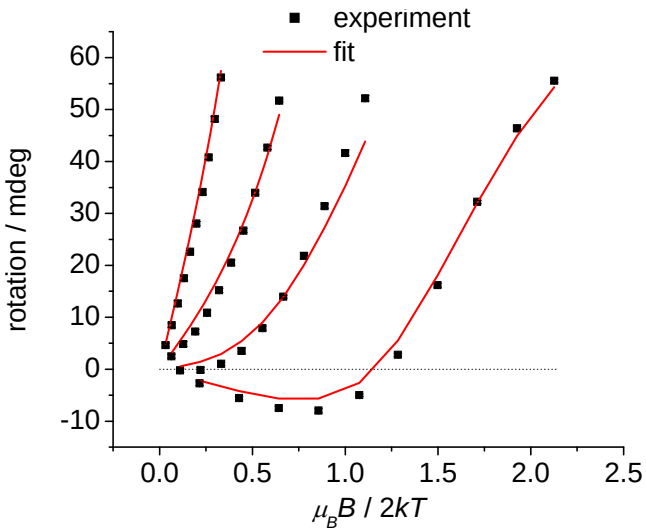


Rhombic fit ($E \neq 0$)

$S = 3/2$
$g = 1.98$
$D = -0.58\ cm^{-1}$
$E / D = 0.1$
$J = -3.5\ cm^{-1}$

Piligkos, Van Slageren, Dalton Trans. 2010

# Ch. 5. Electronic Absorption and Luminescence

## Section 5.1 Theoretical background and experimental considerations



**Magnetic Circular Dichroism. Example 2 $[Ln(Pc)_2]^-$**

- Anions in EtOH:MeOH glass.
- Transitions based on ligand.
- MCD bands have derivative lineshapes: A-term intensity.
- Lowest-energy transition has opposite MCD sign for $Tb^{3+}$ and $Dy^{3+}$.

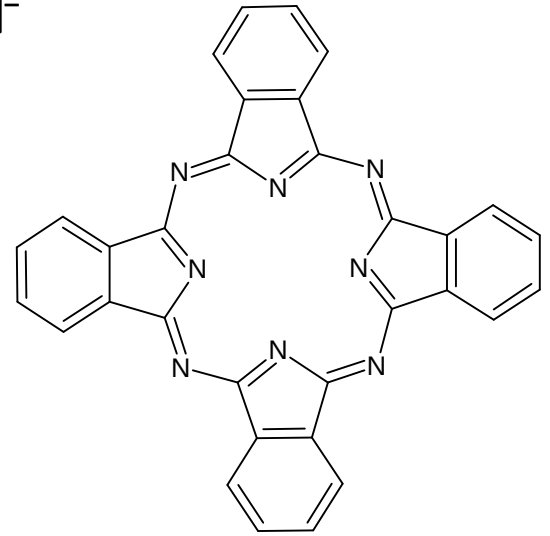

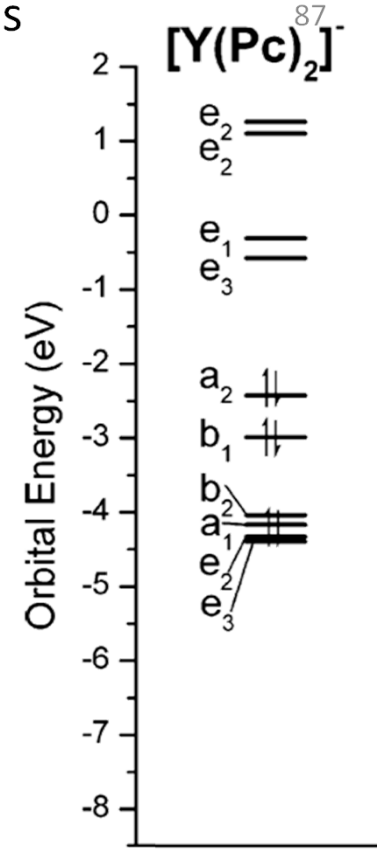


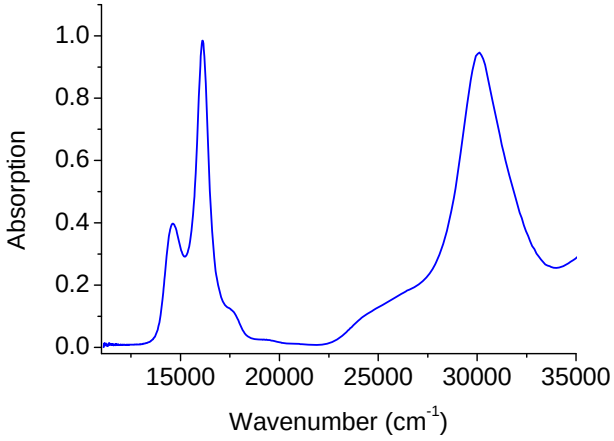


UV/Vis

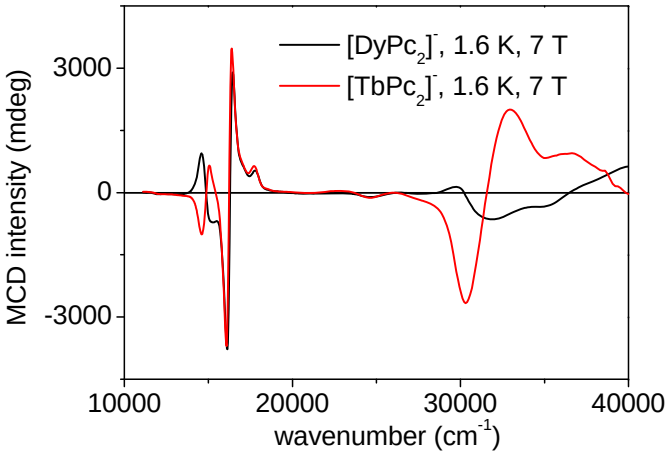


MCD

Krivokapic, Waters, Van Slageren, unpublished

# Ch. 5. Electronic Absorption and Luminescence

## Section 5.3 Magnetic Circular Dichroism



**Magnetic Circular Dichroism. Example 2 $[Ln(Pc)_2]^{0/-}$**

- Hysteresis is observed for all complexes in spite of ligand based nature of transitions.
- For $[DyPc_2]^0$ no hysteresis is observed in powder magnetisation measurements.

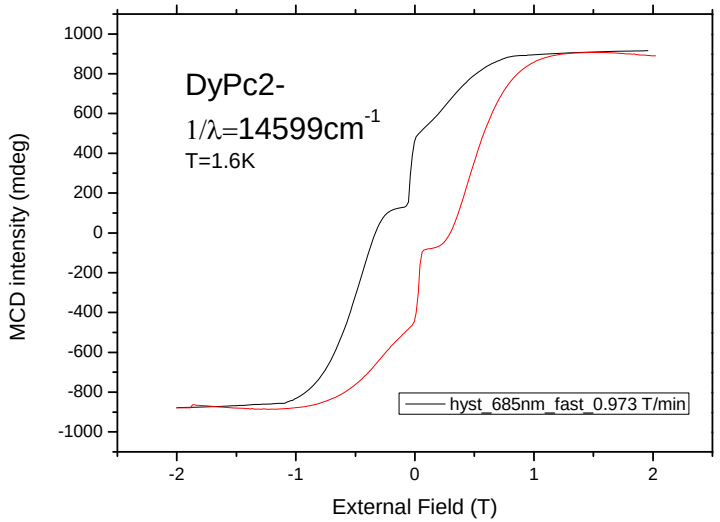


$[DyPc_2]^-$

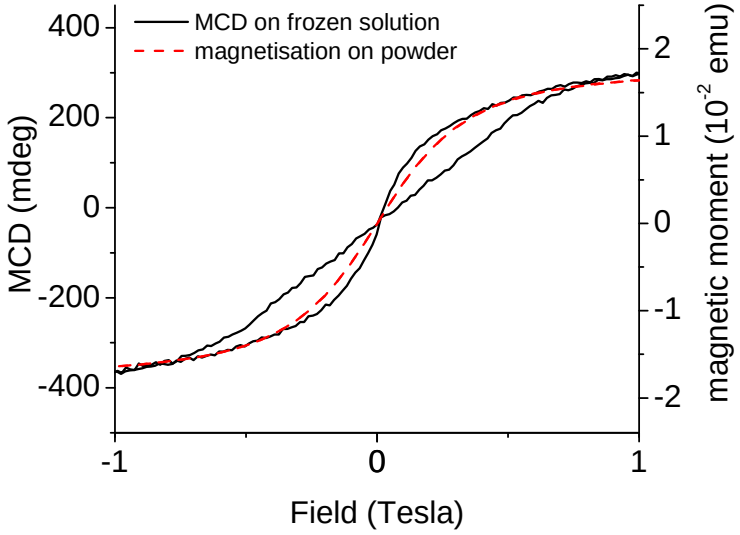


$[DyPc_2]^0$

Krivokapic, Waters, Van Slageren, unpublished; Gonidec, JACS, 2010

# Ch. 5. Electronic Absorption and Luminescence

## Section 5.3 Magnetic Circular Dichroism



**Magnetic Circular Dichroism. Example 3 $[C(NH_2)_3]_5[Ln(CO_3)_4]$ (1-Ln) with Ln = Dy, Er**

- Crystal field split ff transitions

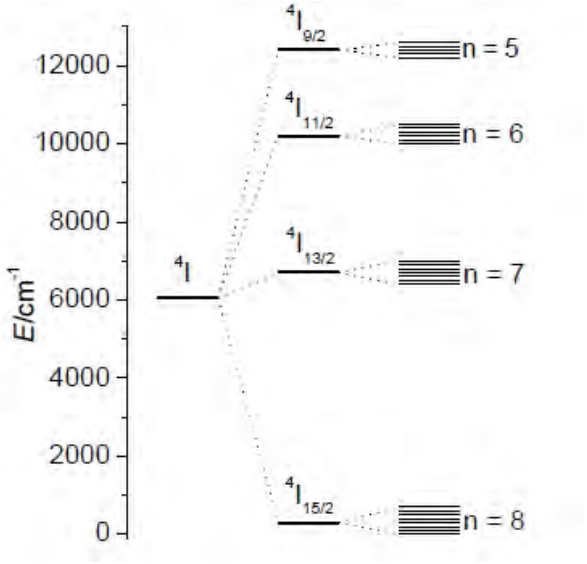


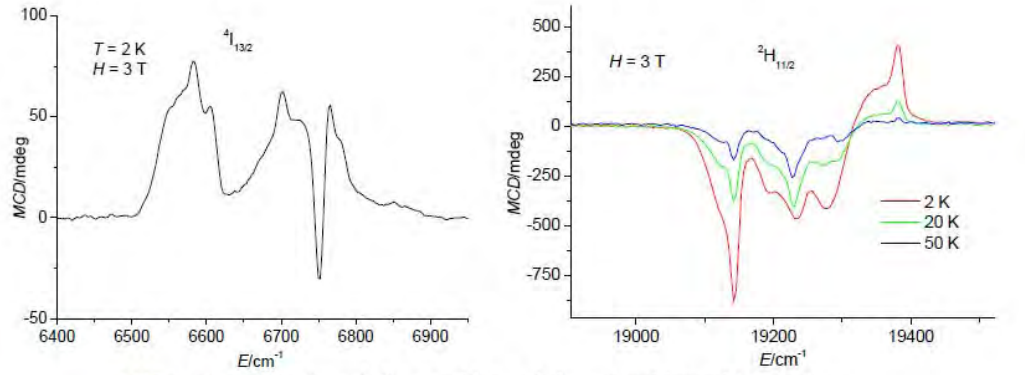


MCD spectra of the $^4I_{13/2} \leftarrow {}^4I_{15/2}$ and $^2H_{11/2} \leftarrow {}^4I_{15/2}$ transitions of **1-Er** at 3 T.

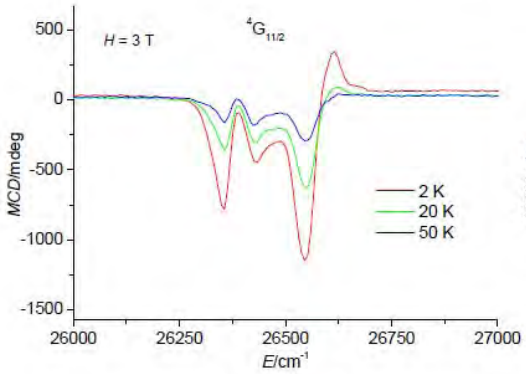


MCD spectra of the $^4G_{11/2} \leftarrow {}^4I_{15/2}$ transition of **1-Er** at 3 T.

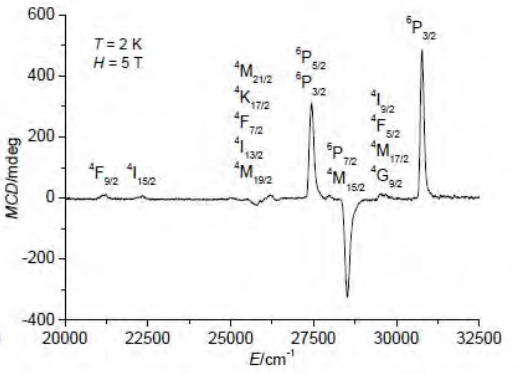


MCD spectrum in the visible region of **1-Dy** at 5 T and 2 K.

Rechkemmer, Van Slageren, unpublished

# Ch. 6. Some words on relaxation of the magnetization

## Section 6.1 Spin-Lattice relaxation



**The fundamental difference between magnetization dynamics in single-ion and polynuclear species**

- In polynuclear TM clusters, Arrhenius behaviour over many orders of magnitude; sharp transition to tunnelling
- In f-elements generally curved Arrhenius plots. Different temperature regime.
- The reason is that in single-ion systems, there are many relaxation pathways with different field- and temperature dependences (direct process, tunnelling, Raman, Orbach, multistep direct process).
- Hence a straight line in the Arrhenius plot is not necessarily expected

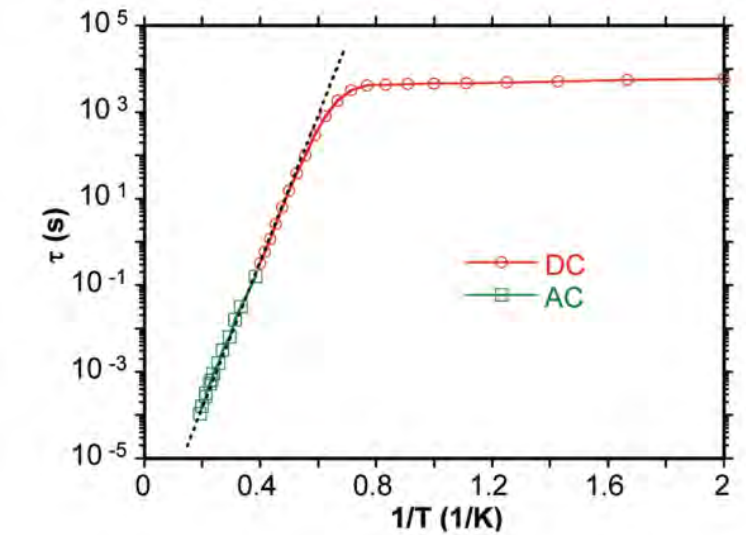


$[Mn_3O(Me\text{-}salox)_3(2,4'\text{-}bpy)_3(ClO_4)]$, Yang, Tsai, *IC*, 2008

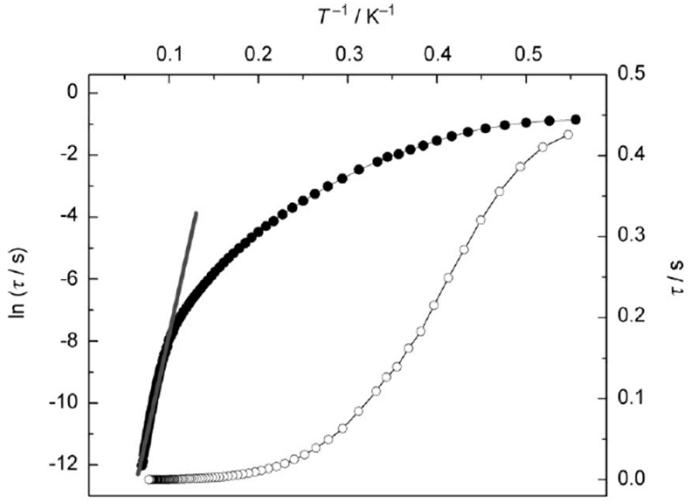


$[Dy(hfac)_3(PyNO)]_2$, Yi, CEJ, 2012

# Ch. 6. Some words on relaxation of the magnetization

## Section 6.1 Spin-Lattice relaxation



**The fundamental difference between magnetization dynamics in single-ion and polynuclear species**

**The first f-element "single-molecule magnets".**

- Relaxation parameters

| | $\Delta E/k_B$ (K) | $\tau_0$ (s) | ref |
|---|---|---|---|
| • Tb/– | 331 | 6.3 x $10^{-8}$ | Ishikawa, *J. Am. Chem. Soc.*, 125, 8694 – 8695 (2003) |
| • Dy/– | 40.3 | 6.3 x $10^{-6}$ | Ishikawa, *J. Am. Chem. Soc.*, 125, 8694 – 8695 (2003) |
| • Tb/0 | 590 | 1.5 x $10^{-9}$ | Ishikawa, *Inorg*. Chem, 43, 5498 – 5500 (2004) |
| • Dy/0 | – | | |

- Many substituted (terbium) double deckers known
- Strong correlation between $\Delta E$ and $\tau_0$.

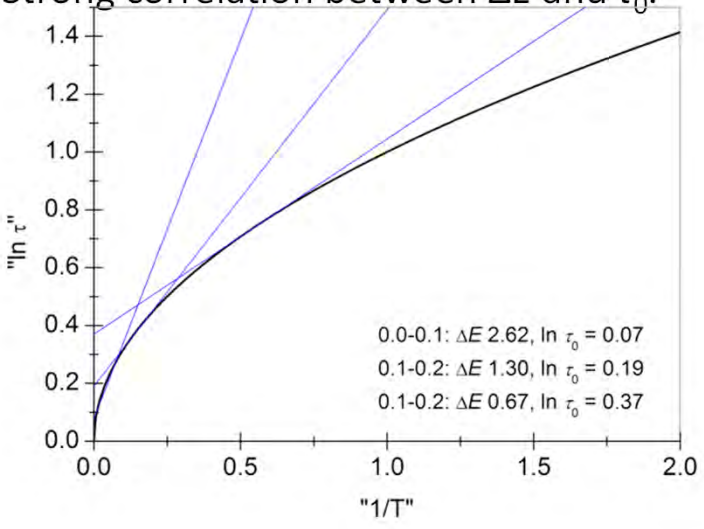


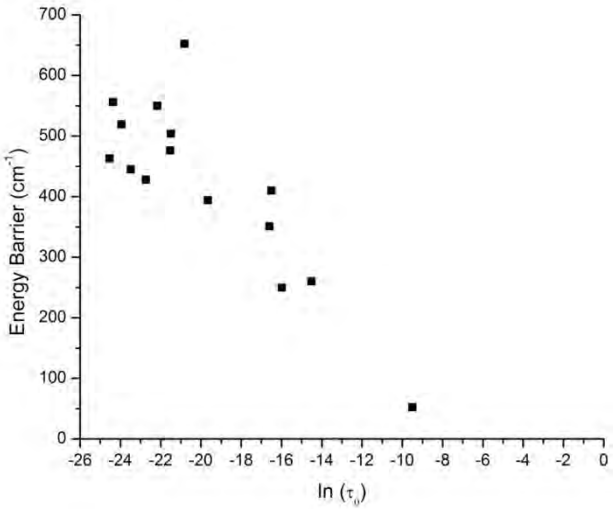


Michael Waters PhD Thesis University of Nottingham, 2013

# Ch. 6. Some words on relaxation of the magnetization

## Section 6.1 Spin-Lattice relaxation



**Basic Spin-Lattice Relaxation Mechanisms in dilute systems**

- assume dilute systems.
- A further mechanism is quantum tunnelling

energy conservation in both steps

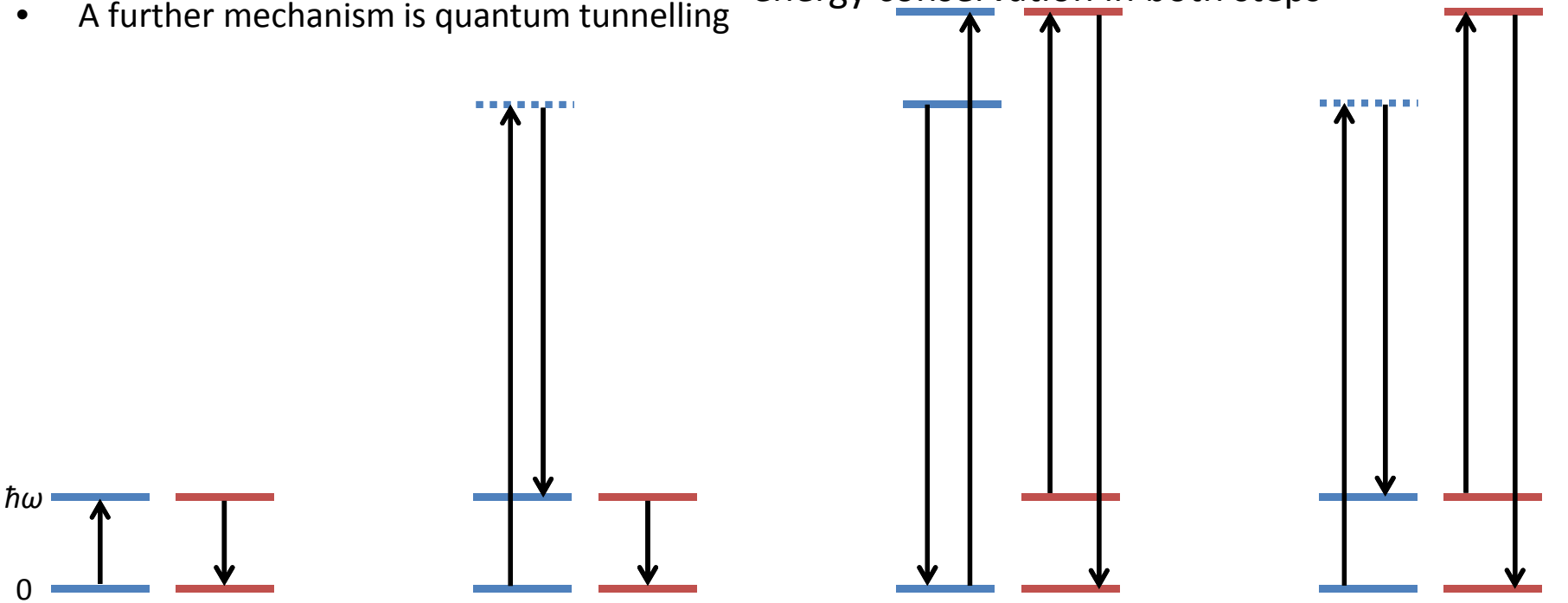


- Note that the figure was changed compared to literature. It seems to be more logical this way

Bertini in Handbook of Electron Spin Resonance, Misra in Multifrequency Electron Paramagnetic Resonance
Orbach in Electron Paramagnetic Resonance, Geschwind (Ed.), 1972; Abragam and Bleaney

# Ch. 6. Some words on relaxation of the magnetization

## Section 6.1 Spin-Lattice relaxation



**General formulas (not considering tunnelling)**

- non-Kramers ions:

$$T_1^{-1} = R_d \left(\hbar\omega\right)^3 \coth\left(\frac{\hbar\omega}{2kT_0}\right) + R_{Or}\Delta^3 \left\{\exp\left(\frac{\Delta}{kT_0}\right) - 1\right\}^{-1} + R_R T_0^7$$

- Kramers ions:

$$T_1^{-1} = R_d \left(\hbar\omega\right)^5 \coth\left(\frac{\hbar\omega}{2kT_0}\right) + R_{Or}\Delta^3 \left\{\exp\left(\frac{\Delta}{kT_0}\right) - 1\right\}^{-1} + R_R T_0^9 + R'_R \left(\frac{\hbar\omega}{k}\right) T_0^7$$